

https://dspace.org/

# An investigation into the use of a compressed air loading mechanism as a means of improving the efficiency of a four stroke spark ignition internal combustion engine

**Mackay, John Bruce**

**2012-07-04**
http://hdl.handle.net/10539/11607

Downloaded from a DSpace repository. https://dspace.org/

# AN INVESTIGATION INTO THE USE OF A COMPRESSED AIR LOADING MECHANISM AS A MEANS OF IMPROVING THE EFFICIENCY OF A FOUR STROKE SPARK IGNITION INTERNAL COMBUSTION ENGINE

John Bruce Mackay

A research report submitted to the Faculty of Engineering and the Built Environment, University of the Witwatersrand, Johannesburg, in partial fulfillment of the requirements for the degree of Master of Science in Engineering.

Johannesburg, 2011

## DECLARATION

I declare that this dissertation is my own unaided work. It is being submitted to the degree of Master of Science in Engineering to the University of the Witwatersrand, Johannesburg. It has not been submitted before for any degree or examination to any other University.

..... (Signature of Candidate)

..... day of ..... year .....

**Abstract**

Internal combustion (I.C.) engines typically exhibit a characteristic efficiency profile which varies with operating load and engine speed, and it is widely known that the operating efficiency is poor under low loading conditions. The objective of this project is to investigate whether an energy storing and recovering process, involving compressing air and subsequently using it for propulsion, could be used to achieve better overall efficiency. An engine so modified would operate in two alternate modes. When using fuel, the engine operates as close to maximum efficiency as practicable, with the excess of engine output over driving requirements being absorbed by air-compression loading - driving an external compressor, charging air into a receiver. Later, under low driving requirements, this air is expanded - using the engine cylinders - as a source of propulsion. Heat transfer from the exhaust gases to the stored compressed air is used to improve engine efficiency. Through modelling and simulation, an overall efficiency improvement of 10% over standard engine operation is predicted to be realisable by applying this modification, and scope exists to further improve this figure through improved heat recovery from exhaust gases and improved loading capability.

## ACKNOWLEDGEMENTS

I would like to thank Dr Bailey-McEwan for his guidance during the course of the research project.

# Contents


**1 Introduction** **1**

1.1 Problem Statement . . . . . 2

1.2 Required features of a compressed air augmentation system . . . . . 2

1.3 Existing applications of the compressed air-augmented I.C. engine . . . . . 3

1.4 Project objectives . . . . . 6

1.5 Outline of research report . . . . . 6

**2 Background** **8**

2.1 How an internal combustion engine works . . . . . 8

2.2 Feasibility of using compressed air to store and release energy . . . . . 9

2.2.1 Efficiency definitions . . . . . 10

2.3 Standard air analysis as an analytical tool for this project . . . . . 11

2.4 Compressed air system model . . . . . 11

2.4.1 First law-based differential equation model . . . . . 12

2.4.2 Second law analysis . . . . . 16

2.4.3 Sources of irreversibility in the compression-expansion processes . . . 18

2.4.4 Differential equation model applied to a compression & expansion stroke 19

2.5 Differential equation model of the Otto cycle . . . . . 21

2.5.1 First law model . . . . . 21

2.5.2 Application of the second law to the dynamic Otto cycle model . . . . 23

2.5.3 Sources of irreversibility . . . . . 24

2.5.4 Discussion . . . . . 25

2.5.5 Efficiency mapping . . . . . 26

2.5.6 Moving toward a more realistic engine model . . . . . 28

2.5.7 Transient effects . . . . . 29

2.5.8 Summary: dynamic Otto cycle model . . . . . 29

2.6 More accurate modelling of feasibility of C.A. augmentation of an engine . . . 30

**3 Application of the compressed air system to engines in existing vehicles** **32**

3.1 Overview: retrofitting to existing vehicles . . . . . 32

3.2 Using compressed air to propel the engine without fuel . . . . . 32
3.2.1 Using an external compressor to expand the air . . . . . 32
3.2.2 Using the engine to expand the compressed air . . . . . 33
3.3 Performance requirements if compressed air propels the engine . . . . . 35
3.4 Varying torque generation when compressed air propels the engine . . . . . 42
3.4.1 Irreversibility due to inlet of compressed air into the cylinder . . . . . 43
3.5 Using compressed air in conjunction with fuel . . . . . 46

**4 Enhanced compressed air system with heat recovery from exhaust gases 51**
4.1 Overview . . . . . 51
4.1.1 Required performance improvement . . . . . 52
4.2 Heat exchange from the exhaust gases to the compressed air . . . . . 53
4.2.1 Overview . . . . . 53
4.2.2 Heat exchanger design . . . . . 55
4.2.3 Heat transfer coefficient for turbulent flow through the exhaust pipe (R1) 58
4.2.4 Heat transfer coefficient for forced convection over heat exchanger area (R2) 59
4.2.5 Heat transfer coefficient for natural convection (R3) . . . . . 61
4.2.6 Heat transfer solution algorithm . . . . . 61
4.2.7 Performance improvement due to heat transfer . . . . . 62
4.3 Energy storage system description . . . . . 64
4.3.1 External compressor specification . . . . . 64
4.3.2 Model description . . . . . 65
4.3.3 System parameters for the compressed air storage model . . . . . 69
4.3.4 Results obtained from the compressed air storage model . . . . . 69
4.3.5 Overall efficiency: combining performance factor and loading capacity 74
4.3.6 Receiver sizing and time taken to reach final receiver pressure . . . . . 77
4.4 Conclusion . . . . . 79

**5 Conclusions and recommendation 80**
5.1 Future work . . . . . 81

**A Finite-time thermodynamics** **A.0**

A.1 Overview . . . . . A.0

A.2 Internal Combustion Engine Model . . . . . A.1

**B Sample calculation for the differential equation model** **B.0**

**C Heat transfer sample calculations** **C.0**

C.1 Heat transfer coefficient from exhaust gas to heat exchanger . . . . . C.0

C.2 Heat transfer coefficient from heat exchanger surface to receiver gases . . . . . C.1

C.3 Heat transfer via natural convection . . . . . C.2

**D Sample calculation for the compressed air storage model** **D.0**

# List of Figures


1.1 Typical engine efficiency mapping . . . . . 3
2.1 Four stroke combustion cycle . . . . . 9
2.2 A graphical representation of the relationship between speed, load and efficiency 10
2.3 Illustration of a crank shaft . . . . . 14
2.4 Otto cycle simulation results . . . . . 23
2.5 Dynamic Otto cycle model: Engine efficiency mapping . . . . . 28
2.6 Viability of loading an internal combustion engine - improved model . . . . . 30
3.1 Schematic diagram of the compressed air system . . . . . 36
3.2 Illustration of possible torque demands made by the driver . . . . . 37
3.3 Typical power-torque-speed curve of a Toyota 4ZZ-FE engine . . . . . 38
3.4 Propulsion by compressed air: cylinder pressure & P-V diagram . . . . . 39
3.5 Propulsion by compressed air: work done vs. receiver pressure . . . . . 42
3.6 Propulsion by compressed air: receiver temperature vs. receiver pressure . . . . 43
3.7 Propulsion by compressed air: useful work lost due to irreversibility . . . . . 45
3.8 The effect on cylinder gas temperature with compressed air injection . . . . . 47
3.9 P-V & T-V diagrams for a standard & modified Otto cycle . . . . . 48
4.1 Energy storage schematic overview . . . . . 53
4.2 Annual saving due to efficiency improvement . . . . . 54
4.3 Heat exchanger - conceptual drawing . . . . . 56
4.4 Heat transfer analogy . . . . . 57
4.5 Exhaust gas temperature and cylinder air mass during an exhaust stroke . . . . 58
4.6 External air compressor P-V diagram . . . . . 65
4.7 External compressor size specification . . . . . 65
4.8 Heat transfer as a function of heat exchanger size . . . . . 70
4.9 Performance factor vs compr. vol. and max receiver pressure, GR 1:1 . . . . . 72
4.10 Performance factor as a function of external compression volume and gear ratio 73
4.11 Overall system efficiency for a range of driver load requirements . . . . . 78
A.1 Finite-time thermodynamic model - Power and efficiency curves . . . . . A.4
A.2 TS diagram representation of an Otto cycle . . . . . A.5

# List of Tables


2.1 Engine model parameters . . . . . 16
2.2 Engine configuration parameters . . . . . 23
2.3 Dynamic Otto cycle model: Magnitude of sources of irreversibility . . . . . 27
2.4 Feasible conditions where loading will improve operating efficiency (revised) . 31
3.1 Using an external compressor to load an IC engine . . . . . 34
3.2 Simulation summary, compressed air injected into cylinder during combustion. 50
4.1 Feasible conditions under which partial loading will improve efficiency . . . . 75
4.2 Extracts from the efficiency-load mapping . . . . . 77
A.1 Sample data for the FTT model . . . . . A.4

## Nomenclature

| | | |
|---|---|---|
| $\beta$ | = | Volumetric coefficient of thermal expansion |
| $\gamma$ | = | Specific heat ratio |
| $\eta$ | = | Engine efficiency |
| $\theta$ | = | Crank angle |
| $\lambda$ | = | Thermal conductivity |
| $\mu$ | = | Viscosity |
| $\Xi$ | = | Exergy |
| $\rho$ | = | Density |
| $\tau$ | = | Torque |
| $\omega$ | = | Angular velocity |
| | | |
| $a$ | = | Crank radius |
| $A$ | = | Area |
| $A_{th}$ | = | Orifice area |
| $B$ | = | Cylinder bore |
| $b$ | = | Gap between heat exchanger fins |
| $\bar{c}$ | = | Mean piston speed |
| $C_h$ | = | Higher heat capacity for a stream in a heat exchanger |
| $C_l$ | = | Lower heat capacity for a stream in a heat exchanger |
| $c_d$ | = | Discharge coefficient, drag coefficient |
| $c_v$ | = | Specific heat constant volume |
| $d$ | = | Diameter |
| $E$ | = | Total energy |
| $F$ | = | Force |
| $G_r$ | = | Gear ratio |
| $g$ | = | Gravitational acceleration constant |
| $Hp$ | = | Heat input |
| $HV$ | = | Heating value |

$h$ = Enthalpy

$\bar{h}$ = Coefficient of heat transfer

$I_r$ = Work lost due to irreversibility

$L$ = Length of fin in vertical flow direction

$l$ = Con rod length

$m$ = Mass

$N$ = Rotational speed (rpm), number of teeth on a gear wheel

$N_{Pr}$ = Prandtl number

$N_{Re}$ = Reynolds number

$m_f$ = Mass of fuel

$r_p$ = Pressure ratio

$p$ = Pressure

$p_r$ = Relative pressure

$Q$ = Heat

$R$ = Ideal gas constant

$R_a$ = Rayleigh number

$R_{ht}$ = Resistance to heat transfer

$s$ = Entropy

$T$ = Temperature

$t$ = Time

$U$ = Internal energy, overall heat conductance

$u_m$ = Mean free stream velocity

$V$ = Volume ($m^3$)

$v$ = Specific volume ($m^3/kg$)

$W$ = Work

## Subscripts

| | | |
|---|---|---|
| $c$ | = | Cold, Combined |
| $cpr$ | = | Compressor |
| $cyl$ | = | Cylinder |
| $d$ | = | Downstream |
| $drv$ | = | Drive |
| $e$ | = | Exhaust |
| $f$ | = | Final, fuel |
| $fmech$ | = | Mechanical friction |
| $fric$ | = | Friction |
| $fpipe$ | = | Friction in pipe |
| $h$ | = | Hot |
| $ht$ | = | Heat transfer |
| $hr$ | = | Heat released |
| $h$ | = | Higher, hot |
| $i$ | = | inlet, initial |
| $l$ | = | Lower |
| $mx$ | = | Mixing |
| $o$ | = | outlet |
| $p$ | = | Products, Process |
| $pl$ | = | Process loaded (effective) |
| $r$ | = | Reactants |
| $rec$ | = | Receiver |
| $req$ | = | Required |
| $supl$ | = | Supplied |
| $th$ | = | Throttling |
| $u$ | = | Upstream |
| $v$ | = | Volumetric |

| | | |
|---|---|---|
| $w$ | = | Wall |
| 0 | = | Dead state |
| $x$ | = | Compression control variable, used to denote cylinder volume when the inlet valve closes or opens |
| $z$ | = | Expansion control variable, used to denote cylinder volume when the exhaust valve closes or opens |
| $1, 2$ | = | State 1, 2 etc |

## Superscripts

| | | |
|---|---|---|
| $k, n$ | = | number of species of products and reactants respectively |

## Glossary of Terms

| | | |
|---|---|---|
| $ABDC$ | = | After bottom dead center |
| $A/F$ | = | Air fuel ratio |
| $BDC$ | = | Bottom dead center |
| $BTDC$ | = | Before top dead center |
| $BSFC$ | = | Brake specific fuel consumption |
| $C.A.$ | = | Compressed air |
| $fmep$ | = | Friction mean effective pressure (kPa) |
| $I.C.$ | = | Internal combustion |
| $idle$ | = | Term used to describe the state of the engine when fully throttled and disengaged from the gear box |
| $LMTD$ | = | Log mean temperature difference |
| $RPM$ | = | Engine speed (revolutions per min) |
| $TDC$ | = | Top dead center |
| $VVT$ | = | Variable valve timing |

# 1 Introduction

Increasing oil prices and a growing concern about global warming places pressure on the automotive industry to improve internal combustion engine technology such that fuel consumption and green-house gas emissions are minimised. To this end, players in the automotive market have responded with numerous innovations including alternative fuels, dynamic valve train systems, exhaust gas recirculation, use of light-weight engine components, hybrid technology, and advanced transmission systems [1, 2, 3]. Hybrid engines are typically designed as follows: an internal combustion engine is mechanically coupled via a planetary gearset to an electric motor, which allows for regenerative braking and for the engine to be operated closest to the point of optimum efficiency [4]. Continuously varying transmissions (CVT) allow the engine to be operated along an optimum torque-speed trajectory thereby decreasing overall fuel consumption, despite a CVT being typically less efficient than a standard manual gearbox [5]. With this in mind, it must be stated that every engine has a specific fuel consumption characteristic which is a function of engine torque and speed. In spark ignition engines, throttling is used as a means of controlling the amount of work done per cycle [6], and hence the output of the engine. Engine efficiency decreases with throttling [7] and by default, engine efficiency is lowest when idling. This is attributed to pumping losses[1] increasing with throttling [8], as the inlet manifold pressure of a throttled engine is lower than atmospheric pressure. Exhaust gas recirculation (EGR) has achieved limited success in reducing throttling losses [2], although the amount of exhaust gas that can be recirculated is restricted[2] [9], and therefore the amount by which throttling losses can be reduced is also limited. Dynamic valve train systems allow for early intake valve closing (EIVC) to greatly reduce throttling losses [1].

The aim of this project is not to re-invent the hybrid engine, as the electrical motor is more efficient acting as the energy transformation and reuse mechanism than any thermodynamic power cycle; nor is it to supersede the use of CVTs. The concept is rather to be developed as a retro-fit to an existing engine for the primary reason that scope exists to improve the operating efficiency of spark ignition vehicles already on the road. Electrical hybridisation of an existing vehicle or the replacement of a standard transmission system with a CVT has installation

[1] Pumping losses are defined as the work done to move air or exhaust gases into or out of the cylinder.

[2] The amount of exhaust gas that can be recirculated is limited because the A/F ratio is limited, to ensure normal combustion.

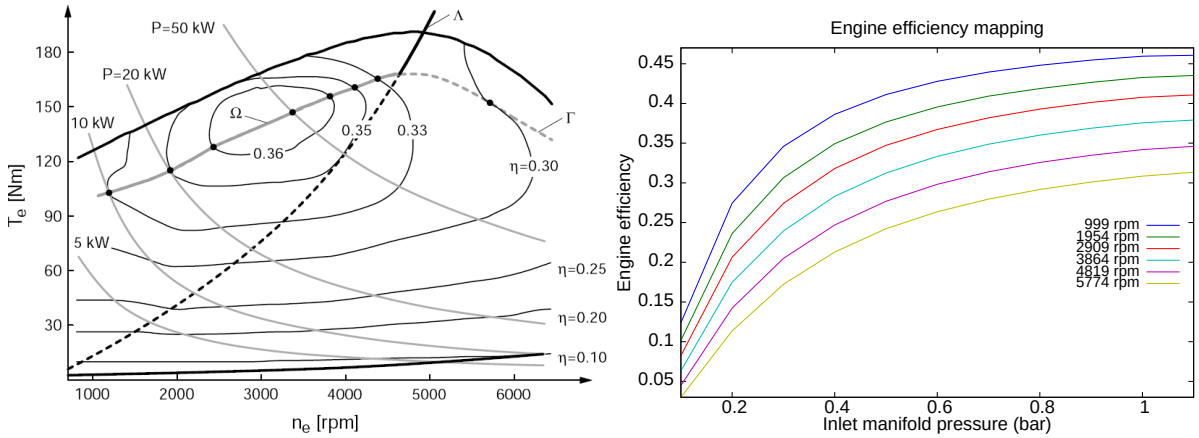
prohibitive practicality and cost implications, hence the investigation into the more practicable alternative of compressed air.

## 1.1 Problem Statement

The modern internal combustion engine is designed for acceleration - it is designed to produce a certain maximum torque, and is most efficient when operating at a value near to this maximum. However motor vehicles are required to operate over a wide range of conditions, and therefore the engine may spend a significant proportion of time operating at a point with an efficiency lower than the optimum efficiency of the engine. An efficiency mapping of a typical spark ignition internal combustion engine is shown in *Figure 1(a)*, demonstrating that the region of optimum efficiency lies at an operating point of approximately 85 % of optimum torque at an engine speed which is half of the maximum engine speed. Engine efficiency is particularly low when torque requirements are low. The proposed mandate for this project is to improve the efficiency of the spark ignition engine when torque requirements are low. *Figure 1(b)* shows an efficiency mapping obtained using a differential equation model (see *Section 2.5*, page 21), and shows the same basic efficiency characteristics as the actual efficiency mapping - which is that the engine has a low operating efficiency when highly throttled. It is proposed that the engine be loaded with a compressed air process when torque requirements are low, and that the compressed air be used independently of or in conjunction with a combustion cycle. The loading mechanism is analogous to an electrical generator-battery-motor energy storage and re-use system in this regard.

## 1.2 Required features of a compressed air augmentation system

Due to the space restrictions of the engine bay, the size (and therefore the energy storage capacity) of the device will be limited. For this reason, the potential efficiency gain obtained using a variety of both external and internal loading mechanisms should be quantified. A belt driven compressor might be used to load the engine externally, or cylinders within the engine might be used to do this air compression, thus loading the engine internally. The loading process must not adversely affect the operation of the engine - the operational characteristics of the loaded engine, such as torque output for a particular throttle setting, must not differ from conventional




(a) Actual engine efficiency mapping obtained from [5]

(b) Efficiency mapping obtained from a differential equation model

Figure 1.1: *Typical engine efficiency mapping*

engine characteristics. The efficiency of the compressed air system must be determined for all candidate loading mechanisms, and this is done using both the first and second laws of thermodynamics. Naturally no process is free of irreversibility, and a method involving regeneration, particularly the transfer of heat energy from the exhaust gases into the compressed air system, is presented to further increase the overall engine efficiency as much as is possible. (Scope also exists for the loading mechanism to be used as a regenerative braking device). The presentation of the proposed solution begins with an investigation into compressed air vehicle applications.

## 1.3 Existing applications of the compressed air-augmented I.C. engine

Before any analysis can be undertaken, the question of whether an internal combustion engine can be powered by compressed air must be addressed. To this end, a brief literature survey was conducted to find relevant examples. The literature survey shows that success has been achieved in this field, with compressed air first used as a motive source at the beginning of the last century. Advances in this field have been made since then.

The concept of using compressed air to drive an engine is not novel. One of the earliest applications of a compressed air engine is the Beaumont engine, which was developed as an alternative power source for a locomotive steam engine in the 1880's. The principle behind this engine was to introduce compressed air into a sequence of cylinders, starting with the cylinder

of the smallest area, until all useful work was extracted from the air. One problem noted with this application was the extremely low temperatures that cylinders and pistons would reach. This was rectified by applying heat to the air as it was expanded into the cylinder [10]. This example of compressed air engine avoids uncontrolled expansion. However, a separate specially designed compressed air expansion device would have to be connected to the engine in order to expand the air in this fashion.

The earliest application of compressed air to an automotive reciprocating four stroke engine was achieved by John Broderick in 1912 [11]. His idea was to enable the driver to use either compressed air or gasoline to propel the vehicle. He also made provision for the engine to be used as an air compressor, as air would be drawn into the cylinder and then forced into a compressed air storage tank through a specially modified exhaust valve. The inlet and exhaust valve timing was altered such that actuation would be achieved twice as often as in the case of a four-stroke engine (i.e. if the inlet valve were to open at $0^{\circ}$ and close at $180^{\circ}$, the exhaust valve would open part way through the compression stroke and close at $360^{\circ}$, allowing air to be compressed into a receiver on the compression stroke). In essence this engine modification not only allowed the car to be powered by compressed air, but also converted it into a hybrid vehicle as otherwise wasted energy could be captured and stored. Cylinders within the engine are used to compress air (and load the engine). This approach was discarded as a possible retrofit option because internal combustion engines typically have large clearance volumes (the engine under investigation has a compression ratio of 10 and clearance volume of 44 $cm^3$, see *Table 2.2*). This would mean that the engine (operating as a compressor) would have a poor volumetric efficiency, and perform very poorly as a compressor. A four stroke engine would also not be properly balanced if one or more of the cylinders were taken out of conventional four stroke operation, without a significantly complicated control algorithm to ensure that every half revolution delivered the same net amount of torque.

Simington invented a modification for the internal combustion engine which allowed it to run on compressed air. This was achieved through a device that allowed compressed air to be injected into the correct cylinder at the correct time through the spark plug holes [12]. The modified engine would still have an inlet and compression stage, both of which being unnecessary in a compressed air engine as the charge of air/fuel mixture need not be inducted or compressed.

This was later achieved by Stricklin through another modification, by replacing the original cam shaft with a new cam shaft: an additional cam is added at an angular displacement of 180° to original cam, such that the valve operates once per revolution of the crank shaft [13]. This idea is more fully explored in *Section 3.5*. The concept of a hybrid internal combustion/compressed air engine has been taken further in recent years through the use of electronic valves. In May 2006, Miller and Froloff were issued a patent for an engine which could be configured to be powered by gasoline or compressed air, could use the compressed air to improve the volumetric efficiency of the combustion process, and could capture braking energy by running the engine as a compressor. All of the modes of operation are obtained by dynamically reconfiguring the engine valve timing [14].

MDI, a French automotive company, have developed an air powered vehicle, and are about to begin producing this vehicle on a commercial scale [15]. This engine offers two modes of operation: the Mono-Energy operating system where the compressed air drives a piston engine equipped with an active chamber and an expansion cylinder; and the Dual-Energy operating system where a burner is used between the compressed-air tank and the engine, in order to achieve a continuous combustion below 900 K, which heats the air to increase its pressure before being injected into the engine. A recent comparative study was conducted where this compressed air engine performs similarly in terms of energy efficiency with an electric vehicle, and exceeds the performance of hybrid vehicles, however the range and maximum speed of this engine are limited. The charging and usage efficiency of the MDI engine running in Mono-Energy mode is stated to be between 62 - 70%, and 43 - 60% respectively, while the charging and usage efficiency of an electric vehicle is stated to be between 64 - 82 %, and 65 - 87 % respectively (depending on battery type) [16]. This does show that the practical efficiency of a compressed air powered vehicle is still poorer than an electically powered vehicle, but compressed air does allow opportunities for energy regeneration from exhaust gases (if applicable) - see *Section 4.2*.

The Cargine-Engineering company have developed a pneumatic engine hybrid which facilitates waste energy capture from braking and exhaust heat. Steam is generated by allowing water to come into contact with exhaust gases via a heat exchanger. This steam is used to drive the engine during every alternative power stroke, as the engine is based on the Hedman combustion cycle, which allows the engine to be powered by compressor strokes alternated with power

strokes [17].

## 1.4 Project objectives

The proposed mandate of the project is summarised by the milestones listed below. These milestones represent the core objectives of the project.

**Core objectives:**

1. To propose a number of loading mechanisms, such that the energy differential between the amount of work per cycle required for driving and the work per cycle delivered at the point of optimum efficiency can be stored. These loading mechanisms can be internal or external to the engine.
2. To develop a macroscopic control routine of the compressed air system such that engine is always correctly loaded despite the states of the air receivers.
3. To derive models of the compressed air system so that irreversibilities like heat transfer, the mixing of gases at different temperatures, throttling and friction can be taken into account. This also allows the states of the air in the cylinder and receivers to be estimated.
4. To develop a model of a spark ignition combustion cycle so that the efficiency of such an engine can be quantified based on the operating conditions of the engine. Various operation related data is also drawn from this model, for instance the amount of energy consumed during a typical exhaust stroke.
5. To use the above mentioned models to analyse process efficiency as affected by engine speed and work done on or by the compressed air system, as well as the effect of injecting compressed air into an engine cylinder part way through a combustion process.
6. To investigate the potential for using heat transfer from the exhaust gases to improve process efficiency through regeneration.

## 1.5 Outline of research report

The background section (*Chapter 2*) begins with a description of how an internal combustion engine works, drawing attention to the characteristically poor part load efficiency (where the

engine is throttled). A solution is then proposed to the problem of poor part load efficiency, which is to load the engine by an air compressor storing compressed air into a receiver to be used later. A differential equation model of the storage and usage of this compressed air is presented. The aim of this model is to illustrate the effect of irreversibility on the overall feasibility of a compressed air augmentation system. Effects such as friction, heat transfer and non-steady flow are then taken into account using a more detailed differential equation based compressed air model.

A differential equation model of an Otto cycle model is then presented and used to generate an efficiency table for a typical engine, and this table is used to show where augmenting an engine with a compressed air system would be most viable.

A detailed description of how the compressed air will be used is then given (*Chapter 3*). Compressed air usage constraints and parameters are specified to ensure that the compressed air is used as efficiently as possible. These constraints are then related to the performance requirements of a typical internal combustion engine, and a balance between these two design objectives (efficient usage of compressed air and meeting internal combustion engine output torque levels) is reached. The efficiency of compressed air usage is presented and discussed.

The way in which compressed air is stored is then discussed (*Chapter 4*), together with how heat transfer from the exhaust gases will be used to improve overall process efficiency. A design for a heat exchanger is proposed, and the analysis of how heat transfer will occur into the compressed air is presented. The design for the air compressor is also proposed, taking into account engine loading requirements (such that the engine operates at a better efficiency) as well as the physical space limitations of the engine bay. The overall performance improvement of the modification is presented.

*Chapter 5* reviews the research report, critically reviews the report and its limitations, and suggests where further work is needed.

# 2 Background

In this chapter an overview of how an internal combustion (IC) engine works is given, together with reasons for poor part load efficiency. The feasibility of using compressed air as a source of motive power in an engine is presented, with emphasis on quantifying process efficiency by including an isentropic efficiency factor. A differential equation based model of such a compressed air process is then presented with the intent of quantifying the effect on process efficiency of various sources of irreversibility present within the system. An air standard Otto cycle is then presented, and used to determine the operating region for which loading an engine with a compressed air process would be feasible. This model is then improved on using a differential equation based model, and the same feasibility analysis is repeated.

## 2.1 How an internal combustion engine works

A typical four stroke spark ignition internal combustion engine works as follows:

1. *Intake stroke:* A fresh mixture of fuel and air (charge) is drawn through the open intake valve while the piston moves from top dead center position to bottom dead center position.
2. *Compression stroke:* The intake valve is closed and the charge is compressed by the piston doing work on the charge. When the piston is close to top dead center, ignition is initiated causing the charge to burn resulting in an increase in the temperature and pressure of the air within the cylinder.
3. *Expansion stroke:* The air within the cylinder expands and does work on the piston, until the piston reaches bottom dead center.
4. *Exhaust stroke :* The burnt gases are then pushed out through the open exhaust valve while the piston moves from bottom dead center to top dead center.

The thermal efficiency of a spark ignition engine with a compression ratio of 10 modelled as a standard ideal Otto air cycle is approximately 60% and is a function of the compression ratio and the specific heat of the air alone [19][pg 378]. This value is calculated for when the engine is operating with the inlet throttle wide open and is greater than the efficiency when the throttle is partially closed.

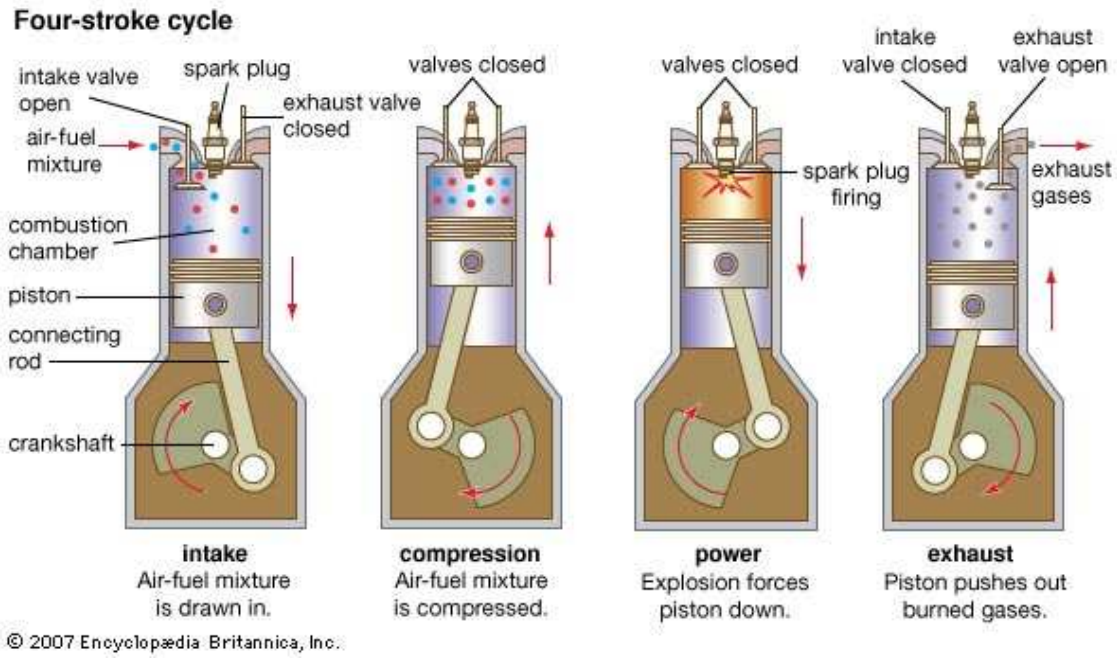



Figure 2.1: Four stroke combustion cycle [18]

In order for the engine to be useful, the amount of output power of the engine must be controlled, and this is done by limiting the supply of fuel to the engine. Spark ignition engines require the stoichiometric ratio between fuel and air to be maintained within flammable limits [20, 21]. This is done by regulating the amount of air supplied to the engine with a throttle valve. The engine must do work against this valve, increasing the pumping loss area on the PV diagram relative to the amount of work produced by the cycle. The residual exhaust gas fraction in the cylinder also increases as the load decreases [21], and these two factors contribute toward inefficient engine operation during low load conditions.

## 2.2 Feasibility of using compressed air to store and release energy

The proposed solution to this problem is to unthrottle and load the engine such that it operates at a point nearer to the point of optimum efficiency. *Figure 2.2* shows that engine efficiency increases as BMEP increases.

It is proposed that the engine be loaded either externally, by an external compressor attached to the drive output of the engine via a belt and pulley arrangement; or that the engine be loaded

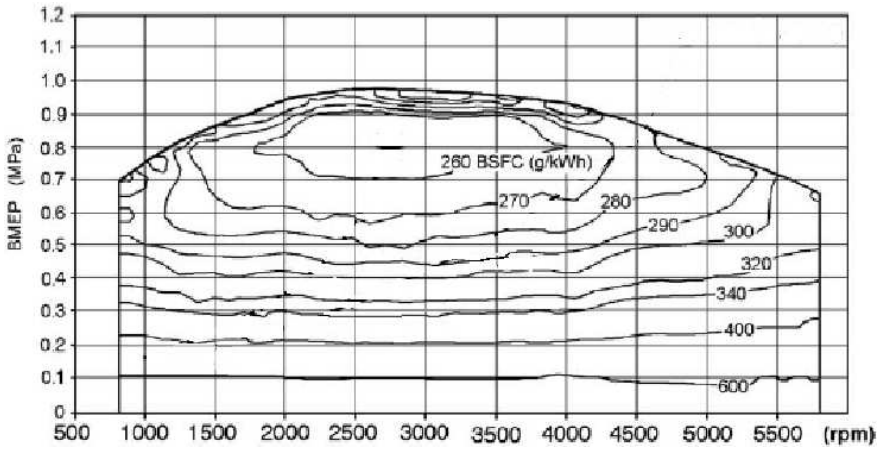



Figure 2.2: A graphical representation of the relationship between speed, load and efficiency for a standard engine, and an engine loaded such that it operates at the point of greatest efficiency for a particular speed [21]

internally, using cylinders within the engine to load the engine sufficiently. Compressed air will be the mechanism by which energy will be stored and released as needed.

### 2.2.1 Efficiency definitions

The efficiency of using (or storing) compressed air by expanding it from (or compressing it into) a storage tank with a piston-cylinder arrangement is now discussed. Consider the injection of a quantity of high pressure air into a cylinder from a high pressure receiver. During the expansion an amount of work will be done on this cylinder's piston, thereby decreasing the internal energy and mass of the air left in the receiver.

$$Energy\ out \quad = \quad -h_e \Delta m_e \tag{2.1}$$

The expansion process is not isentropic, and in practice an isentropic efficiency factor is used to account for irreversibility present in the system. The work done during an expansion process of the air in a cylinder is given by $h_1 - h_2$, where $h_1$ and $h_2$ correspond to the initial and final enthalpy respectively. The maximum amount of work obtainable without external heat input achievable by the system is given by $h_1 - h_{s2}$, and this is for a case where the air expands isentropically to state 2s. Using the above, the isentropic efficiency of an expansion process is

given by:

$$\eta_e = \frac{h_1 - h_2}{h_1 - h_{2s}} \tag{2.2}$$

If air was to be compressed between two states, the isentropic efficiency of the compression process would be given by:

$$\eta_c = \frac{h_{2s} - h_1}{h_2 - h_1} \tag{2.3}$$

## 2.3 Standard air analysis as an analytical tool for this project

Examples of work done to analyse Otto [22] and refrigeration cycles [23] based on standard air analysis techniques have been used successfully, where polytropic models are used to describe compressed air processes and isentropic efficiency factors are used to account for irreversibility. Such models of compression and expansion processes are useful, as good approximations of the amount of work done or absorbed during a process, as well as of the final state of the system, can be obtained. These models predict the behaviour of a compressor which is operating at steady state, with the initial and final temperatures of the process given by the average inlet and exhaust temperatures of the compressor [23]; but this has limited benefit when dealing with coupled processes. For instance: when modelling the discharge of air from a cylinder at one state into a receiver at another state, the receiver and cylinder cannot be considered as one system with the total volume of the system being equal to the sum of the cylinder and receiver volumes, because the states for the cylinder or receiver may not necessarily be equal, and the effects of the flow restriction between the receiver and cylinder, heat transfer and friction cannot be included.

The air standard analysis approach relies on estimates of the isentropic efficiency of each process to have been determined beforehand by experiment. The approach taken for this project was to estimate the isentropic efficiency numerically using a differential equation based method developed by Bejan [24].

## 2.4 Compressed air system model

In this section a compressed air process is described by a differential equation which is then used in conjunction with the second law of thermodynamics to characterise the amount of

useful work destroyed due to irreversibility and hence determine overall process efficiency. This approach does not characterise the entropy generated during the compression or expansion strokes, but rather the effect on entropy due to heat transfer, mixing of gases at different states, and friction. The differential equation modelling approach has been applied to combustion engines [25, 26, 27, 28] and to refrigeration compressors [29].

### 2.4.1 First law-based differential equation model

Extensive use of the differential equation modelling approach has been used to model internal combustion engines. Most of these models are derived as a first step to proposing a form of control algorithm. An assortment of papers from which insight into cylinder state dynamics was drawn are introduced briefly below. Differential equation models of the cylinder state were (possibly still are) too complex for microprocessor technology used for control to compute, but serve to describe processes for further analysis. Works have thus attempted to abstract these models such that they are compatible with existing automotive engine controller computational capabilities. Research avenues include: a control oriented perturbation model of a differential equation model describing cylinder pressure [30], a non-linear sliding observer [31], and an approximation of cylinder pressure using the maximum-likelihood method [32]. The differential equation modelling techniques presented in the above mentioned papers are based on the first law of thermodynamics and form the basis for the differential equation model used for this project. The temperature and pressure in the cylinder are governed by *Equations* 2.5 and 2.9, which are then integrated numerically. The rate of change of pressure in the cylinder (*Equation 2.5*) was arrived at by the differentiation of $pV = mRT$ with respect to the angular position of the crank shaft. The differential equation model is integrated with an integration step size of $\pi/50$ *rad* of a crankshaft revolution.

*Cylinder pressure:*

$$pV = mRT \tag{2.4}$$

Differentiating with respect to time:

$$\begin{aligned} \dot{p}V + \dot{V}p &= R(\dot{m}T + \dot{T}m) \\ \dot{p} &= \frac{R(\dot{m}T + \dot{T}m) - \dot{V}p}{V} \end{aligned} \tag{2.5}$$

Modifying the partial differential equation such that it can be integrated with respect to the angular position of the crank shaft (this applies to all further differentials with respect to time):

$$\frac{dp}{d\theta} = \frac{dp}{dt} \times \frac{dt}{d\theta} \tag{2.6}$$

*Charge temperature:* The rate of change of the cylinder temperature was obtained from the first law of thermodynamics, shown below:

$$\dot{U} = \dot{Q} - \dot{W} + h_i\dot{m} - h_e\dot{m} \tag{2.7}$$

$$\begin{aligned} & using: \ U = mu, \\ \dot{m}u + m\dot{u} &= \dot{Q} - p\dot{V} + h_i\dot{m} - h_e\dot{m} \end{aligned} \tag{2.8}$$

$$\begin{aligned} & using: \ \dot{T} = \frac{1}{c_v}\dot{u}, \\ \dot{T} &= \frac{1}{mc_v}[\dot{Q} - p\dot{V} + h_i\dot{m} - h_e\dot{m} - u\dot{m}] \end{aligned} \tag{2.9}$$

*Mass flowrate [33, pg 907]:* . Where $\dot{m}$ is positive if the inlet pressure $p_1$ is larger than the cylinder pressure $p_2$.

$$\dot{m} = \begin{cases} \frac{C_D A_{th} P_1}{\sqrt{RT_1}} \gamma^{\frac{1}{2}} \left(\frac{2\gamma}{\gamma+1}\right)^{\frac{\gamma+1}{2(\gamma-1)}} & \text{if } \frac{P_2}{P_1} > \frac{2}{\gamma+1}^{\frac{\gamma+1}{2(\gamma-1)}} \\ \frac{C_D A_{th} P_1}{\sqrt{RT_1}} \left(\frac{P_2}{P_1}\right)^{\frac{1}{\gamma}} \left[\frac{2\gamma}{\gamma-1}\left(1 - \frac{P_2}{P_1}^{\frac{\gamma-1}{\gamma}}\right)\right]^{\frac{1}{2}} & \text{if } \frac{P_2}{P_1} \leq \frac{2}{\gamma+1}^{\frac{\gamma+1}{2(\gamma-1)}} \end{cases} \tag{2.10}$$

Receiver pressure and temperature are obtained from Equations 2.5 and 2.9 respectively with $\dot{V}$ as zero because the receiver volume is assumed constant.

*Receiver pressure:*

$$\dot{p} = \frac{R[\dot{m}T + \dot{T}m]}{V} \tag{2.11}$$

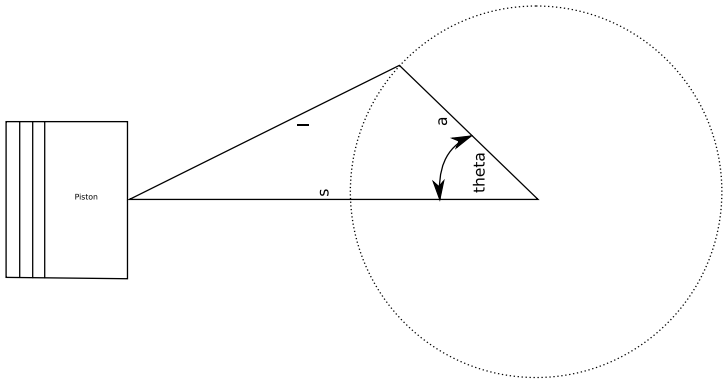



Figure 2.3: Illustration of a crank shaft for the derivation of *Equation 2.16*

*Receiver temperature:*

$$\dot{T} = \frac{1}{mc_v}[\dot{Q} + h_i\dot{m} - h_e\dot{m} - u\dot{m}] \tag{2.12}$$

*Heat transfer (cylinder):* Heat transfer between the cylinder and the engine walls is given by the Annand expression [25, 34, 28] :

$$\dot{Q}_{ht} = A_{cyl}\left[0.3\lambda\frac{N_{Re}^{0.7}}{D}(T_{cyl} - T_w) + 1 \times 10^{-8}({T_{cyl}}^4 - T_w^4)\right] \tag{2.13}$$

Where:

| | | |
|---|---|---|
| $\lambda$ | = | Thermal conductivity (W/K.m) |
| $D$ | = | Cylinder bore (m) |
| $N_{Re}$ | = | Reynolds Number |
| $T_{cyl}$ | = | Temperature of air in the cylinder (K) |
| $T_w$ | = | Temperature of cylinder wall (K) |

The surface area of the combustion chamber is derived below:

$$Area = A_{ch} + A_p + \pi B(l + a - s) \tag{2.14}$$

Where ($a$, $l$ and $s$ are depicted in *Figure 2.3*):

$A_{ch}$ = Cylinder head surface area (m)

$A_p$ = Piston crown area(m)

$a$ = Connecting rod length (m)

$l$ = Crank radius (m)

$s$ = Position of piston pin to crank centre (m)

$$s = a\cos(\theta) + \sqrt{l^2 - (a\sin(\theta))^2} \tag{2.15}$$

Resulting in [33, pg 44]:

$$Area = \pi(B/2)^2 + \pi(B/2)^2 + \pi B(l + a - a\cos(\theta) + \sqrt{l^2 - (a\sin(\theta))^2}) \tag{2.16}$$

The Reynolds number (Re) is given by $\rho D\bar{c}/\mu$, where $c$ is the mean piston speed and $\rho$, $\mu$ are the density and viscosity of the gas respectively.

*Mechanical friction:* Mechanical friction is incorporated into the model according to an empirical approach developed by Rakopoulos *et al* [26], which describes the relationship between engine speed ($N$), peak cylinder pressure ($p_{max}$) and friction. A similar model was proposed by Heywood, but the effect of peak cylinder pressure on friction is not included [33]. Friction is given in bar and must be multiplied by the rate of change of cylinder volume to determine the amount of power required to overcome mechanical friction.

$$fmep = 0.137 + 0.005p_{max} + 0.0108N \tag{2.17}$$

*Fluid friction:* Pipe friction is included in the model through the Darcy-Weisbach equation [35, pg 271] (*Equation 2.18* below) and has to be calculated iteratively, as pipe friction and mass flow rate are dependent on one another. Pipe friction and mass flow rate are calculated according to the following algorithm:

- Step 1. Assuming pipe friction is zero, calculate mass flow rate
- Step 2. Calculate pipe friction using this flow rate
- Step 3. Recalculate flow rate incorporating the effects of pipe friction
- Step 4. Repeat the above until mass flow rate converges

$$p_{fric} = \frac{64}{\mathrm{Re}} \frac{1}{D} \frac{\rho V^2}{2} \tag{2.18}$$

Thermal conductivity ($\lambda$) [36] and fluid viscosity ($\mu$) [37] are given by the following equations:

$$\lambda = 1.0184 \times 10^{-4} T - 3.9333 \times 10^{-4} \tag{2.19}$$

$$\mu = (18.27 \times 10^{-6}) \Big( \frac{411.15}{T + 120} \Big) \Big( \frac{T}{291.15} \Big)^{1.5} \tag{2.20}$$

The following engine parameters are assumed [38]:

Table 2.1: Engine model parameters

| | |
|---|---|
| Cylinders | 4 |
| Bore (m) | 0.08 |
| Compression ratio | 10 |
| Clearance volume ($m^3$) | $4.407 \times 10^{-5}$ |
| Swept Volume ($m^3$) | $3.967 \times 10^{-4}$ |

***Comment:*** This first-law model has merit in that time-varying system states can be predicted based on the parameters specified. However, the system should be modelled as closely to a real system as possible, in that aspects such as heat transfer and the mixing of gases at two different states are taken into account; as well as the effects of pipe friction. A means to measure the degradation of useful energy (available for work) due to such real world irreversibilities is obtained from the second law of thermodynamics.

### 2.4.2 Second law analysis

Second law analysis will be used to evaluate how much useful energy (available for work) might be degraded by various sources of irreversibility present in the system during a particular compression or expansion stroke. Process efficiency (affected by the degradation of useful energy) may be affected by various operational requirements as well as changing system states. Examples were found in literature which take this approach in quantifying the second law efficiency

[25, 29] of a thermodynamic process. First law analysis is used to describe the variation in the state of the system according to the differential equation model presented in *Section 2.4.1*, and the amount of useful energy which has been degraded is quantified using exergy analysis techniques. The exergy of a system in a given state is defined as the maximum amount of useful work which could be obtained from the combination of the system and the surrounding atmosphere, as the system goes through reversible processes to equilibrate with the atmosphere [25]. Irreversible processes give rise to a ”lost” work term which is quantifiable in terms of the entropy produced, through a relationship known as the Gouy-Stodola theorem; where the amount of energy made unavailable to do work due to irreversibility is proportional to the amount of entropy produced by a process. The proportionality constant is dependent on the system of interest [24, pg 24].

$$\dot{W_{lost}} = T_0 \dot{S_{gen}} \tag{2.21}$$

Where:

$T_0$ = constant of proportionality, taken to be the temperature of the surroundings (300 K)

$\dot{S_{gen}}$ = rate at which entropy is produced during a process.

The compressed air loading process is dynamic in the sense that the conditions surrounding the system change, and the model provides a means for the effect of the changing surroundings on process efficiency to be quantified. Using *Equation 2.21*, one can quantify the amount of useful work lost due to heat transfer, mixing of air streams at different states, and friction; all of which are present in the loading process under investigation. The amount of ”lost” work can be used to quantify a process efficiency, which is defined as the amount of work absorbed or released during a complete a process (compression, expansion etc) taking into account the amount of useful energy (available for work) degraded during this process, divided by the work required for that a process if it were to occur without irreversibility. This efficiency is known as the second law efficiency (*Equation 2.22*), as given by Bejan [24].

$$\eta_{II} = 1 - \frac{\dot{W}_{lost}}{\dot{W}_{max}} \tag{2.22}$$

Where:

$$\dot{W}_{max} = \sum_{in} \dot{m}(h - T_0 s) - \sum_{out} \dot{m}(h - T_0 s) - \frac{d}{dt}(E - T_0 S) \tag{2.23}$$

### 2.4.3 Sources of irreversibility in the compression-expansion processes

The following relationships are based on work done by Bejan [24]. Sources of irreversibility present in the envisaged compression or expansion processes are the mixing of air streams at different states, pressure drops due to friction between air and piping, mechanical friction and heat transfer. Loss of useful energy due to friction between the cylinder walls and piston rings is given by *Equation 2.24*.

Note:

| | | |
|---|---|---|
| $T_w$ | = | Cylinder wall temperature |
| $T_0$ | = | Temperature at the reference state |
| $R$ | = | Ideal gas constant |
| $\dot{m}$ | = | Mass flow rate |
| $P_u$, $T_u$ | = | Up stream pressure and temperature |
| $P_d$, $T_d$ | = | Down stream pressure and temperature |
| $\dot{I}r_{fmech}$ | = | Irreversibility due to mechanical friction |
| $\dot{I}r_{fpipe}$ | = | Irreversibility due to pipe friction |
| $\dot{I}r_{mx}$ | = | Irreversibility due to mixing |
| $\dot{I}r_{th}$ | = | Irreversibility due to throttling |
| $s$ | = | Entropy at the inlet |
| $s'$ | = | Entropy at the outlet |
| $h$ | = | Enthalpy at the inlet |
| $h'$ | = | Enthalpy at the outlet |

$$\dot{I}r_{fmech} = \dot{W}_{fmech}\left(1 - \frac{T_w - T_0}{T_w}\right) \tag{2.24}$$

Friction between the gas and pipe tubing results in a pressure drop and an associated loss of useful energy given by *Equation 2.25* [24]. In addition to pipe friction, a pressure drop occurs

across the engine valves, which varies with engine speed [39]. Steady flow has been assumed.

$$\dot{I}r_{fpipe} = T_0 S_{gen} = T_0 mR\ln\left(\frac{p_{in}}{p_{out}}\right) \tag{2.25}$$

A key design aim of this project is to avoid uncontrolled expansions (mixing of air at different pressures) as much as possible, but the mixing of air streams at different temperatures seems unavoidable (air will be discharged into a receiver and mix with its contents not necessarily at the same state as the air exhausted from the compressor), with the loss in useful work arising from such an event given by *Equation 2.26*.

$$\dot{I}r_{mx} = \dot{m}T_0 C_p\left(\ln\left(\frac{T_1}{T_2}\right) - \frac{T_1 - T_2}{T_1}\right) \tag{2.26}$$

A certain amount of uncontrolled expansion is expected as valve actuation will not be ideal, and the corresponding loss in useful work is given by *Equation 2.27*. The expansion (when mixing gases at different pressures) is assumed to be isenthalpic. The reference state is taken to be 300 $K$, $1 \times 10^5$ $pa$. The irreversibility directly associated with the act of compressing or expanding the air within the cylinder is not included in this model. This could have been modelled using finite element thermodynamics, but this was beyond this project's scope. These processes have been modelled as isentropic.

$$\dot{I}r_{th} = T_0\dot{m}(s' - s) \tag{2.27}$$

Where: $h' = h$

Alternatively one could evaluate the loss of available work due to mixing by using the following expression [28]:

$$\dot{I}r_{th} = T_0\dot{m}\left[c_p\ln\left(\frac{T_u}{T_d}\right) - R\ln\left(\frac{p_u}{p_d}\right)\right] \tag{2.28}$$

### 2.4.4 Differential equation model applied to a compression followed by an expansion stroke

An idea of compressed air process efficiency is obtained from the dynamic model presented above. Air is compressed from a volume of $4.407 \times 10^{-4}$ $m^3$ and a state of 1 $bar$, 300 $K$ to a volume of $4.407 \times 10^{-5}$ $m^3$ and a state of 23 $bar$, 700 $K$, and then expanded to the initial volume and a state of 0.92 $bar$, 275 $K$. Heat transfer and friction are both included in the simulation,

hence the difference between initial and final states. The process was modelled in Octave - a mathematical simulation package similar to Matlab.

The process efficiency is 67 %. The compression mechanism modelled here is isentropic, so the actual efficiency of a compression stroke followed by an expansion stroke is expected to be lower than 67%.

## 2.5 Differential equation model of the Otto cycle

The air standard approach to Otto cycle analysis has been developed and expressions for maximum power and efficiency as functions of various parameters have been obtained. The results obtained using this approach are not realistic and so have not been used, but the methodology is presented in *Section A* of the Appendix.

The differential equation based model of a conventional spark ignition internal combustion engine allowed investigation into the use of high pressure air injection to improve the efficiency of the existing combustion cycle directly. Such a model would also allow a more accurate efficiency mapping of an engine to be obtained (more accurate than an air standard analysis approach). However this mapping would only provide a qualitative understanding of engine efficiency; the efficiency of a combustion engine would be determined through experiment for most accurate results.

Other operational related data required for the analysis of various aspects of this project are also drawn from the differential equation model. This includes work done during a typical expansion, compression, intake, or exhaust stroke; as well as the exhaust gas state and outlet mass flow rate used for heat transfer analysis.

### 2.5.1 First law model

When simulating a combustion process, the rate of heat release is dependent on the rate at which fuel is burned, which is approximated by a Weibe function [33, pg 390]:

$$m_b = m_f\left(1-\exp\left[-a\left(\frac{\theta-\theta_0}{\Delta\theta}\right)^{m+1}\right]\right) \tag{2.29}$$

Where $a$ and $m$ are constants used to match the Weibe function to experimentally obtained data on to burn profiles. Real burn fraction curves have been fitted to a Weibe function with $a = 5$ and $m = 2$ [28, 40]. The amount of the heat released is given by:

$$\dot{Q}_{hr} = Q_{LHV}\dot{m}_b\eta_b \tag{2.30}$$

where:

$Q_{LHV}$ = Lower heating value

$\dot{m}_b$ = Mass burn rate

$\eta_b$ = Burn efficiency

Combustion efficiency can be included into the model using an empirical model [28]:

$$\eta_b = 0.9(4.6509\lambda - 2.0764\lambda^2) \tag{2.31}$$

where $\lambda$ represents the excess air in the cylinder, but it has been assumed that the air fuel mixture is stoichiometric so $\lambda = 0$, and $\eta_b = 0.9$ accordingly.

$$\dot{T} = \frac{1}{mCv}[\dot{Q}_{hr} - \dot{Q}_{ht} - p\dot{V} + h_i\dot{m} - h_e\dot{m} - u\dot{m}] \tag{2.32}$$

Valve and ignition timing settings are as shown in *Table 2.2*. The differential equation model provides a means to observe the effect of valve and ignition timing on engine operational efficiency. For instance: altering the ignition timing has an effect on the amount of work done, because the point at which cylinder pressures peak changes accordingly. Closing the inlet valve after BDC results in the induction of more air into the cylinder, and experimentation with this model indicates that the inlet valve should close at 35° after BDC at an engine speed of 6000 *RPM*.

The breathing characteristics are dependent on the structure of the engine and the inertia of the air, and have been included into the model through an empirical model of volumetric efficiency (*Equation 2.33*), based on work done by Williams [41]. Other empirical methods of characterising intake flow rate were found in [42, 43, 44].

$$\eta_v(n,p) = 0.597071 + n5.15605 \times 10^{-5} + p9.30417 \times 10^{-7} \tag{2.33}$$

Where:

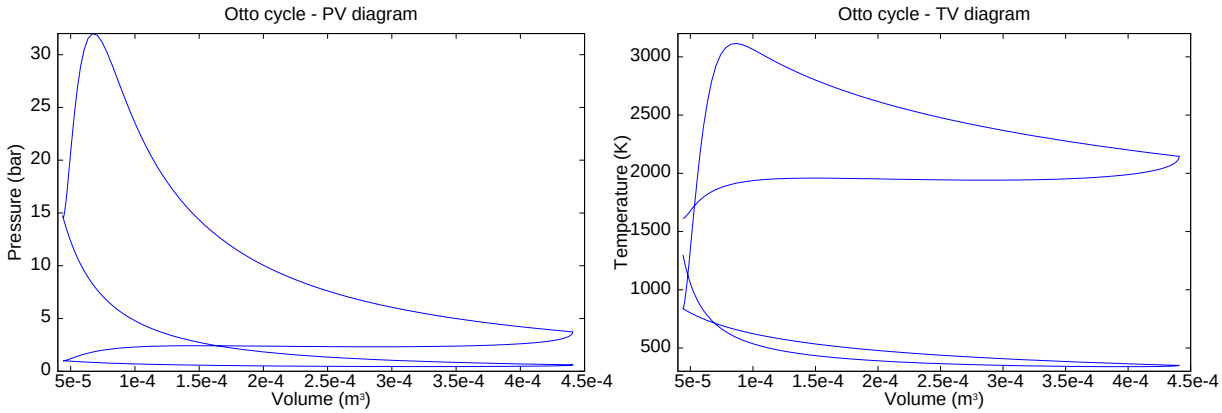
$n$ = engine speed

$p$ = peak cylinder pressure

The efficiency model is expanded using exergy analysis, so that the effect of certain irreversibilities on process efficiency can be quantified. This approach is based on work done by Rakopoulos [25] and Ribeiro et al [28]. P-V and T-V diagrams of a typical simulation are presented in *Figure 2.4*.

Table 2.2: *Engine configuration parameters* [38]

| | |
|---|---|
| Bore | 0.08 *m* |
| Stroke | 0.077 *m* |
| Burn duration | 0.628 *rad* |
| Ignition | 10° BTDC |
| Inlet valve open | TDC |
| Inlet valve close | 15° ABDC |
| Exhaust valve open | BDC |
| Compression ratio | 10 |
| Air fuel ratio (A/F) | 14.7 |




(a) Pressure-volume diagram

(b) Temperature-volume diagram

Figure 2.4: *Otto cycle simulation results*

### 2.5.2 Application of the second law to the dynamic Otto cycle model

The second law of thermodynamics is used to obtain an efficiency model of the engine when it is operating at a constant load and speed. The analysis presented in *Section 2.4.3* is extended to encompass irreversibility and associated loss of useful work due to combustion and the exhaust of hot air into the surroundings (known as gas transfer). This is based predominantly on work done by Rakopoulos and Heywood [33, 45]. The approach taken by Rakopoulos is to model the combustion processes according to first law principles, going as far as to include detail about the nature of the chemical reactions taking place within the cylinder. This aspect of combustion modelling has not been included in the model presented here. A Weibe function

is used to describe the combustion process as indicated above, without taking into account the irreversibility due to the change in chemical species of the reactants and products. Modelling of the burn profile as an empirical function (i.e. Weibe function) is the generally accepted practice, as the combustion profile can be fitted to experimental data [26].

### 2.5.3 Sources of irreversibility

Irreversibility due to the combustion process was evaluated by Ribeiro et al [28] according to *Equation 2.34* below. During experimentation they noted that the irreversibility due to combustion evaluated according to this method was much less than irreversibility due to valve throttling for example, which is not consistent with other results obtained by Heywood [33, pg 795]. Using *Equation 2.34*, the amount of "lost" work due to combustion is approximately 14 $J$ per cycle, which is not correct. Irreversibility due to combustion accounts for about a third of the total irreversibility of the engine [33].

$$\dot{I}r_{comb} = \sum_{i=1}^{k} \dot{m}_{pi} s_{pi} - \sum_{i=1}^{n} \dot{m}_{ri} s_{ri} \tag{2.34}$$

where:

| | | |
|---|---|---|
| $m$ | = | mass |
| $s$ | = | entropy |
| $p$ | = | products |
| $r$ | = | reactants |
| $k, n$ | = | number of species of products and reactants respectively |

Instead of using the method described above, the beginning and end states of the combustion process are used to determine the destruction of exergy due to the irreversibility associated with combustion, in accordance with Rakopoulos and Heywood [25, 33]. The change in exergy due to combustion is given by *Equation 2.35* below. Using *Equation 2.35*, the amount of "lost" work due to combustion is approximately 213 $J$ per cycle (with engine unthrottled, and configured according to *Table 2.2*). This is more in line with the results presented in the above mentioned literature.

$$\Xi_2 - \Xi_1 = -T_0 m(s_2 - s_1) \tag{2.35}$$

Irreversibility due to gas transfer is taken into account with *Equation 2.36* [25], and represents the loss of useful energy during the exhaust process.

$$d\Xi = dm[h - h_0 - T_0(s - s_0)] \tag{2.36}$$

Aspects which have been included in, and omitted from the differential equation model are listed below.

***Aspects included in the dynamic Otto cycle model***

- Uncontrolled expansion.
- Irreversibility due to combustion
- Heat transfer between cylinder walls and cylinder contents.
- Mechanical friction, through an empirical model.
- Flow through valves.
- Engine breathing characteristics (through a simple empirical model).
- The effect of valve and ignition timing.

***Aspects not included in the Otto cycle model***

- Nature of the combustion products during exhaust. Chemical potential energy will be present in combustion products which are subsequently exhausted to the atmosphere.
- Exergy generated during the reaction process.
- Residual exhaust gases in the cylinder.
- Heat transfer between the reactants and products.

### 2.5.4 Discussion

A combustion cycle was configured according to the parameters in *Table 2.2*, and the simulation results are presented in *Table 2.3*. The simulation was performed for two throttled conditions (inlet manifold pressure of 0.3 *bar* and 0.5 *bar* respectively) for a speed of 1000 *RPM*, and for two unthrottled conditions (the inlet manifold pressure is 1 *bar*), for an engine speed of 1000 *RPM* and 3000 *RPM*. The sum of the amounts of energy made unavailable to do useful

work due to irreversibilities and the net work output of the engine should equal the amount of energy released during the combustion, which although very close (1245 as opposed to 1324), is not quite the case as shown in *Table 2.3*. This is attributed to some expressions for work lost due to irreversibility including assumptions about the ambient environment.

For instance when evaluating ”lost” work due to mechanical friction and heat transfer, it is assumed that cylinder wall temperature is 400 $K$ and that ambient air temperature is 300 $K$ - in other words, the irreversibility is scaled by constant factors which may have been incorrectly selected.

In *Table 2.3*, the net irreversibility due to uncontrolled expansion (as evaluated by *Equation 2.27*) decreases as the amount by which the engine is throttled increases. For an increase in throttling, further investigation reveals that the irreversibility due to uncontrolled expansion increases during the intake stroke, but then decreases during the exhaust stroke as low peak cylinder pressures result in lower cylinder pressures at the end of the expansion stroke - and therefore results in less irreversibility due to uncontrolled expansion during the exhaust stroke. Peak pressures are less because less fuel-air mixture has been combusted. Pumping work under throttled conditions is higher than under unthrottled conditions as expected, and this is observable by plotting work done against angular displacement for a particular throttling condition.

Comparing the cases where the unthrottled engine operates at 1000 *RPM* and 3000 *RPM*: heat transfer decreases as engine speed increases as there is less time for heat transfer to occur. Irreversibility due to uncontrolled expansion increases with engine speed as the pressure difference across the inlet valve increases. There is less time available for charge mixture to be drawn into the cylinder, therefore irreversibility due to combustion decreases because there is less charge to be combusted. Friction irreversibility increases with piston speed, and irreversibility due to gas transfer is higher because the energy content of air in the cylinder after expansion is larger, in turn because less heat transfer out of the cylinder has occurred.

### 2.5.5 Efficiency mapping

The engine efficiency mapping was generated through simulation (see *Figure 2.5*), but does not display the behavioral characteristics common to real engines, particularly a decrease in engine efficiency at high load, and limited increases in efficiency with engine speed due to improved

Table 2.3: Dynamic Otto cycle model: Magnitude of various sources of irreversibility.
*Two throttling conditions are presented for partially throttled conditions (throttled such that the inlet manifold pressure is* 0.3 *bar and* 0.5 *bar) for an engine speed of* 1000 *RPM. Two unthrottled conditions are presented (inlet manifold pressure is* 1 *bar), for the engine speeds of* 1000 *RPM and* 3000 *RPM respectively. The engine was set up as in Table 2.2. It is assumed that the ambient pressure is* 1 *bar.*

| ***Throttling condition*** | *Work* (J) | *Mechanical friction*(J) | *Gas transfer*(J) | *Heat transfer*(J) | *Uncontrolled* exp (J) | *Combustion*(J) | $\sum$ (J) | *Net heat input*(J) |
|---|---|---|---|---|---|---|---|---|
| *unthrottled (1 bar)* | 434 | 108 | 274 | 280 | 29.5 | 211 | 1245 | 1324 |
| *low load (0.5 bar)* | 153 | 87 | 122 | 175 | 6.2 | 107 | 650 | 674 |
| *idle (0.3 bar)* | 40 | 68 | 69 | 126 | 2.3 | 66 | 371 | 411 |
| *unthrottled 3000 rpm* | 207 | 276 | 307 | 218 | 37 | 202 | 1247 | 1273 |

breathing characteristics. High load at high speed results in poor combustion. An example of an actual fuel consumption model is shown in *Figure 2.2*, and one can see that in this instance maximum efficiency is at about 80% of maximum torque, with a global optimum efficiency at an engine speed which is 50% of maximum. Considering the optimum engine operating point as a starting point: at a constant load, increasing speed from this point results in increased friction losses, increasing load at a constant speed increases air flow limitations, and the mixture is subsequently enriched [33].

Another factor not included in the model is cylinder turbulence, particularly the effect that this has on heat transfer and fuel mixing, resulting in better mixing and burning of fuel [46], despite a decrease in the volumetric efficiency. The model does provide an understanding of engine efficiency magnitudes at a range of operating conditions, but where these above ignored phenomena begin to take effect, it is inadequate.

The engine is most efficient when completely unthrottled according to the model derived for this project. Each efficiency value is calculated under the assumption that the engine is operating at steady state. Engine efficiency is defined below:

$$\eta = \frac{work\ done\ per\ cycle}{work\ done\ per\ cycle + work\ lost\ to\ irreversibility\ per\ cycle}$$

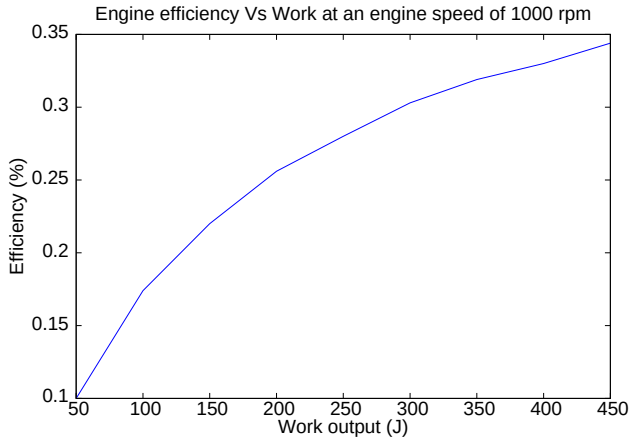



Figure 2.5: Dynamic Otto cycle model: Engine efficiency mapping

### 2.5.6 Moving toward a more realistic engine model

Typically BSFC mappings are determined through experiment [33, 47]: engine torque, speed and fuel consumption will be measured over a wide range of operating conditions, and the mapping will be generated accordingly. A method (developed by Goering and Cho) has been developed to generate efficiency mapping models without conducting many tests. In this method empirical models of torque, friction, and thermal efficiency are used to generate the mapping [47]. This mapping approach lends itself well to the intended future focus of the project, as a wide variety of engines may be fitted with the loading mechanism, and an efficiency mapping test would probably need to be done on each of the candidate engines. The efficiency mapping method developed by Goering and Cho is outlined below:

$$\begin{aligned} \eta_{engine} &= \frac{\pi\tau\, rpm}{30 HV_l \dot{m}_f} \\ &= \frac{\eta_{therm}}{1+\frac{fmep}{bmep}} \end{aligned} \tag{2.37}$$

After equating the above:

$$\begin{aligned} \dot{m}_f &= \frac{\pi\tau\, rpm(bmep+fmep)}{30 bmep HV_l} \\ BSFC &= \frac{\dot{m}_f}{Output\ power} \end{aligned} \tag{2.38}$$

where:

$bmep$ = Brake mean effective pressure

$fmep$ = Friction mean effective pressure

$rpm$ = Engine speed in rev/min

$m_f$ = Mass of fuel

$BSFC$ = Brake specific fuel consumption

$HV_l$ = Lower heating value of the fuel

### 2.5.7 Transient effects

No attempt has been made at modelling the efficiency of the engine at an accelerating transient state. A recent study has shown that during fast accelerating transients, measured fuel consumption is up to twice as much as during the corresponding steady-state load conditions [48]. The transient fuel consumption model presented in the above mentioned reference is based on the sum of the static fuel consumption properties of an engine and a transient fuel consumption correction factor, which is based on measured engine performance data. Given that fuel efficiency is low under accelerating transient conditions, it may prove beneficial to use compressed air to accelerate the engine, which is proposed as a topic for future work. One would begin by assuming that fuel consumption under accelerating transient conditions is 50% higher than normal (i.e. efficiency is 50 % poorer), and then determine engine efficiency if compressed air is used as means of accelerating the engine.

### 2.5.8 Summary: dynamic Otto cycle model

This section develops the models used to simulate two modes of operation of an I.C. engine: conventional operation with fuel, and propulsion by compressed air. The dynamic Otto cycle model was used to predict the amount of work associated with each of the four strokes of a combustion cycle, and allowed the amount and state of exhaust gases exiting an engine during an exhaust stroke to be evaluated. Expressions relating maximum power and efficiency to operational parameters such as engine speed and throttle setting (amongst others) were also developed from this model.

## 2.6 More accurate modelling of feasibility of compressed air augmentation of an engine

This model is used to demonstrate where loading the engine with the compressed air system could be applied. *Table 2.4* indicates that the effectiveness of the modification decreases as the combined compressed air storage and usage efficiency decrease, and serves to show that the efficiency gain decreases as the amount of required loading decreases. Consider the engine operating with an inlet pressure of 0.42 bar, producing 100 J of work per cycle at an efficiency of 17%. If the engine were fully loaded, 360 *J* of energy would be available to be used by the compressor. Of course, as noted in *Section 2.4*, not all this energy will be available for reuse. For the purposes of the explanation, assume that the combined efficiency of the air compression-expansion process is 70%; 252 *J* of energy is available for reuse, and the effective efficiency ($\eta_{pl}$) of the engine after taking this energy into account is 27% (which is greater than if the engine were operated partially loaded). The region of feasibility has been summarised in *Figure 2.6*.

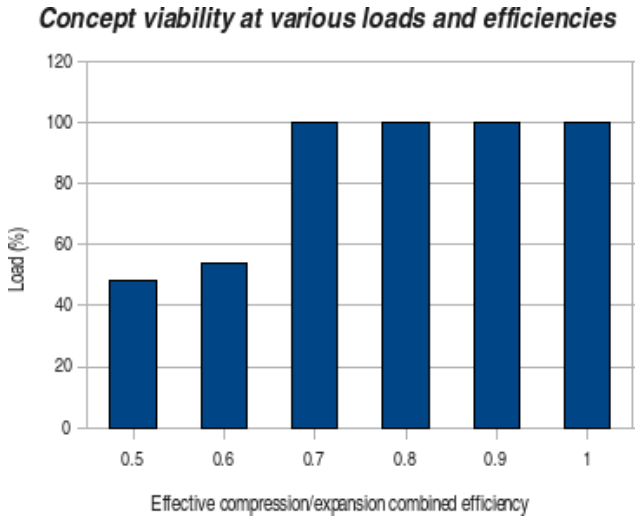



Figure 2.6: Viability of loading an internal combustion engine for various compression-expansion process efficiencies and different required loading conditions

Table 2.4: Feasible conditions where loading will improve operating efficiency (revised)

| | | | | $\eta_c$ | 1 | | 0.9 | | 0.8 | | 0.7 | | 0.6 | | 0.5 | |
|---|---|---|---|---|---|---|---|---|---|---|---|---|---|---|---|---|
| **Load** | **IP (bar)** | $\eta_p$ | **W** | $\mathbf{H_p}$ | **ER (J)** | $\eta_{pl}$ | **ER (J)** | $\eta_{pl}$ | **ER (J)** | $\eta_{pl}$ | **ER (J)** | $\eta_{pl}$ | **ER (J)** | $\eta_{pl}$ | **ER (J)** | $\eta_{pl}$ |
| 2 | 0.05 | 0.03 | 10 | 384.62 | 450 | 0.35 | 405 | 0.31 | 360 | 0.28 | 315 | 0.25 | 270 | 0.21 | 225 | 0.18 |
| 4 | 0.28 | 0.05 | 20 | 400.00 | 440 | 0.35 | 396 | 0.31 | 352 | 0.28 | 308 | 0.25 | 264 | 0.21 | 220 | 0.18 |
| 9 | 0.32 | 0.09 | 40 | 444.44 | 420 | 0.35 | 378 | 0.32 | 336 | 0.28 | 294 | 0.25 | 252 | 0.22 | 210 | 0.19 |
| 13 | 0.35 | 0.12 | 60 | 491.80 | 400 | 0.35 | 360 | 0.32 | 320 | 0.29 | 280 | 0.26 | 240 | 0.23 | 200 | 0.20 |
| 17 | 0.38 | 0.15 | 80 | 533.33 | 380 | 0.35 | 342 | 0.32 | 304 | 0.29 | 266 | 0.26 | 228 | 0.23 | 190 | 0.20 |
| 22 | 0.42 | 0.17 | 100 | 574.71 | 360 | 0.35 | 324 | 0.32 | 288 | 0.29 | 252 | 0.27 | 216 | 0.24 | 180 | 0.21 |
| 28 | 0.46 | 0.20 | 130 | 637.25 | 330 | 0.35 | 297 | 0.32 | 264 | 0.30 | 231 | 0.27 | 198 | 0.25 | 165 | 0.22 |
| 35 | 0.51 | 0.23 | 160 | 698.69 | 300 | 0.35 | 270 | 0.32 | 240 | 0.30 | 210 | 0.28 | 180 | 0.26 | 150 | 0.23 |
| 41 | 0.56 | 0.25 | 190 | 763.05 | 270 | 0.35 | 243 | 0.33 | 216 | 0.31 | 189 | 0.29 | 162 | 0.27 | 135 | 0.25 |
| 48 | 0.61 | 0.27 | 220 | 823.97 | 240 | 0.35 | 216 | 0.33 | 192 | 0.31 | 168 | 0.29 | 144 | 0.27 | 120 | 0.26 |
| 54 | 0.66 | 0.28 | 250 | 886.52 | 210 | 0.35 | 189 | 0.33 | 168 | 0.32 | 147 | 0.30 | 126 | 0.28 | 105 | 0.27 |
| 61 | 0.70 | 0.30 | 280 | 949.15 | 180 | 0.35 | 162 | 0.33 | 144 | 0.32 | 126 | 0.31 | 108 | 0.29 | 90 | 0.28 |
| 67 | 0.75 | 0.31 | 310 | 1013.07 | 150 | 0.35 | 135 | 0.34 | 120 | 0.32 | 105 | 0.31 | 90 | 0.30 | 75 | 0.29 |
| 74 | 0.79 | 0.32 | 340 | 1075.95 | 120 | 0.35 | 108 | 0.34 | 96 | 0.33 | 84 | 0.32 | 72 | 0.31 | 60 | 0.30 |
| 80 | 0.85 | 0.33 | 370 | 1138.46 | 90 | 0.35 | 81 | 0.34 | 72 | 0.33 | 63 | 0.33 | 54 | 0.32 | 45 | 0.31 |
| 87 | 0.90 | 0.33 | 400 | 1201.20 | 60 | 0.35 | 54 | 0.34 | 48 | 0.34 | 42 | 0.33 | 36 | 0.33 | 30 | 0.32 |
| 93 | 0.94 | 0.34 | 430 | 1264.71 | 30 | 0.35 | 27 | 0.34 | 24 | 0.34 | 21 | 0.34 | 18 | 0.34 | 15 | 0.34 |
| 100 | 0.99 | 0.35 | 460 | 1325.65 | 0 | 0.35 | 0 | 0.35 | 0 | 0.35 | 0 | 0.35 | 0 | 0.35 | 0 | 0.35 |

# 3 Application of the compressed air system to engines in existing vehicles

## 3.1 Overview: retrofitting to existing vehicles

Efficiency mappings released by manufacturers[21] as well as the simulation results of the previous chapter show that a typical spark-ignition internal combustion engine is least efficient when the amount of torque required by the engine is low. For existing vehicles, this is the reason for proposing that a compressor be used to load the engine when it is producing torque below a certain threshold, by compressing air into a receiver, allowing it to operate in a more efficient zone (as throttling could be decreased). The compressed air will then be used to propel the engine in some way at a later stage: either in place of conventional fuel, or in conjunction with it.

This chapter contains a description of how the compressed air will be used, the performance requirements of the compressed air augmentation system, how the torque developed by this system will be controlled, and expected efficiency of usage of the compressed air. The idea of using compressed air in conjunction with conventional fuel is presented and reasons are given why this avenue of investigation is not pursued.

## 3.2 Using compressed air to propel the engine without fuel

### 3.2.1 Using an external compressor to expand the air

An external compressor could be used to expand compressed air in order to supplement driving requirements. Bearing in mind that this external compressor will be small in order to fit into the engine bay, the amount of torque that this external compressor can produce will be limited. This means that the external compressor will have to work in conjunction with the IC engine to produce the amount of torque required by the driver. The overall efficiency of such a process would have to be quantified, and this is done by means of a numerical example, assuming that the external compressor is sized such that it can load the engine by 30 $N.m$ (94 J stored per stroke), that the performance factor of the energy storage process is 2.4 through the effects of regenerative heat transfer (see *Section 4.2.7* for more details on performance factor and regenerative heat transfer). The specifications of the external compressor have arisen from analysis

presented in Chapter 4. The isentropic efficiency of compressed air usage will be assumed to be 0.8 [49].

The reader is referred to *Table 3.1*. Driver requirements at the time of loading are assumed to be 51 $N.m$ (160 J per stroke), and the external compressor will provide 94 J of additional loading per stroke. Heat transfer into the system will mean that 225 J is effectively stored. When it comes to using the stored energy: 94 J can be supplied by the external compressor, but only 75 J is useful (due to an isentropic efficiency of 0.8), and the engine must supply the remainder of the requirement. The efficiency of this process is evaluated by calculating the net amount of energy delivered by the IC engine (160 J + 85 J) plus the surplus energy stored as compressed air which was not available to be used for propulsion due to expansion capacity limitations [3] of the external compressor, but could be used in future expansion strokes. This figure is then divided by the energy input as fuel.

This modification results in a performance improvement over standard operation, and it is practical to implement as no modification to the valve system of the engine is required. The weakness of this modification is that the engine is still required to operate under compressed air expansion mode, at a reduced torque output and subsequently a poor operating efficiency. For this reason, using the engine to expand the compressed air is also considered.

### 3.2.2 Using the engine to expand the compressed air

Compressed air will be used in place of conventional fuel under certain operational conditions. When these conditions are met, normal four stroke combustion processes will stop (no more fuel will be injected, and conventional valve operation will stop), and the engine will be used to expand compressed air directly. This will be done through a separate valve and pipe system connected to a receiver containing the stored compressed air, as shown in *Figure 3.1*. The conventional inlet valves would no longer operate as normal - because air will no longer be drawn into the cylinder from the atmosphere, but rather injected directly into the cylinder from a receiver as compressed air. The inlet valves would have to be closed and then disengaged during compressed air operation by modifying the way in which the camshaft actuates these

[3] The amount of energy available for later use is: $(225-94)\times 0.8$, or the energy not used after storage, multiplied by the usage efficiency.

Table 3.1: Using an external compressor to load an IC engine, and expand the compressed air to reduce the work requirement on the engine at a later stage.

| | Modified | | Unmodified | |
|---|---|---|---|---|
| **Driver requirement** | 160 J | | 160 J | |
| **Energy storage** | | | | |
| Amount of loading | 94 J | | 0 J | |
| Amount of energy stored | 225 J | | 0 J | |
| Engine work requirement | 160 + 94 J | | 160 | |
| IC engine efficiency | 0.28 | | 0.23 | |
| Energy consumed as fuel | 775 J | | 695 J | |
| **Energy usage** | | | | |
| Energy supplement from ext. compr. | 75 J | | 0 J | |
| Engine work requirement | 160 - 75 J | | 160 J | |
| IC engine efficiency | 0.15 | | 0.23 | |
| Energy consumed as fuel | 584 J | | 695 | |
| **Overall efficiency** | | $\frac{160+85+0.8\times(225-94)}{775+584}$ $= 0.26$ | | $\frac{160+160}{695+695}$ $= 0.23$ |

valves - possibly by shifting the camshaft forward so that it no longer pushed on the valve stems. Compressed air would have to be admitted through its own valve system. The conventional exhaust valves would also not be able to be used because the exhaust valve will have to operate twice as often, *Section 3.3* contains further details.

A four cylinder four stroke engine [38] is the candidate engine type for retrofitting with the compressed air modification. This means that at any point in time, two pistons will be moving towards top dead center and two pistons will be moving towards bottom dead center, as each cylinder must perform one of the four strokes (intake - downward stroke, compression - upward stroke, expansion - downward stroke, exhaust - upward stroke). This allows two cylinders to be used to expand compressed air concurrently. Air can only be expanded on a downward stroke, and four downward strokes will occur per revolution.

The essential structure of this modification is to connect a small auxiliary compressor to the

drive shaft on the engine, which will be responsible for compressing air into the receiver. When receiver pressure is sufficient, the engine will be able to enter compressed air mode (indicated by *Figure 3.1*[4]), where all four conventional strokes cease, and compressed air is allowed to enter cylinders currently at the beginning of an expansion stroke. The charging of compressed air into the receiver will also cease, as there is no longer a need to alter the torque requirement of the engine through loading.

Driver requirements (inferred from the accelerator pedal position) will not be constant, and may at times be larger than what the compressed air system can produce. For these reasons, an overall control philosophy must be defined in order to avoid some undesirable operating conditions. For instance, if the driver requirements are quite close to what the compressed air system can supply (the dotted line labelled B in *Figure 3.2*), the system will only supply the maximum torque available. If driver requirements increase even more and exceed this level (the line labeled A), then compressed air usage will stop and the engine will again run on conventional fuel. A time dead band is imposed so that if torque requirements drop suddenly, the engine will not revert back to compressed air operation unless the time dead band has expired (i.e. the engine has been operating on conventional fuel for some time). This is to prevent excessive switching of operation between the two systems.

## 3.3 Performance requirements if compressed air propels the engine

This augmentation system is intended for a typical motor vehicle as a retrofit to improve performance, and it should therefore be able to do (in part) what the engine could do under normal operation. Considering an engine that produces 70 kW at 6000 rpm, one can determine that the torque at this speed is:

$$\begin{aligned} Torque &= \frac{70 \times 10^3}{2\pi \times 100} \\ &= 111.4\ N.m \end{aligned} \tag{3.1}$$

The maximum torque produced by the engine varies with engine speed (see *Figure 3.3* for an example of a 4ZZ-FE Toyota engine), with peak torque produced typically just over halfway

[4]The external compressor is omitted from this drawing because it will not run while the engine is propelled by compressed air

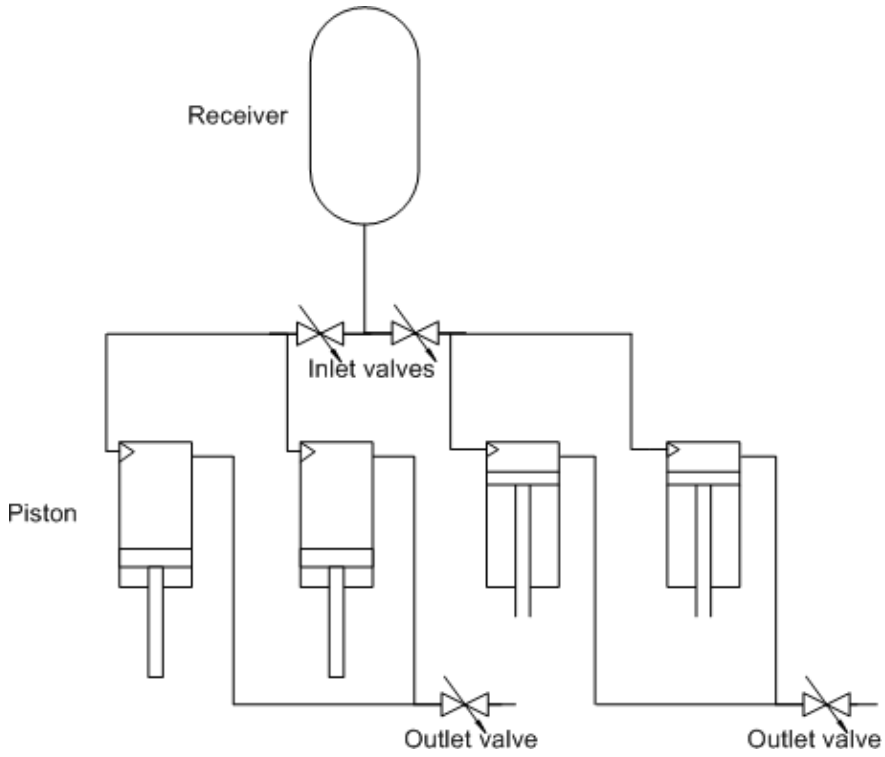



Figure 3.1: Schematic diagram of the envisaged compressed air augmentation system.

between the maximum and minimum speed of the engine. The variation with speed is not excessive; in the diagram used as an example, engine torque varies from a minimum of 100 $N.m$ to a maximum of 120 $N.m$, and for the remainder of this section it is assumed that the datum engine torque of our sample engine is 110 $N.m$. It must be noted that this value of torque is measured when the engine is completely unthrottled. The total amount of work done by the engine to produce 110 N.m of torque over one revolution is $110 \times 2\pi = 691\ J$.

$$torque = work\ per\ revolution / 2\pi \tag{3.2}$$

Bearing in mind that this is a four stroke, four cylinder engine; two expansion strokes occur for every revolution (when operating on conventional fuel), which means that 345 $J$ of work is done per expansion stroke (this is the net amount of work done). The pumping losses incurred by the other cylinders have already been included within *Figure 3.3*, where the torque is the net torque output of the engine. Under the normal four stroke internal combustion mode of operation, each cylinder performs one of the four stroke processes (either intake, compression,

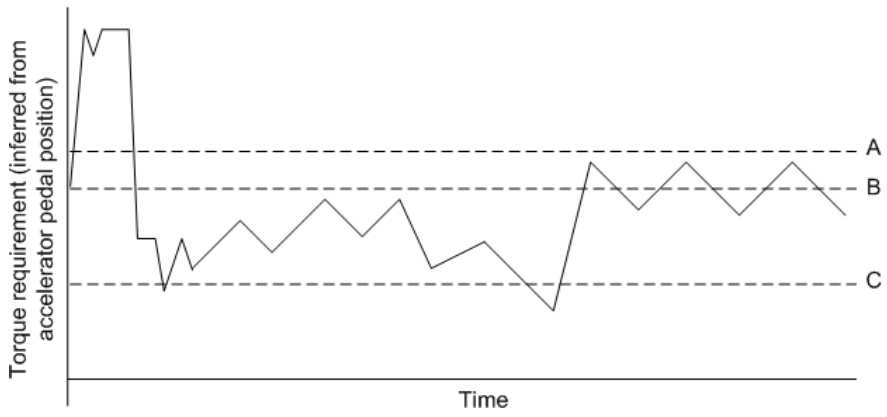



Figure 3.2: Illustration of possible torque demands made by the driver. Line A represents the torque requirement at which the engine will revert to conventional operation. Line B represents the maximum torque that the augmented system can provide. Line C represents the minimum amount of torque that the augmented system can provide.

expansion, exhaust), at any instant in time. The piston moves downward on the intake and expansion strokes, and it moves upwards on the compression and exhaust strokes. This can be used to advantage when expanding the compressed air, as two cylinders could work in parallel to produce the required amount of work. For example, if the driving requirements at the time are such that 110 $N.m$ of torque is required, each piston would have to do 345 $J$ of work per expansion stroke (if using conventional fuel). However, if using compressed air two cylinders can be combined to produce this amount of work, so each cylinder would produce 172.5 $J$ of work. The benefit of this is that lower operational pressures are required for the compressed air retrofit.

This value of work done per expansion stroke gives an indication of the kind of pressures that would be required for this engine retrofit to operate. Uncontrolled expansions must be avoided as much as possible (to ensure that the combined compressed air storage and usage efficiency be as high as possible), which means that the pressure of the air within the cylinder at the end of an expansion stroke must be sufficiently high enough to overcome the back pressure due to the exhaust pipe (say 1.5 *bar* gauge). The requirement that the air pressure in the cylinder be approximately 1.5 bar at the end of the expansion sets the maximum cylinder pressure at the beginning of the expansion. The estimation of what this pressure could be is done assuming

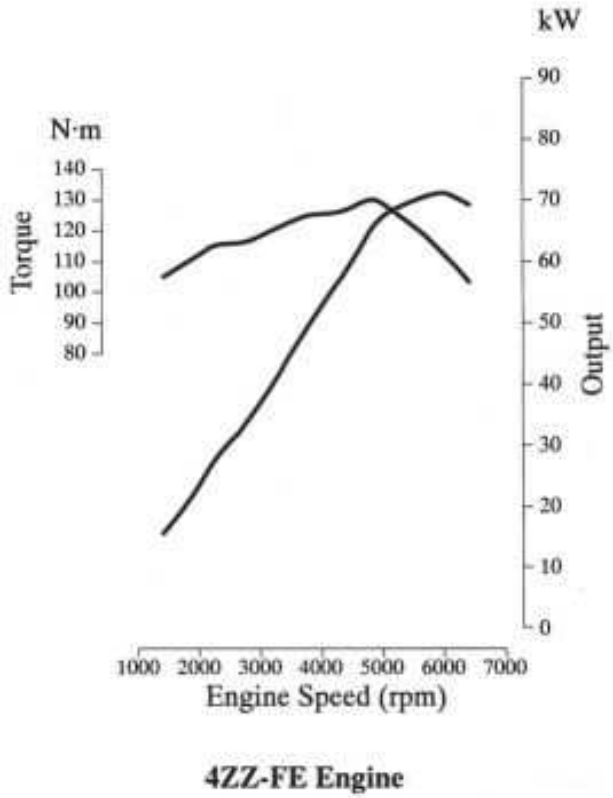
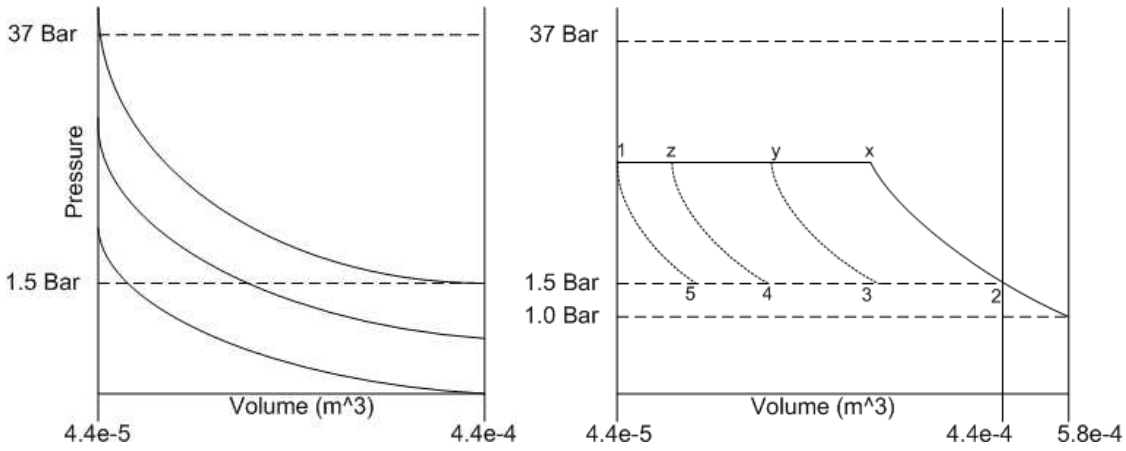



Figure 3.3: Typical power-torque-speed curve of a Toyota 4ZZ-FE engine [50].

that the compressed air is modelled as an ideal gas, and the expansion process is modelled as an isentropic expansion process:

$$\begin{aligned} \frac{p_2}{p_1} &= \left(\frac{V_1}{V_2}\right)^{\gamma} \\ p_2 &= p_1\left(\frac{V_1}{V_2}\right)^{\gamma} \\ &= p_1\left(\frac{4.407\times10^{-4}}{4.407\times10^{-5}}\right)^{1.4} \\ &= 1.5\times10^{5}\times25.11 \\ &= 37.66\ bar \end{aligned} \tag{3.3}$$

This figure is the start of the top curve in *Figure 3.4*a. The amount of work done if air is allowed to expand from this pressure to 1.5 bar can also be estimated (assuming an isentropic expansion




(a) Implication of cylinder geometry on initial cylinder pressure

(b) Proposed P-V diagram for the expansion of compressed air process):

Figure 3.4: Propulsion by compressed air: maximum cylinder pressure & proposed P-V diagram for the cylinders expanding compressed air.

$$
\begin{aligned}
work &= \frac{p_1V_1 - p_2V_2}{1-\gamma} \\
&= \frac{(1.5\times10^5)(4.407\times10^{-4}) - (37.66\times10^5)(4.407\times10^{-5})}{1-1.4} \\
&= 249.65\ J
\end{aligned} \tag{3.4a}
$$

$$
\begin{aligned}
work &= p(V_1 - V_2) \\
&= 1.01\times10^5(4.407\times10^{-5} - 4.407\times10^{-4}) \\
&= -40.05\ J
\end{aligned} \tag{3.4b}
$$

One must also take into account that the other side of the piston will be exposed to roughly atmospheric pressure[5] [51], and this will decrease the net amount of work done on the crank shaft by 40 $J$, as shown by *Equation 3.4b*. The result of the sum of *Equation 3.4a* and *Equation 3.4b* indicates the operational range of the compressed air system.

The fact that the engine (with its fixed geometry) is used to expand the compressed air poses a challenge because if air at an initial pressure less than 37 bar is expanded, the air

[5]A PCV valve system is used to regulate crank case pressure as a high crank case pressure leads to oil leakage from seals and gaskets. The pressure conscious valve (PCV) regulates the crank pressure by allowing air to flow into the inlet manifold.

pressure will always drop to some value below atmospheric pressure, which will result in an energy wastage when the exhaust valve opens as air at atmospheric pressure would rush into the cylinder. *Figure 3.4*a illustrates this point - only the curve with an initial pressure of 37 bar expands to approximately 1.5 bar. All other initial pressures will expand to some other value and cause irreversibilities. The exhaust valve could be opened when cylinder air pressure equaled atmospheric pressure in order to circumvent this wastage of energy. Another option is to lower the operational pressures of the system, but allow compressed air to flow from the receiver into the cylinder for a longer duration (see *Figure 3.4*b). The cylinder pressure and compressed air inlet duration would be carefully selected to ensure that cylinder pressures were still close to atmospheric at the end of the expansion stroke. The disadvantage of lowering receiver pressure is that the engine torque range that can be reached by the compressed air system is reduced. The advantages of lowering the receiver pressure are:

a. The pressure difference between the air in the cylinder at the beginning of the compressed air injection and the pressure in the receiver would be lower, resulting in lower energy wastage due to throttling.
b. A cheaper external compressor would be required. The external compressor would need to supply compressed air at a lower pressure, so its internal components would not need to be quite as robust.
c. Lower receiver pressure results in a lower receiver temperature, and this improves the capacity for heat transfer from the exhaust gases to occur.
d. Lower receiver pressure means that the receiver does not have to be built as strongly.

Looking at *Figure 3.4*b, the expansion processes have a period where cylinder pressure is constant with volume, and another where the cylinder pressure changes with volume. The points at which the cylinder pressure begins to decrease are the points where the valve between the receiver and the cylinder is closed (labelled x,y & z). The work done during this stroke is given by *Equation 3.5* below. The maximum and minimum work done per stroke was plotted against receiver pressure (see *Figure 3.5*), and it will be seen that the work done per stroke increases rapidly up to a point (approximately 10 *bar*), after which the curve begins to flatten off. Maximum work done per stroke corresponds to 1-x-2 on *Figure 3.4*b, and minimum work

done per stroke corresponds to 1-5-2. This minimum amount of work does not create a problem for the driver who wants a very low torque output, because the losses incurred with expanding compressed air are actually higher than this minimum amount of work. See *Section 3.4.1* following.

$$work = p_1(V_x - V_1) + \frac{p_2V_2 - p_1V_x}{1-\gamma} - 1.01 \times 10^5(V_2 - V_1) \tag{3.5}$$

Where:

$p_1$ = Receiver pressure

$V_x$ = Cylinder volume at which the inlet of compressed air stops

$V_1$ = Cylinder volume at top dead center

$p_2$ = Cylinder pressure at bottom dead center

$V_2$ = Cylinder volume at bottom dead center

$\gamma$ = Specific heat ratio

The receiver temperature is also a function of receiver pressure, and a graph of receiver temperature vs. receiver pressure has been generated (*Figure 3.6*) based on the assumption that the air can be modelled as an ideal gas, and that the compression process is isentropic (*Equation 3.6*):

$$\frac{T_f}{T_i} = \frac{p_f}{p_i}^{(\gamma-1)/\gamma} \tag{3.6}$$

Where:

$T_f$ = Final cylinder air temperature

$T_i$ = Initial cylinder air temperature

$p_f$ = Final cylinder air pressure

$p_i$ = Initial cylinder air pressure

$\gamma$ = Specific heat ratio

*Figure 3.6* shows that the relationship between receiver temperature and pressure is roughly linear, but a lower receiver pressure results in lower receiver temperature and allows for improved heat transfer between the exhaust gases and the air within the receiver. Heat transfer will take place between a heat exchanger (through which exhaust gases will flow), and the air in the receiver because the heat exchanger is located in the receiver. This heat exchanger is considered in *Section 4.2*.

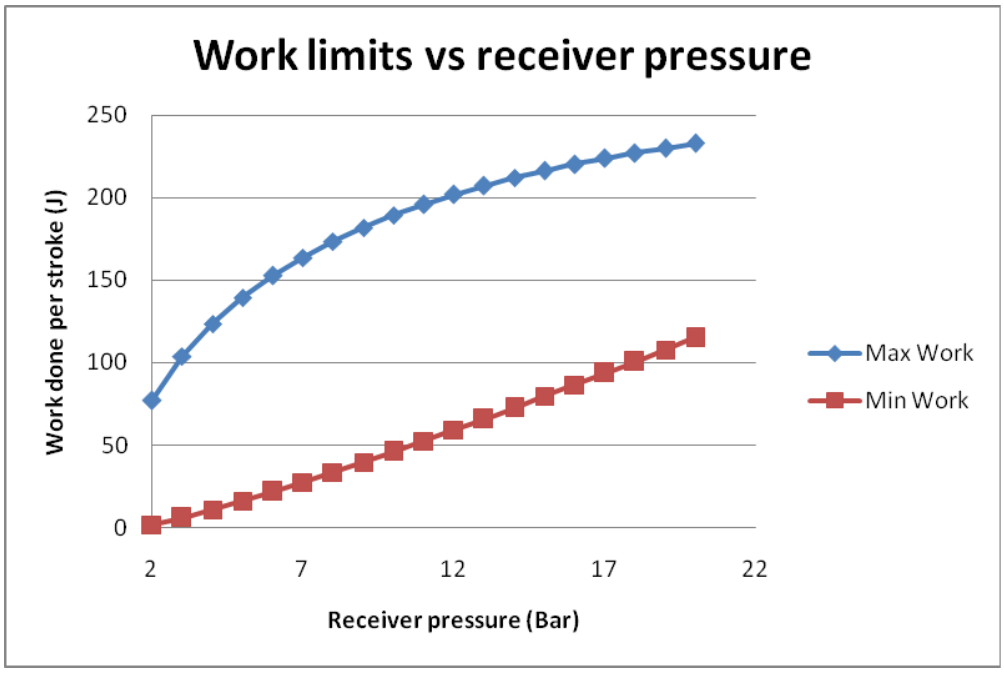



Figure 3.5: Propulsion by compressed air: variation of work done per stroke vs. receiver pressure.

### 3.4 Varying torque generation when compressed air propels the engine

A mechanism must be implemented to control how much torque is produced. Referring back to *Figure 3.4*b, there are three dotted expansion lines beginning at points x, y and z. Each of these points corresponds to a cylinder volume at which the valve between the compressed air receiver and the cylinder is closed, and the expansion process then begins. Cylinder air pressure will reach atmospheric pressure before the end of the expansion stroke, so the exhaust valve of the cylinder must be opened in order to prevent the cylinder drawing a vacuum and absorbing energy from the crank shaft unnecessarily. The point at which the inlet valve closes can be calculated from *Equation 3.7*:

$$V_x = \frac{\textit{required work per stroke} \times (1-k) + p_1V_1(1-k) - p_2V_2}{-kp_1} \tag{3.7}$$

Mass will flow out of the receiver during compressed air usage, decreasing both the pressure and temperature of the air in the receiver. The decrease in pressure will have an effect on the maximum torque that the engine can provide when being propelled by compressed air, as indicated in *Figure 3.5*.

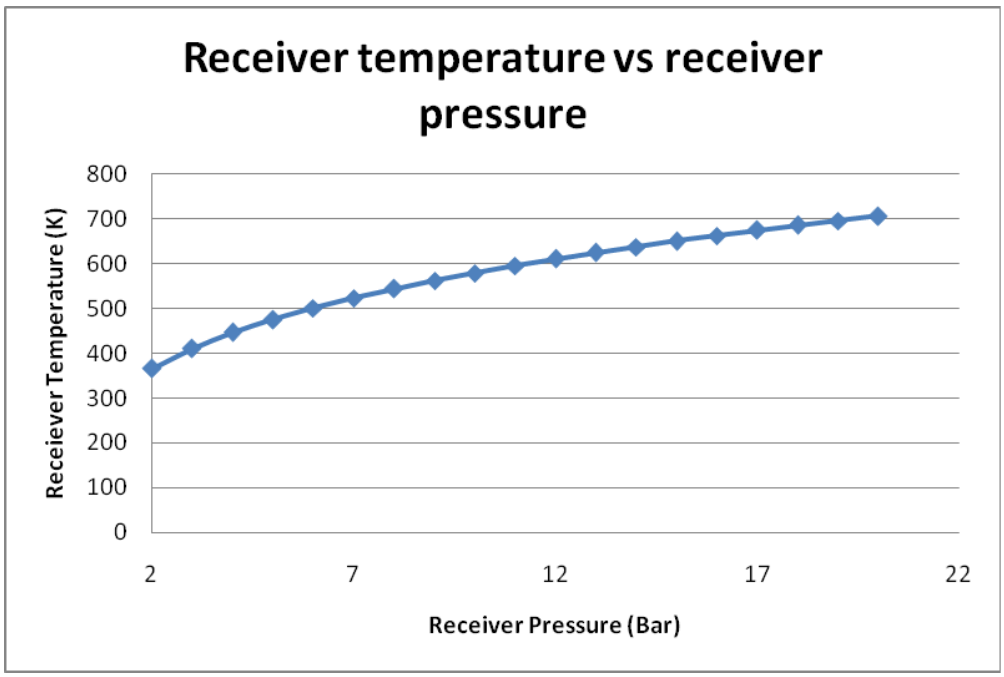



Figure 3.6: Propulsion by compressed air: variation of receiver temperature vs. receiver pressure.

### 3.4.1 Irreversibility due to inlet of compressed air into the cylinder

Energy wastage due to uncontrolled expansion will be large when air at receiver pressure is allowed to flow into the cylinder at atmospheric pressure. This loss will be minimised if the inlet pressure is reduced, thereby reducing the pressure difference across the inlet valve. The amount of irreversibility can be determined considering that the throttling across this valve is an isenthalpic process, and work lost due to throttling can be calculated from *Equation 2.28*. The compressed air has been modelled as an ideal gas, so the temperature does not change across the expansion valve [52, pg 145] i.e. the Joule-Thomson co-efficient has been assumed to be zero.

The air pressure within the cylinder will rise as the air enters the cylinder, resulting in a time varying pressure across the inlet valve. This can be calculated using the model described in *Section 2.4* (the equations of which are summarised in the equation block below), with cylinder volume fixed and heat transfer into or out of the cylinder ignored. Mass flow rate through the valve is given by *Equation 2.10*.

$$\dot{p} = \frac{R(\dot{m}T + \dot{T}m)}{V} \tag{2.5}$$

$$\dot{T} = \frac{1}{mc_v}[h_i\dot{m} - u\dot{m}] \tag{2.9}$$

$$\dot{I}r_{mx} = \dot{m}T_0C_p\left(\ln\left(\frac{T_u}{T_d}\right) - \frac{T_u - T_d}{T_u}\right) \tag{2.26}$$

$$\dot{I}r_{th} = T_0\dot{m}\left[-R\ln\left(\frac{p_u}{p_d}\right)\right] \tag{2.28}$$

Once through the valve, the air will mix with air already in the cylinder. The temperature of this air is determined by assuming that the air is modelled as an ideal gas initially at 1000 K and was expanded from a volume of 44.07 $cm^3$ to 440.7 $cm^3$, resulting in a final temperature[6] of 400 $K$. In reality this final temperature may be considerably lower (see *Section 4.2.7* - heat transfer from the exhaust gases does not occur fast enough to raise the receiver temperature to 1000 K, even though exhaust gas temperature is near this value), and therefore the irreversibility due to mixing of gases at different temperatures will be less than the amount calculated here. This calculation gives the worst case scenario.

The irreversibility due to mixing gas at different temperatures is given by *Equation 2.26*. A plot has been generated of work lost due to irreversibility for various values of receiver pressure, and is shown in *Figure 3.7*. If a cylinder pressure of 12 *bar* is selected (see *Section 4.3.4* for details), 202 $J$ of work would be done per expansion stroke with no irreversibilities present, 9.3 $J$ of energy will be wasted due to the irreversibilities of throttling and mixing gases at different temperatures; 25 $J$ of energy will be lost due to friction (calculated according to the model described in *Section 2.4.1*, where maximum cylinder pressure is specified at 12 bar, and engine speed is 1000 RPM), 19.1 J will be lost because air is expanded to 1.5 bar and not to atmospheric pressure, and 108.6 $J$ of work is done during this stroke - resulting in a stroke

[6] $\frac{T_2}{T_1} = \left(\frac{V_1}{V_2}\right)^{1-1.4} = 1000 \times 10^{-0.4} = 398\ K$

efficiency of 53.7%.

$$
\begin{aligned}
work &= work\ done\ at\ particular\ receiver\ pressure \\
&\quad - work\ done\ by\ piston\ against\ the\ atmosphere \\
&\quad - work\ lost\ due\ to\ friction \\
&\quad - work\ lost\ due\ to\ throttling \\
&\quad - work\ lost\ due\ to\ uncontrolled\ expansion \\
&= 202 - 40 - 25 - 9.3 - 19.1 \\
&= 108.6
\end{aligned} \tag{3.8}
$$

$$
\begin{aligned}
\eta &= \frac{108.6}{202} \\
&= 53.7\% \qquad (3.9)
\end{aligned}
$$

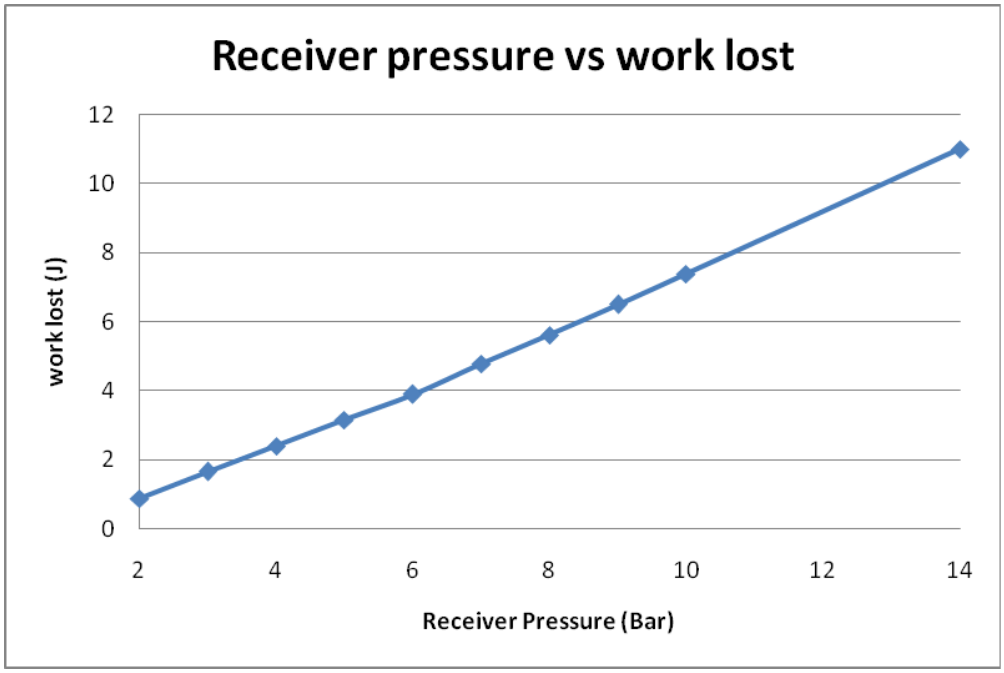



Figure 3.7: Propulsion by compressed air: variation of useful work lost due to irreversibility (specifically irreversibility due to throttling and the mixing of air at different temperatures) vs. receiver pressure.

## 3.5 Using compressed air in conjunction with fuel

This section gives an overview of the investigation into using compressed air in conjunction with conventional fuel. Compressed air could be injected directly into the cylinder at some point during a combustion cycle, in much the same way as Simington has done [12]. The question of when the compressed air should be injected now arises; it can be done prior to, during, or after the combustion process. If the compressed air injection is done prior to ignition, the ensuing combustion will be very lean (i.e. the air-fuel ratio will be greater than 1). This has both positive and negative ramifications: combustion efficiency is improved and heat transfer loss is decreased, but flame speed is reduced [53] and nitrogen oxide (NO) emissions increase [54]. Fuel-air mixture of a sufficient richness must surround the spark plug to ensure ignition, which may place limitations on injecting the compressed air prior to combustion, as such an injection may make the fuel air mixture too lean for ignition. This approach is possible, but the added control complexity eliminates this option as a potentially feasible retrofit candidate. It may be possible to inject compressed air into the cylinder during the combustion, although the complex relationship sure to exist between the compressed air wave and the flame front would best be investigated experimentally as opposed to mathematically, as the differential equation model developed for the analysis of cylinder states may not provide an accurate description of the process[7]. Additionally, combustion must not be arrested by the injection of compressed air, although this is unlikely as the auto ignition temperature of petrol is $246^{\circ}C$ [55], and the temperature of the air within the cylinder (after compressed air injection) is predicted to be still greater than the auto ignition temperature of the mixture, as shown by *Figure 3.8*, which was generated using the Otto cycle model from *Section 2.5* but with compressed air allowed to enter the cylinder 0.23 rad after combustion had been initiated. The remaining alternative is to inject the compressed air into the cylinder after or during the final stages of combustion so as to supplement the amount of fuel injected into the cylinder per cycle.

Compressed air injection will also reduce the exhaust gas temperatures which may decrease the potential for efficiency improvements through regeneration. Exhaust gas pressure will be

[7] A finite element or multidimensional burn model approach is probably required for meaningful analysis here. Combustion is modelled with a Weibe function in this work, which is empirical in nature - based on measurements of an actual combustion process [33, pg 145].

higher than in standard operation, causing more irreversibility due to uncontrolled expansion during the exhaust stroke. This can be seen in *Figure 3.9* where final cylinder gas temperatures of the system with compressed air injection are lower than those of the standard cycle, and cylinder gas pressures are higher than those of the standard cycle. Irreversibility due to mixing of gases at different temperatures would increase.

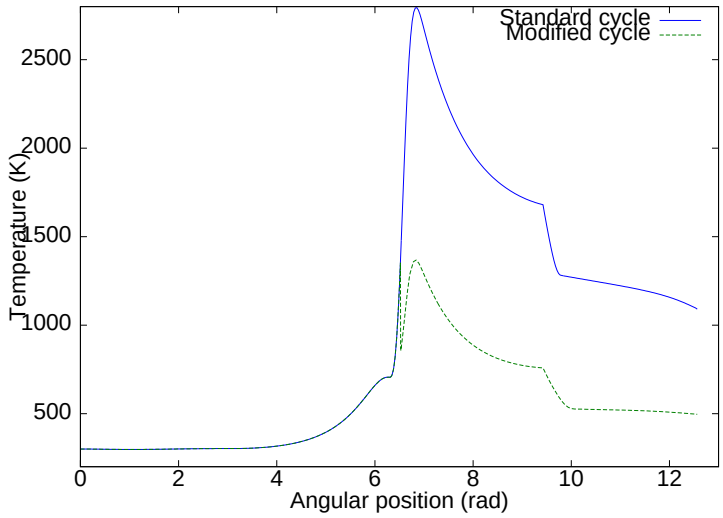
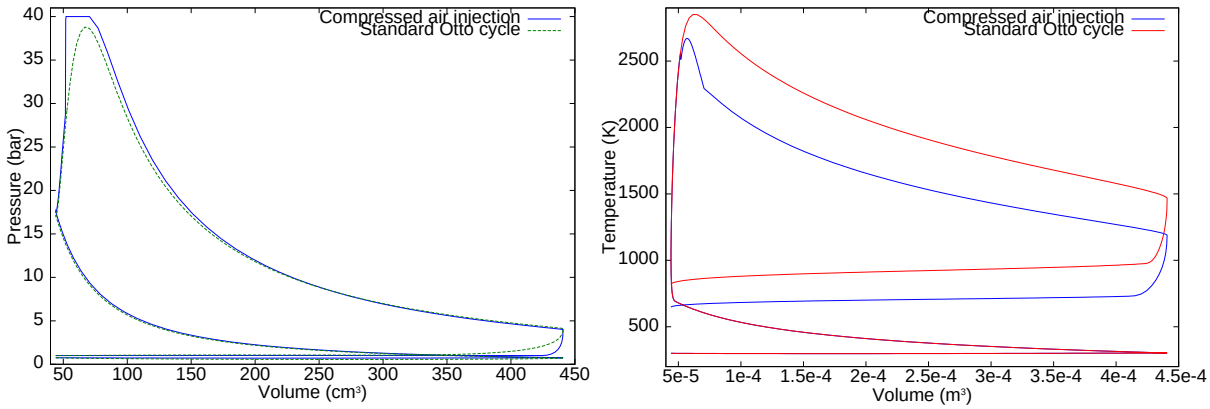



Figure 3.8: *The effect on cylinder gas temperature with compressed air injection. Cylinder gas temperature drops when compressed air is injected, but not to a level lower than the auto ignition temperature of the fuel air mixture.*

The mixture of oxygen rich air with hot exhaust gases may also have an impact on the amount of emissions produced by the engine, as unreacted CO may then react with the $O_2$ to form $CO_2$. This would need to be verified with an emissions analyser. Additionally, injecting compressed air into the cylinder post-combustion will increase the amount of free oxygen present in the exhaust gases, resulting in less NO gases being reduced into $N_2$ and $O_2$ by a typical gasoline type catalytic converter [56]. A NO absorber (commonly used for diesel engine emission control due to the characteristically lean operation of such engines) may be required in order to meet emission regulations.

Using the compressed air in conjunction with conventional fuel was investigated by performing simulations in which the differential equation models of the Otto cycle derived in the previous chapter were modified, so that compressed air was injected into the cylinder towards




(a) P-V diagram

(b) T-V diagram

Figure 3.9: *P-V and T-V diagrams for a standard Otto cycle and an Otto cycle with compressed air injection. The injection pressure and temperature are* 40 *bar and* 600 *K respectively, and the injection duration is* $\pi/15$ *rad. The model used to analyse the compressed air system is presented in Section 2.5.*

the end of the combustion process and used to generate *Figure 3.8* and *Figure 3.9*. The results of these simulations show an improvement in operational efficiency over a standard cycle, but the receiver pressures required were very large (simulations show a range from 40 *bar* - 75 *bar*, depending on the current load requirement of the engine - for the required amount of compressed air to be forced into the cylinder in the time available), and so a very powerful external compressor would be required to generate the required pressures. An additional negative factor was that the differential equation models were not comprehensive enough to simulate the interaction between combustion flame fronts and the compressed air - thereby affecting the combustion process without fully simulating the effects thereof. So this is definitely not recommended as a retrofit option, but simulations of compressed air injection into the cylinder were done, and the results are presented in *Table 3.2* - where the amount of compressed air injected during the combustion process is varied for a particular throttle setting (in this case yielding an inlet manifold pressure of 0.55 *bar*). The engine is still loaded with an external compressor which supplies air to the receiver. Air is compressed adiabatically assuming an isentropic efficiency of 0.80, resulting in a work input per kg of compressed air of 690 kJ/kg.

Note - air temperature if compressed isentropically from atmospheric conditions to 40 bar is 859 K.

$$\begin{aligned} compression\ work &= h(859) - h(300) \\ &= (887.23 - 300.19)/0.80 \\ &= 690.6\ kJ/kg \end{aligned} \tag{3.10}$$

The overall engine efficiency must be found iteratively as the energy source of the external air compressor is the engine itself; the overall efficiency is used to determine the equivalent fuel cost (input heat cost) of compressing a certain quantity of air. A sample efficiency calculation is shown in *Equation 3.11* below, on the bases of 80% of the work input to the compressor being used to create the pressure rise. The amount of energy added to the system as compressed air is determined by multiplying the mass of air injected by the work input of the compressed air (*Equation 3.10* above).

$$\begin{aligned} \eta_{engine} &= \frac{work\ output}{energy\ input} \\ &= \frac{work\ output\ to\ drive\ shaft + \eta_c(work\ extracted\ by\ compressor)}{heat\ input + air\ energy\ input/\eta_{engine}} \end{aligned} \tag{3.11}$$

For the calculation below, the value are the final ones obtained by iteration, causing both sides of the equation to balance.

$$\begin{aligned} air\ energy\ input &= 1.5 \times 10^{-4} \times 690 \times 10^3 \\ &= 103J \\ \eta &= \frac{(269 - 183) + 0.8 \times 183}{746 + 103/0.1734} \\ &= 17.34\% \end{aligned} \tag{3.12}$$

As seen from *Table 3.2*, injecting compressed air into the cylinder directly results in a very limited efficiency advantage for the torque output range which will be useful to the driver. The results are good for a very low output range (less than 50 J per stroke) but this is not very useful to the driver. This is a complex modification with high compressed air pressures, and will not be considered as a candidate retrofit option for this project.

Table 3.2: *Simulation summary - compressed air injected into the cylinder during combustion. The work input of compressing air from atmospheric conditions to receiver pressure is* 690 $kJ/kg$. *The engine is loaded by the amount of* 183 $J$ *per stroke to produce compressed air at* 40 $bar$. *Net heat input is* 746.4 $J$. *This table was generated using the modified dynamic Otto cycle model.*

| *Air injection duration (rad)* | $\pi/12.5$ | $\pi/15$ | $\pi/17.5$ | $\pi/20$ | $\pi/25$ | $\pi/30$ |
|---|---|---|---|---|---|---|
| Irreversibility due to : | | | | | | |
| *Gas transfer (exhaust)(J)* | 153.6 | 147.56 | 144.24 | 142.18 | 139.86 | 131.5 |
| *Heat transfer (J)* | 43.8 | 43.89 | 44.32 | 44.69 | 45.25 | 45.0 |
| *Throttling (J)* | 21.27 | 16.7 | 14.14 | 12.58 | 10.86 | 9.3 |
| *Mixing (J)* | 34.48 | 25.8 | 19.76 | 15.41 | 9.94 | 7.6 |
| *Combustion (J)* | 101.4 | 101.4 | 101.4 | 101.4 | 101.4 | 101.4 |
| *Gross work done (J)* | 304.0 | 269.8 | 247.6 | 232.4 | 214 | 203.0 |
| *Net work done (J)* | 121 | 86.8 | 64.6 | 49.4 | 31 | 20 |
| *Injected air mass (kg* $\times 10^4$*)* | 2.1 | 1.5 | 1.1 | 0.82 | 0.51 | 0.4 |
| *Overall efficiency (%)* | 16.72 | 17.34 | 18.69 | 19.0 | 19.32 | 18.7 |
| *Unmodified engine efficiency (%)* | 19.6 | 15.8 | 12.92 | 10.6 | 7.3 | 5 |

# 4 Enhanced compressed air system with heat recovery from exhaust gases

## 4.1 Overview

An external reciprocating compressor will be used to store compressed air into a receiver, because the pressure ratio of the compressor will vary with the state of the receiver, and therefore the point at which the outlet valve must open will change. This can be overcome by using the type of reed valve commonly found in small refrigeration compressors. The reed valve opens automatically once the pressure within the cylinder is greater than the pressure in the receiver [57, pg 141]. The engine drive shaft and compressor must also be able to be disconnected (through an electrical clutch mechanism similar to those used for car air conditioners) when driver torque requirements are high and loading is not needed. The throttling of the engine would also have to be automatically controlled such that the engine is automatically unthrottled when it is loaded with the external compressor. *Figure 4.1* shows a schematic diagram of the system.

The efficiency of compressed air usage is low (53.7% as shown in the previous chapter), and the use of heat from the exhaust gas is investigated as a way of improving the overall process efficiency. The exhaust gases present a source of ”free” energy in the sense that under normal conditions exhaust gases are not used by the engine (if considering a normally aspirated engine, as in this research report). It is envisaged that heat from the exhaust gases would be transferred into the receiver, thereby increasing the temperature of the air therein, and ultimately the useful work output of the system. As an illustration, consider heat transfer to an ideal gas stored in a receiver (of constant volume) initially at 9 bar and 562 K, such that the final temperature of the receiver is 800 K:

$$\begin{aligned} p_2 &= p_1 \times \frac{T_2}{T_1} \\ &= 9 \times \frac{800}{562} \\ &= 12.8\ bar \end{aligned} \tag{4.1}$$

Assuming a constant pressure expansion from the receiver into the cylinder:

$$\begin{aligned} work &= p(V_1 - V_2) \\ work_1 &= 9 \times 10^5 (4.407 \times 10^{-5} - 4.407 \times 10^{-4}) \quad (without\ heat\ recovery) \\ &= -356.3\ J \end{aligned} \tag{4.2}$$

$$\begin{aligned} work_2 &= 12.8 \times 10^5 (4.407 \times 10^{-5} - 4.407 \times 10^{-4}) \quad (with\ heat\ recovery) \\ &= -507.6\ J \end{aligned} \tag{4.3}$$

The above illustration shows that the potential for work from the receiver is far larger because the receiver pressure is higher, so overall process efficiency can be improved using heat from the exhaust that would otherwise be wasted. The heat exchanger would be placed in the receiver to maximise the time available for heat transfer to take place.

A model was created to simulate how the system will be affected by certain system parameters. This model is created assuming that air is an ideal gas, and all compression processes are isentropic, and therefore serves to demonstrate the performance of the system. The model does allow for the effects on process efficiency of a number of system parameters to be observed, including:

- Exhaust gas temperature and mass flow rate
- Heat exchanger area
- External compressor size
- Receiver size
- Gear ratio between the external compressor and the engine

This chapter describes how the model was created, how heat transfer from the exhaust gas is expected to occur, and how effectively the energy storage system mitigates the losses incurred when using compressed air to propel the engine.

### 4.1.1 Required performance improvement

An indication of the performance required by the improvement must be explored in order to specify a design of the heat exchanger and external compressor. The modification will have a certain outlay cost but would yield an efficiency improvement. It is assumed that the vehicle will

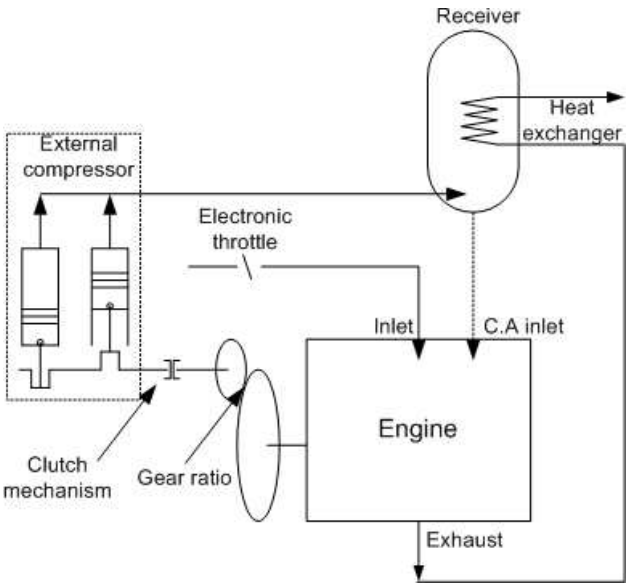



Figure 4.1: Energy storage schematic overview.

be driven between 1500 - 2500 km per month, the fuel price is taken to be *R 10*/*l* and the fuel consumption of the unmodified engine is taken to be 10*l*/100km. This data is used to calculate how much money would be saved over a year for a range of monthly driving distances, and this has been summarised in *Figure 4.2*. The feasibility of this modification ultimately depends on the cost of the retrofit and the envisaged life span of the vehicle, but for the purposes of this investigation it is assumed that an efficiency improvement of 10% is required for economic feasibility.

## 4.2 Heat exchange from the exhaust gases to the compressed air

### 4.2.1 Overview

Heat from the exhaust gases will be used to make up for the irreversibilities incurred when expanding the compressed air, however this heat transfer must take place between the exhaust gases and the compressed air, and therefore requires the use of a heat exchanger. Heat must be transferred into the compressed air of the receiver to gain an increase in process efficiency (through the increase in receiver pressure). The engine has been designed with a specific back pressure from the exhaust system in mind, and the heat exchanger must not affect this excessively. Fouling will also build up along the exhaust pipe over time, which will affect the

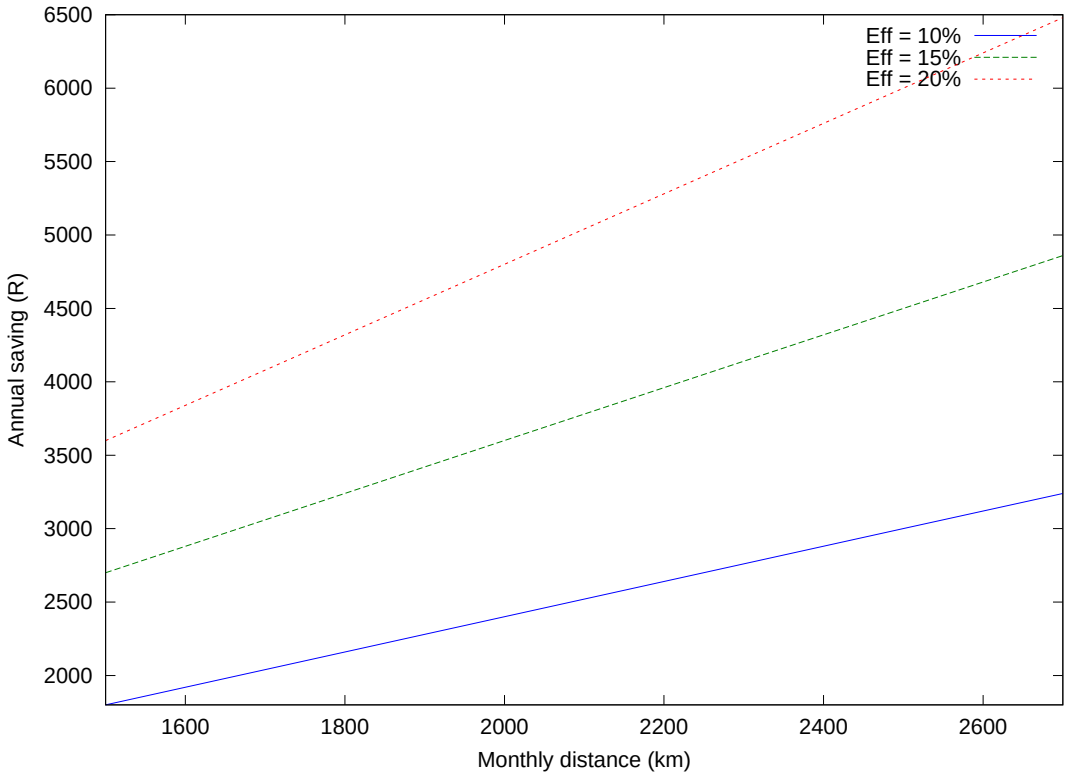



Figure 4.2: Annual saving due to efficiency improvement.

effectiveness of the heat exchanger as well.

### 4.2.2 Heat exchanger design

In deciding on which type of heat exchanger would best suit this application, a number of possible exchanger options were investigated. These include[58, pg 13]:

- Double-pipe heat exchanger - which is made up of two concentric pipes, where one fluid flows through a center pipe and the other flows through the annular space between the pipes.
- Shell and tube heat exchanger - which is made up of a bundle of tubes mounted in a cylindrical shell. One fluid flows in the tubes and the other fluid flows over the tubes, within the shell.
- Plate type heat exchanger - which consists of a number of stacked plates between which the hot fluid and cold fluid flow.

It was decided that the heat exchanger should be placed in series with the exhaust pipe and have minimum frictional resistance so as to affect the system as little as possible. For this reason it was decided that the heat exchanger be a pipe with an extended surface area (achieved by adding fins to the pipe). As stated earlier, the heat exchanger will be placed in the receiver, and the air inlet from the external compressor will be directed such that forced convection takes place over a portion of the surface of the heat exchanger. Heat transfer via natural convection will occur from the remainder of the heat exchanger surface, and this will allow heat exchange to take place even when no compressed air is flowing into the receiver. *Figure 4.3* is a conceptualisation of the heat exchanger.

The rate at which heat transfer can occur into the receiver air must also be considered. There are four components which act to inhibit heat transfer, a representation of which is shown in *Figure 4.4*. $R_1$ is the resistance to heat transfer between the exhaust gas and the heat exchanger, $R_2$ is the resistance between the heat exchanger surface and the air within the receiver with forced convection present, $R_3$ is the resistance between the heat exchanger surface and the air within the receiver with only natural convection present, and $R_4$ is the resistance due to the metal of the pipe - and is omitted from this analysis since its resistance to heat transfer is much

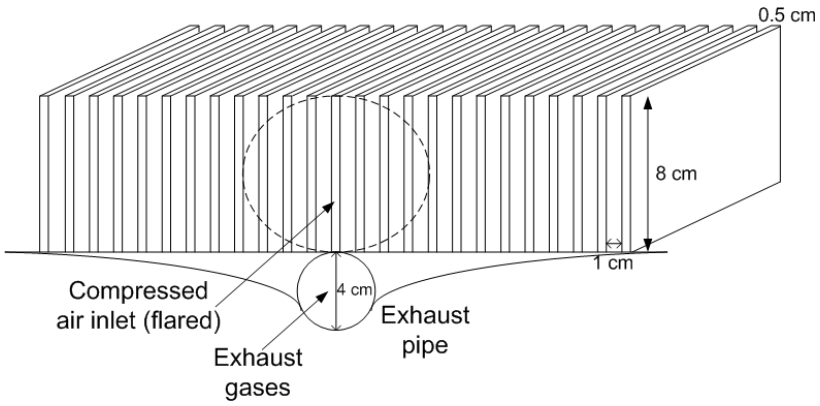



Figure 4.3: Heat exchanger - conceptual drawing

lower than the other resistances. The derivation of each of these resistances to heat transfer is presented in Sections 4.2.3 to 4.2.5 below.

Each source of resistance to heat transfer is a complex function of variables, all of which change with the operating state of the system. For example, the heat transfer coefficient between the exhaust gases and the heat exchanger increases as the engine speed increases due to increased mass flow and turbulence in the exhaust pipe; heat transfer from the surface of the heat exchanger due to forced convection decreases as the flow rate of air over the surface decreases, yet heat transfer due to both forced and natural convection increases as the pressure in the receiver increases.

Exhaust gases will have to be diverted around the heat exchanger when compressed air is used to power the engine, otherwise heat transfer from the receiver into the exhaust gases will occur, and process efficiency will decrease.

Heat transfer into the air within the receiver is dependent on the overall heat transfer coefficient ($U$), the surface area of the heat exchanger which is in contact with the air in the receiver, and the log mean temperature difference (LMTD - *Equation 4.5*) between the temperature of the exhaust gases and the temperature of the air in the receiver. The heat exchanger is mounted in the receiver, so there is no cold receiver inlet ($t_1$) and hot receiver outlet ($t_2$), rather just a receiver air temperature[8] ($t_{rec}$) when evaluating the LMTD between the exhaust gas and receiver

[8]Receiver air temperature will not be uniform, but has been assumed so to simplify modelling complexity.

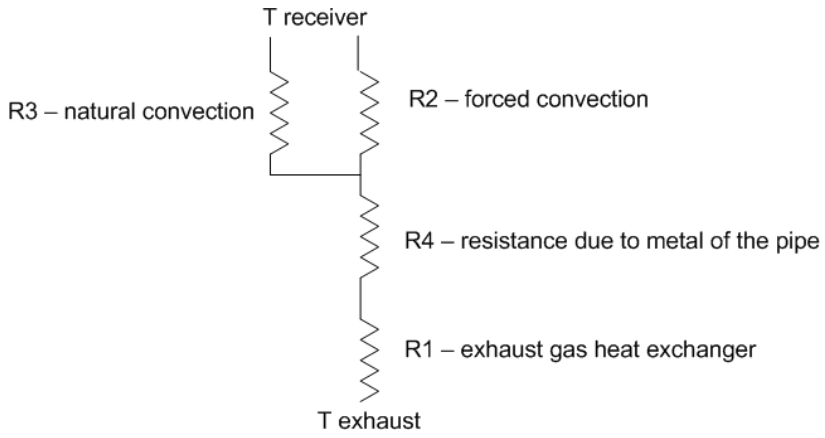



Figure 4.4: Heat transfer analogy - each resistor represents a source of resistance to heat transfer.

air.

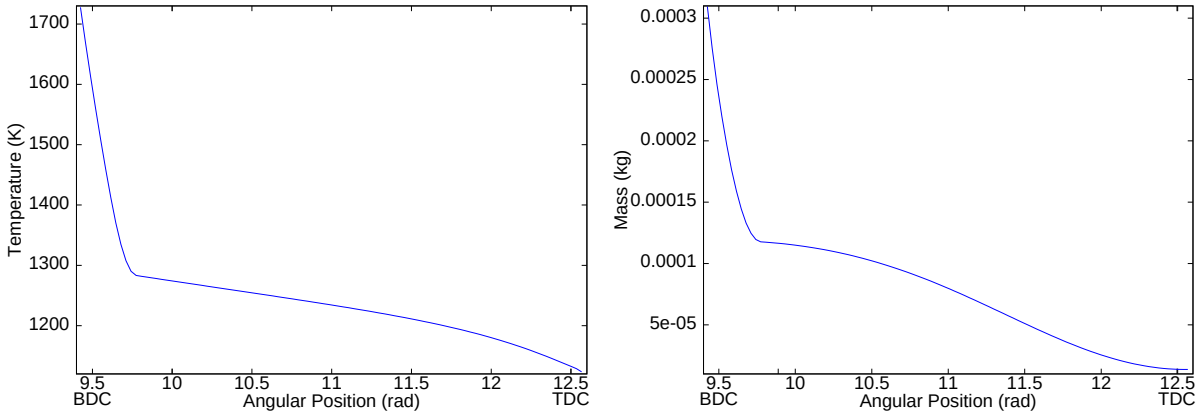
$$\dot{Q} = U \times A \times LMTD \tag{4.4}$$

Where:

$$\begin{aligned} LMTD &= \frac{(T_1 - t_2) - (T_2 - t_1)}{\ln \frac{T_1 - t_2}{T_2 - t_1}} \\ &= \frac{(T_1 - t_{rec}) - (T_2 - t_{rec})}{\ln \frac{T_1 - t_{rec}}{T_2 - t_{rec}}} \end{aligned} \tag{4.5}$$

And:

| | | |
|---|---|---|
| $A$ | = | Area of the heat exchanger in contact with the air in the receiver ($m^2$) |
| $T_1$ | = | Exhaust stream inlet temperature ($K$) |
| $T_2$ | = | Exhaust stream outlet temperature ($K$) |
| $t_1$ | = | Cold stream inlet temperature ($K$) |
| $t_2$ | = | Cold stream outlet temperature ($K$) |
| $t_{rec}$ | = | Temperature of the air in the receiver ($K$) |
| $LMTD$ | = | Log mean temperature difference ($K$) |
| $U$ | = | Overall heat transfer coefficient ($W/m^2K$) |




(a) Exhaust gas temperature

(b) Mass of the exhaust gas

Figure 4.5: *Exhaust gas temperature and cylinder air mass during an exhaust stroke.* The sharp fall in exhaust gas temperatures is due to the rapid decompression of the cylinder during the blow-down phase of the exhaust stroke, also seen by the rapid decrease in cylinder mass in 5(b). The simulation was done for the engine described in *Section 2.5*, but with an inlet pressure of 0.6 *bar* (typical driving requirement) - producing approximately 70 $N.m$ of torque (gross).

### 4.2.3 Heat transfer coefficient for turbulent flow through the exhaust pipe (R1)

The descriptions of turbulence from *Foust et al*[59, pg 152] are based on turbulence that is fully developed - occurring where there is no further change in the velocity pattern of the fluid with the progression of the fluid. Exhaust gas flow will be pulsed (due to four cylinders exhausting gas sequentially), and simulation results from *Section 2.5* (reproduced as *Figure 4.5*) show that mass flow during each stroke will also not be constant (due to the blow down and cylinder pumping phases of the exhaust stroke) but an averaged value for exhaust gas mass flow is assumed. The mass flow rate is estimated based on the current air density in the cylinder, the displacement of the cylinder, and the time it will take for the cylinder to displace all the gas inside of it (this is related to the engine speed - 1/RPM gives the period in minutes for two strokes, one ”up” stroke and one ”down” stroke).

$$\bar{\dot{m}} = \frac{\Delta m}{\Delta t}$$

*where* :

$$\begin{aligned} \Delta m &= \rho(V_i - V_f) \quad (\textit{mass of air charged per stroke}) \\ \Delta t &= \frac{30}{N} \quad (\textit{period in seconds for one stroke}) \end{aligned} \tag{4.6}$$

The model used to describe how much heat is transferred from the exhaust gas is described below. It is based on theory presented in *Foust et al* [59, pg 168] and *Incropera et al* [60, pg 354]. The convective heat transfer coefficient for turbulent flow in circular tubes is dependent on the Reynolds number and the Prandtl number (characterising the dependence of heat transfer on the fluid properties). This value of the heat transfer coefficient is taken for the case where cooling of the fluid is occurring (heating of the fluid is modelled using a different exponent for the Prandtl number).

$$\begin{aligned} \bar{h} &= 0.023\frac{\lambda}{d}(N_{Re})^{0.8}(N_{Pr})^{0.3} \\ &= 0.023\frac{\lambda}{d}\left(\frac{u_m d\rho}{\mu}\right)^{0.8}\left(\frac{c_p\mu}{\lambda}\right)^{0.3} \end{aligned} \tag{4.7}$$

Where:

- $d$ = Diameter of the exhaust pipe ($m$)
- $u_m$ = Mean free stream velocity ($m/s$)
- $\bar{h}$ = Heat transfer coefficient from exhaust gases to the heat exchanger surface ($W/m^2.K$)
- $\lambda$ = Thermal conductivity of the exhaust gas ($W/K.m$)
- $\mu$ = Viscosity of the exhaust gas ($N.s/m^2$)
- $c_p$ = Specific heat of the exhaust gas ($kJ/kg.K$)

### 4.2.4 Heat transfer coefficient for forced convection over heat exchanger area (R2)

Heat transfer due to forced convection will occur where the air is directed over the heat exchanger surface. This is not expected to occur over the entire surface - rather just a portion

of it. The size of this portion is dependent on how the compressed air inlet into the receiver is designed - one could flare this inlet more to allow the air to pass over more segments, but this in turn will decrease the velocity (because there will now be more space through which the same amount of air will flow) and lower the heat transfer coefficient due to forced convection, ultimately yielding a heat transfer coefficient comparable to that of natural convection.

*Equation 4.8* below is valid for a Reynolds number less than $5 \times 10^5$ and a Prandtl number greater than 0.6 [61]. Air is directed along the length of the heat exchanger surface, and no attempt has been made to analyse how the air flow will rise as it progresses along the length of the heat exchanger surface, as it has been assumed that the air will move much faster along the surface of the heat exchanger than it will rise from the surface of the heat exchanger.

$$\begin{aligned} N_{Re} &= \frac{L\rho u_m}{\mu} \\ N_{Pr} &= \frac{c_p \mu}{\lambda} \\ \bar{h} &= \frac{\lambda (N_{Re}{}^{\frac{1}{2}})(N_{Pr}{}^{\frac{1}{3}})}{L} \end{aligned} \tag{4.8}$$

### 4.2.5 Heat transfer coefficient for natural convection (R3)

By placing the heat exchanger inside the receiver, heat transfer will also take place when no forced convection occurs. In this case, there are many adjacent fins (much like a heat sink for a microchip), and so the standard relationships for heat transfer due to natural convection cannot be used. Heat transfer relationships due to natural convection specific to heat sinks have been used [62, 63, 64, 65].

$$\begin{aligned} h &= \frac{\lambda\, R_a\, b}{24\, L}\left(1 - e^{-\frac{35}{R_a\, b}}\right)^{0.75} \\ R_a &= \frac{\rho\, g\, \beta\, c_p\, b^3\, \Delta\, T}{\mu\, \lambda} \end{aligned} \tag{4.9}$$

Where:

| | | |
|---|---|---|
| $b$ | = | Gap between fins ($m$) |
| $R_a$ | = | Rayleigh number |
| $\beta$ | = | Volumetric coefficient of thermal expansion ($K/m^3$) |
| $\Delta T$ | = | Temperature difference from surface to air ($K$) |
| $L$ | = | Length of fin in vertical flow direction ($m$) |

### 4.2.6 Heat transfer solution algorithm

In the elementary design of the heat exchanger, the outlet temperature has to be solved for iteratively, which is done according to the following algorithm:

1. Guess a value for the outlet temperature of the exhaust gas from the heat exchanger. In this case the initial guess was made according to $T_2 = t_{rec} + \frac{T_1 - t_{rec}}{2}$, because it is known that the outlet temperature must lie somewhere between the exhaust gas inlet temperature and the receiver temperature.
2. Calculate the $UA$ and $LMTD$ and hence the amount of heat transferred.
3. A new value for the outlet enthalpy ($h_e$) and hence temperature is then calculated, based on the known mass flow rate, inlet enthalpy, and previously calculated heat transfer value

using *Equation 4.10*.

$$h_e = \frac{-\dot{Q} + h_i \dot{m}_i}{\dot{m}_i} \tag{4.10}$$

4. Steps 1. to 3. are repeated until $T_2$ converges, which is reached when the value of $T_2$ from the previous iteration differs from the value of $T_2$ by a small margin, i.e. $T_{2old} - T_2 < 0.1$

At times it was found that the solution became unstable (in which case the outlet temperatures from the heat exchanger never converge). This was found to happen when the algorithm guessed a heat exchanger outlet temperature which was less than the temperature of the air in the receiver - which is impossible. In order to prevent such instability, the process would be repeated (from step 1 above), but now step 3 was changed as follows: $T_2 = T_2 - \frac{T_2 - T_{2old}}{2}$. This has the effect of slowing down the rate of the convergence of the algorithm, and eliminated solution instability. Sample calculations for each of the three types of heat transfer have been included in Appendix C.

### 4.2.7 Performance improvement due to heat transfer

Heat transfer into the receiver has the effect of raising the temperature and pressure of this air, thereby reducing the amount of work that the external compressor is required to do in order to raise the pressure of the receiver to the maximum level. Performance of this process can be quantified by comparing the amount of work required to raise receiver pressure by a certain amount when no heat is transferred into the system (i.e. with no heat exchanger), to the case where heat is transferred into the system. This comparison results in a factor which gives an indication of how effective the system will be. For example, if no heat is transferred into the receiver 69.4 *kJ* of work would have to be done to raise the pressure of a receiver from 6 *bar* to 12 *bar*. If heat is transferred into the receiver, 58.8 *kJ* of work is required to increase the receiver pressure from 6 *bar* to 12 *bar*, and the performance of the system can be quantified as:

$$\begin{aligned} performance\ factor &= \frac{Work\ done\ without\ heat\ transfer}{Work\ done\ with\ heat\ transfer} \\ &= \frac{693.8}{588.9} \\ &= 1.18 \end{aligned} \tag{4.11}$$

To put this figure into perspective, if 100 $J$ of energy were to be released from the receiver, 84 $J$ would have actually have been expended by the external compressor, and 26 $J$ would be ”recovered energy” which would mitigate some of the other irreversibilities incurred while using the compressed air to propel the engine. For example if 100 $J$ were to be released using a compressor with an isentropic efficiency of 50 %, then the overall efficiency of the process (from energy storage to energy usage) would be:

$$\begin{aligned} \eta_c &= performance\ factor \times \eta_{usage} \\ &= 1.18 \times 0.5 \\ &= 59\% \end{aligned} \tag{4.12}$$

## 4.3 Energy storage system description

### 4.3.1 External compressor specification

As mentioned above, loading is achieved using an external compressor. Ideally the engine would be loaded by the difference between what is required by the driver and the output torque at which the engine operates most efficiently. This external compressor has to fit inside the engine bay so that it can be driven off the engine drive shaft, and so space limitations exist. The aim was to specify a compressor roughly similar in size to a car air conditioning system compressor, or alternator - so an estimate for a practical dimension was taken to be approximately 10-15 cm long, 10-15 cm high, and 5-10 cm wide.

The external compressor must be designed to compress air at atmospheric pressure up to receiver pressure, at which point the valve between the receiver and external compressor will open, and compressed air will flow into the receiver. The cylinder volume at the end of the compression stroke will be approximately zero, and at this point an inlet valve will open and air at atmospheric pressure will be drawn in. An example of such a process is shown in *Figure 4.6*, and the work required by this process is given by *Equation 4.13*.

$$\begin{aligned} V_b &= V_i / \left(\frac{p_{rec}}{p_{in}}\right)^{1/\gamma} \\ work &= p_{rec}(V_f - V_b) + \frac{p_{rec}V_b - p_{in}V_i}{1-\gamma} \end{aligned} \tag{4.13}$$

The initial compressor volume can be calculated from *Equation 4.14*.

$$V_i = (\tau \times \pi)/(P_{rec}(-1/X) + (P_{rec}/X - P_{in})/(1-\gamma)) \tag{4.14}$$

Where:

$$X = \left(\frac{P_{rec}}{P_{in}}\right)^{\frac{1}{\gamma}}$$

Using:

$\gamma$ = Specific heat ratio

$P_{rec}$ = Receiver pressure

$P_{in}$ = Inlet pressure

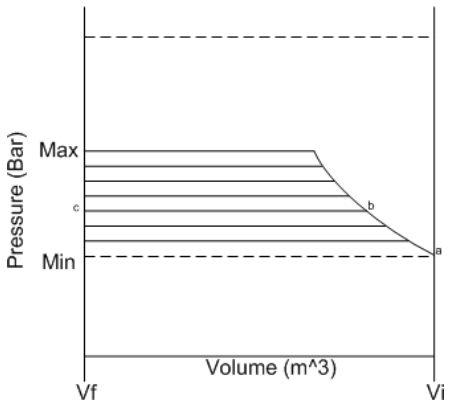



Figure 4.6: External air compressor P-V diagram for charging receiver to various pressures.

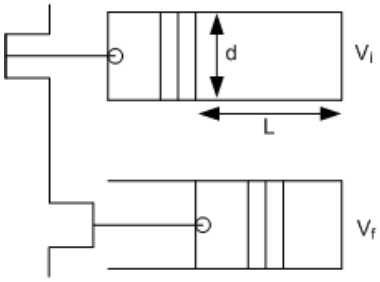



Figure 4.7: External compressor size specification.

It is also desired that the loading of the engine be as constant as possible. If using a reciprocating compressor, work input is only required for half of a revolution of the external compressor; this being on the upward stroke - the downward stroke draws fresh air into the cylinder chamber for compression. For this reason, the external compressor should comprise of two cylinders, with the pistons out of phase by 180° on the shaft driving the compressor, so that one cylinder will require some work input from the engine at all times - thereby providing a more constant source of load for the engine.

### 4.3.2 Model description

The performance of the energy storage system is a function of the amount of work done on the air in the receiver, and the amount of heat transferred into it, which are functions of many different system parameters. The objective of developing the model was to allow the effect of certain parameters on the energy storage system to be investigated. Such parameters include:

- Exhaust gas temperature and mass flow rate
- Heat exchanger area
- External compressor size
- Receiver size
- Gear ratio between the external compressor and the engine
- Engine speed

This allows estimation of the key measures of performance of the system including:

- Heat transfer into the receiver
- Exhaust gas temperatures after passing through the heat exchanger
- Total work done on the receiver
- Mass added to the receiver
- Number of compression strokes required to fill the receiver
- Final receiver temperature
- Maximum receiver pressure
- Heat exchanger area

Some of these factors are predetermined and are out of the bounds of control by the intended modification, yet their impact on system performance is still of interest. Examples of such factors are:

- Exhaust gas temperature and pressure
- Compressed air inlet temperature and pressure

Each stroke of the compressor must raise the pressure of air at atmospheric pressure to receiver pressure (denoted a-b in *Figure 4.6*), and then push it into the receiver (denoted b-c in *Figure 4.6*). The work required to perform this action is dependent on the receiver pressure, and is given by *Equation 4.15* below. The equation is idealised for the purpose of simplification, as receiver volume is not taken into account when calculating the work required per compression stroke. In reality, receiver pressure will not be constant while air is forced into it, but if the re-

ceiver volume is assumed to be much larger than the cylinder volume[9], then this rise in pressure is small, in which case *Equation 4.15* provides a good approximation for the work required.

The temperature of the air in the cylinder at point b is estimated by assuming that the gas is ideal, compression is adiabatic, and is determined by *Equation 4.16*. The volume at which the pressure of the air in the cylinder reaches the pressure of the air in the receiver is determined using *Equation 4.17*. The density of the air in the cylinder is given according to *Equation 4.18*. The amount of mass added to the receiver per compression stroke is calculated using *Equation 4.19*. The final receiver temperature after a compression stroke is calculated using *Equation 4.20*. The equations listed in the above paragraph are used by a program (Octave) to simulate compression into the receiver.

[9]If the receiver is at a pressure of 6 bar, then the amount of mass added to the receiver per stroke is: $\rho_{cpr}(Vcpr_f - Vcpr_i) = \frac{6\times10^5}{\frac{8314}{28.97}500}(2.2\times10^{-4} - 2.2\times10^{-5}) = 8.27\times10^{-4}\ kg$. If the receiver has a volume of 0.5 $m^3$ (and an initial mass of 2.09 *kg*), resulting in a new pressure of 6.016 *bar*.

$$work = p_b(V_b - V_c) + \frac{p_a V_a - p_b V_b}{1-\gamma} \tag{4.15}$$

$$T_b = T_a\left(\frac{p_b}{p_a}\right)^{\frac{\gamma-1}{\gamma}} \tag{4.16}$$

$$V_b = \frac{V_a}{\left(\frac{p_b}{p_a}\right)^{\frac{1}{\gamma}}} \tag{4.17}$$

$$\rho_b = \frac{p_b}{RT_b} \tag{4.18}$$

$$\Delta m = \rho_b(V_b - V_c) \tag{4.19}$$

$$u_f = \frac{h_{in} \times \Delta m + \Delta Q + u_i m \times rec_i}{\Delta m + mrec_i} \tag{4.20}$$

Where:

$V_a$ = Cylinder volume at bottom dead center ($m^3$)

$V_b$ = Cylinder volume at which cylinder pressure equals receiver pressure ($m^3$)

$V_c$ = Cylinder volume at top dead center ($m^3$)

$p_a$ = Atmospheric pressure ($bar$)

$p_b$ = Pressure of the air within the receiver ($bar$)

$T_a$ = Atmospheric temperature ($K$)

$T_b$ = Temperature after compression (to receiver pressure) ($K$)

$\rho_b$ = Density of the air in the cylinder once at receiver pressure ($kg/m^3$)

$\Delta m$ = Mass of air added to the receiver per compression stroke ($kg$)

$mrec_i$ = Initial mass of the receiver ($kg$)

$u_i$ = Initial specific internal energy of the receiver ($kJ/kg$)

$u_f$ = Final specific internal energy of the receiver ($kJ/kg$)

$h_{in}$ = Enthalpy at the inlet to the receiver ($kJ/kg$)

$\Delta Q$ = Heat transfer into the receiver ($kJ$)

$\gamma$ = Specific heat ratio

### 4.3.3 System parameters for the compressed air storage model

A number of the parameters which affect the performance of the modification will vary with the requirements of the driver at the time, and therefore average values over the expected range have been used for the simulation. Exhaust gas temperature is a function of a number of factors, namely throttle position and engine speed, and simulations from the engine model presented in *Section 2.5* show exhaust gas temperature to vary between $900\ K - 1300\ K$, so this is assumed to be $1100\ K$. The mass flow rate of the exhaust gas depends on the engine speed and the pressure in the cylinder when the exhaust valve opens. The model shows that this pressure ranges from between $3 - 5$ *bar* for a range of operating condition, and is assumed to be 4 *bar* for this simulation. The engine speed is selected to be 2000 *RPM*, because it is envisaged that the modification will be most feasible under low torque and engine speed requirements. Air will enter the external compressor at a pressure and temperature of 1.01 *bar* and 300 *K* respectively. A sample calculation for this model has been included in Appendix D.

### 4.3.4 Results obtained from the compressed air storage model

**4.3.4.1 Heat exchanger area parameters** Two components of the size of the heat exchanger play a dominant role: referring back to *Figure 4.4*, R1 and R2//R3 are the resistance to heat transfer between exhaust gas and the heat exchanger body, and the heat exchanger surface and the air within the receiver respectively. R1 is dependent on the length of the exhaust gas pipe through the heat exchanger, and can be increased by increasing the number of 180 degree bends through it. R2//R3 is dependent on the surface area of the heat exchanger in contact with the air in the receiver, namely the number of fins of the heat exchanger. A simulation for a range of these parameters was completed - from 1-9 passes of the exhaust pipe, and for each of these permutations, 1-50 fins. The simulation shows that the amount of heat transferred increases with increasing surface area, but does so in a diminishing manner (*Figure 4.8*). The number of passes is selected to be five, and the number of fins is selected to be forty for this reason.

The limiting factors for this design decision are the back pressure exerted by the pipe bends onto the engine, and whether the heat exchanger will fit into the receiver. The effects of the back pressure could be mitigated by removing the silencer. Typically, the back pressure in the exhaust pipe is about 1.5 *bar* - and so the back pressure due to the heat exchanger should not

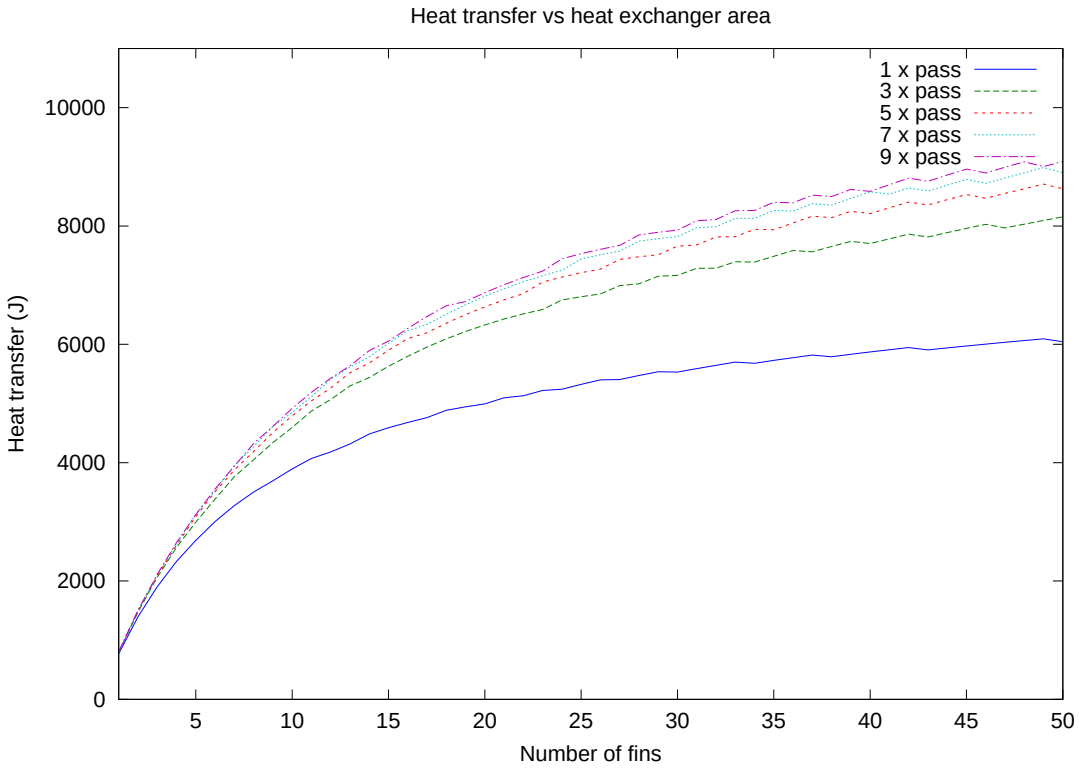



Figure 4.8: Heat transfer into the receiver while compressing from an initial pressure of 6 bar to a final pressure of 12 bar as a function of heat exchanger size.

exceed this value. Assuming that the pressure drop through the heat exchanger will be mainly dependent on the number of 180 degree bends of the exhaust pipe, the pressure drop can be evaluated as follows [66]:

$$\Delta p_b = 0.5 K \rho V^2 \tag{4.21}$$

Where:

$p_b$ = Pressure drop due to the bend ($pa$)

$K$ = Bend constant associated with the type of bend (1.6)

$\rho$ = Gas density ($kg/m^3$)

$V$ = Gas velocity ($m/s$)

Calculations show that each bend and each length of pipe will contribute about 448 pa and 168 pa towards the total pressure drop respectively. A configuration of five passes will

contribute $4 \times 448 + 5 \times 168 = 2632$ *pa* of pressure loss, which should not negatively affect the performance of the engine, and a silencer could still be used.

#### 4.3.4.2 Effects of definable parameters on system performance:

1. Increasing the gear ratio between the engine drive shaft and external compressor will allow the external compressor to load the engine more, but it will also cause the compressor to rotate faster. This results in a larger mass flow rate through the compressor and improves the heat transfer coefficient between the incoming air and heat exchanger surface. However, it also means that the air is moving much faster over the heat exchanger, and there is less time available for heat transfer to take place.
2. A larger compressor swept volume will allow the external compressor to load the engine more effectively, but it also means that the mass flow rate across the heat exchanger will be greater, resulting in less time for heat transfer to take place, as in point 1 above.
3. Increasing maximum receiver pressure will allow the engine to be loaded more effectively, but the temperature of the compressed air flowing across the heat exchanger will also be greater, and allow less opportunity for heat transfer.

A range of maximum receiver pressures were simulated for a range of external compressor swept volumes, and these results are shown in *Figure 4.9*, at a gear ratio of 1:1 between the engine and external compressor. The trend observed is that the performance factor will decrease as the swept volume and maximum receiver pressure increase, and for this reason a maximum receiver pressure of 12 bar will be selected. Note: the minimum receiver pressure is limited to 6 bar, as by *Equation 4.13*, the loading capacity at a lower pressure and for the swept volume selected in *Section 4.3.5* below would not load the engine sufficiently.

The effect of the gear ratio between the external compressor and engine was then investigated, the results of which are shown in *Figure 4.10*, with increases in the gear ratio resulting in a degradation in performance factor. Both the gear ratio between the external compressor and the engine, and the swept volume of the external compressor increase the amount of loading that the compressor can exert on the engine.

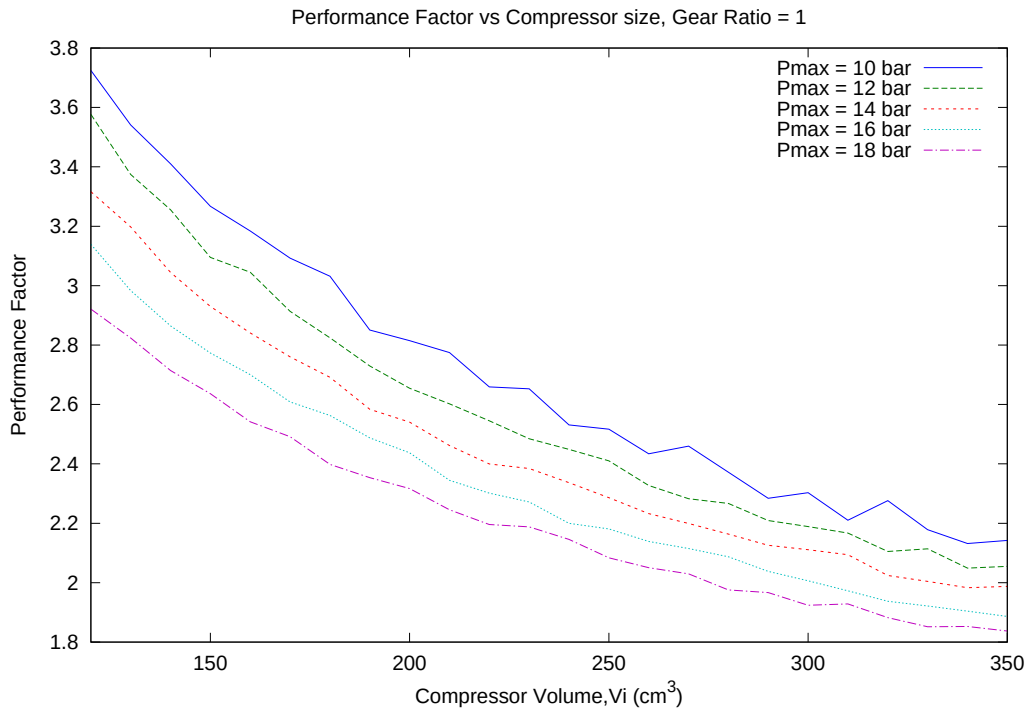



Figure 4.9: Performance factor as a function of external compression volume and maximum receiver pressure, for a gear ratio of 1:1.

**4.3.4.3 General Observations** Simulations show that the final temperature of the receiver (once it has reached maximum pressure) is less than the exhaust gas temperature, which shows that there is still potential for heat transfer to take place. Once the receiver reaches 12 *bar*, the external compressor would be disengaged, and forced convection across the heat exchanger surface would cease. The coefficient of heat transfer due to natural convection would then become the controlling resistance to heat transfer. Heat transfer due to natural convection will still occur from the heat exchanger into the air in the receiver once the external compressor has been disengaged from the engine, but this is not ideal because once the system has reached maximum pressure, the air within the receiver must be used to propel the engine so that receiver pressure will be at a minimum and the loading process can begin again. The rate of heat transfer due to natural convection will also be very low, and will contribute minimally to raising receiver pressure. Two other effects on the performance factor were noted, but are not controllable:

- The performance factor improves as the exhaust gas temperature increases, as heat transfer

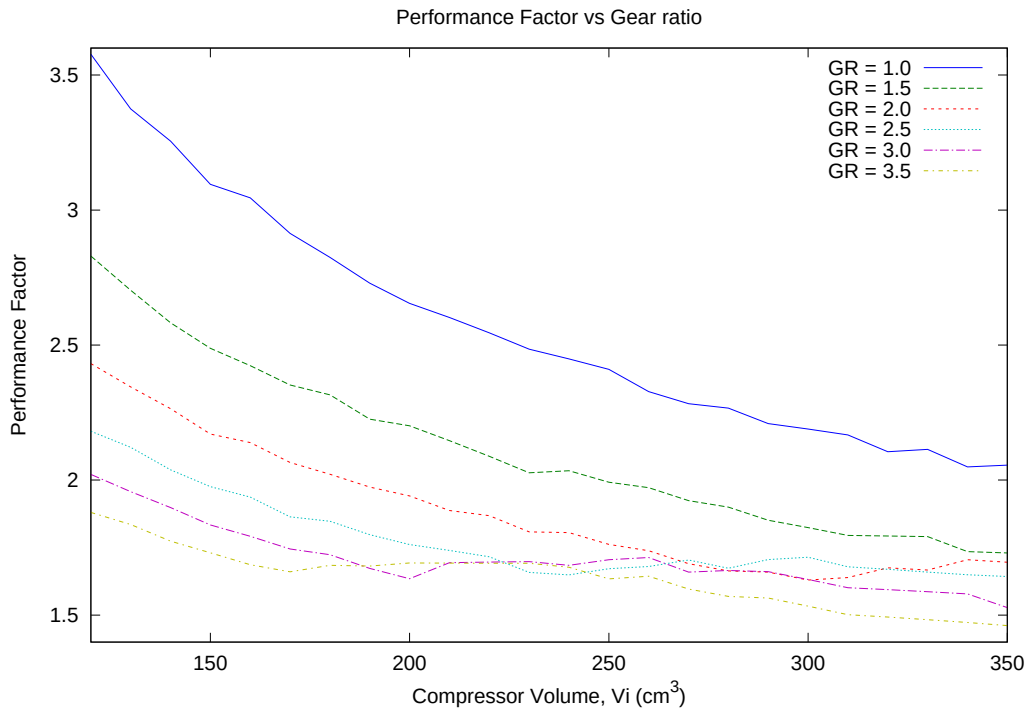



Figure 4.10: Performance factor as a function of external compression volume and gear ratio, for a reciever pressure range of between 6 and 12 bar.

increases.

- The performance factor improves as the engine speed decreases, as more time is available for heat transfer to occur (as the external compressor will be rotating slower and take longer to compress the receiver to maximum pressure).

### 4.3.5 Overall efficiency: combining performance factor and loading capacity

It has been shown in *Table 2.4* that loading the engine with an external compressor where the overall efficiency of compressed air usage and storage is 60%, is viable up to a load of 48% of full torque. This table was generated under the assumption that the engine could be loaded by the difference between the current torque requirement of the driver, and the maximum torque of the engine. This is not possible with the external compressor being considered due to loading capacity limitations, and simulations show that the performance factor is significantly degraded when high loading capacity is required. A new table was generated accordingly, where the engine is loaded by a fixed amount - chosen[10] for the purposes of this explanatory example in this case to be 60 N.m. This equates to a 188 J of work per stroke:

$$work_{per\ rev} = torque \times 2\pi \tag{4.22}$$
$$= 376\ J$$
$$work_{per\ stroke} = work_{per\ rev}/2 \tag{4.23}$$
$$= 188\ J$$

The first five columns represent the engine only - and are the same as the first five columns of *Table 2.4*. The sixth and seventh columns (at a combined compression-expansion [usage] efficiency of 70%) represent the net work requirement (per stroke) of an engine loaded by the external air compressor, and the efficiency of the engine when operating at this load point. The eighth and ninth, and tenth and eleventh columns are at a combined usage efficiencies of 60% and 50% respectively. Consider the sixth row of the table where the work requirement of the driver is 100 J. The engine is loaded by 188 J, so the net load requirement of the engine (column labelled **W+L**) is 288 J, and the engine has an efficiency of 30% when operating at this point.

If the combined efficiency of storing and using the 188 J of energy stored by the external compressor is 70%, then $0.7 \times 188 = 131.6\ J$ of energy is available to be reused to propel the

[10] Fixed in order to generate the table. In reality the amount of work absorbed by the compressor will depend on receiver pressure (will vary up to a maximum of 73 N.m in this case)

Table 4.1: Feasible conditions under which partial loading by an external compressor will improve efficiency. This table is similar to *Table 2.4* except that the engine is loaded by a fixed amount (188 J in this case), and not the difference between driver requirements and the maximum torque.

| | | $\eta_c$ | Loaded | engine | 0.7 | | 0.6 | | 0.5 | |
|---|---|---|---|---|---|---|---|---|---|---|
| **W** (J) | $\eta_W$ | **HP** (J) | **W+L** (J) | $\eta_{W+L}$ | **ER** (J) | $\eta$ | **ER** (J) | $\eta$ | **ER** (J) | $\eta$ |
| 10 | 0.03 | 792.00 | 198 | 0.25 | 131.6 | 0.18 | 112.8 | 0.16 | 94 | 0.13 |
| 20 | 0.05 | 832.00 | 208 | 0.25 | 131.6 | 0.18 | 112.8 | 0.16 | 94 | 0.14 |
| 40 | 0.09 | 844.44 | 228 | 0.27 | 131.6 | 0.20 | 112.8 | 0.18 | 94 | 0.16 |
| 60 | 0.12 | 918.52 | 248 | 0.27 | 131.6 | 0.21 | 112.8 | 0.19 | 94 | 0.17 |
| 80 | 0.15 | 957.14 | 268 | 0.28 | 131.6 | 0.22 | 112.8 | 0.20 | 94 | 0.18 |
| 100 | 0.17 | 960.00 | 288 | 0.3 | 131.6 | 0.24 | 112.8 | 0.22 | 94 | 0.20 |
| 130 | 0.20 | 1025.81 | 318 | 0.31 | 131.6 | 0.26 | 112.8 | 0.24 | 94 | 0.22 |
| 160 | 0.23 | 1087.50 | 348 | 0.32 | 131.6 | 0.27 | 112.8 | 0.25 | 94 | 0.23 |
| 190 | 0.25 | 1145.45 | 378 | 0.33 | 131.6 | 0.28 | 112.8 | 0.26 | 94 | 0.25 |
| 220 | 0.27 | 1236.36 | 408 | 0.33 | 131.6 | 0.28 | 112.8 | 0.27 | 94 | 0.25 |
| 250 | 0.28 | 1288.24 | 438 | 0.34 | 131.6 | 0.30 | 112.8 | 0.28 | 94 | 0.27 |

engine. The overall efficiency of the engine is:

$$\begin{aligned}\eta &= \frac{\textit{energy out}}{\textit{energy in}} \\ &= \frac{\textit{driver requirements} + \textit{energy available from compressed air}}{(W+L)/\eta_{W+L}} \\ &= \frac{100+131.6}{288/0.3} \\ &= 0.24 \end{aligned} \tag{4.24}$$

Comparing *Table 2.4* with *Table 4.1*, it will be seen that the efficiency improvement of the engine has been degraded, but is still more efficient than the unmodified engine. The decrease in efficiency can be explained by the fact that the engine is no longer always operating at its point of maximum efficiency, but is still operating at a better efficiency than it would have been if it were to operate unloaded. The model is now at the point where the overall efficiency of the engine is a function of the amount by which the engine is loaded, and the performance factor of the system. This is presented in *Figure 4.11*. *Table 4.1* is used as a basis of this figure, where the efficiency is plotted against the amount of loading, for a particular compressed air usage and storage efficiency (this is the performance factor $\times$ efficiency of compressed air usage). Three distinct driver load requirements are selected corresponding to 60 *J*, 100 *J*, 160 *J* per stroke, and each driver load requirement results in a family of curves. The curves marked with a "+", "-", and "*" correspond to driver requirements of 60 *J*, 100 *J*, and 160 *J* respectively. The unmodified engine efficiencies are also indicated for each family of curves; the horizontal lines marked with a "+", "o", and "*" are the unmodified engine efficiency for driver requirements of 60 *J*, 100 *J*, and 160 *J* respectively. This figure is used to show the efficiency range for a range of possible loading options and driver requirements, and allows the final specification of the system to be defined for a desired performance outcome. It was stated above that a performance requirement of 10% over an unmodified engine is required.

Referring to *Figure 4.11*, 150 *J* of loading is required to ensure a 10% efficiency improvement when driver requirements are 160 *J* (family of curves marked with "*"). This must be with a compressed air usage and storage efficiency of 1.2, which corresponds to a performance factor of 2.4 assuming a compressed air usage efficiency of 0.5. A lower performance factor will theoretically require more loading to achieve the same efficiency improvement. The required amount of loading is obtained by looking at the horizontal line marked with a "*", adding 0.1,

and reading off the required amount of loading from the curve corresponding to a compressed air efficiency of 1.2.

The swept volume and gear ratio can be specified using *Figure 4.10*. A performance factor of 2.4 will intersect the curve corresponding to a gear ratio of 1:1 and 1.5:1 at a swept volume of 250 $cm^3$ and 157 $cm^3$ respectively. Selecting the greatest amount of loading for the lowest of the two gear ratios: i.e. a swept volume of 250 $cm^3$ and a gear ratio of 1:1 which results in a loading capacity of between $83 - 116$ *J* as the receiver pressure increases from $6 - 12$ *bar* (from *Equation 4.13*). From *Figure 4.11*, the modified engine efficiency will be between 0.29 and 0.31, depending on the current amount of loading.

This does not reach the performance improvement target of 10%. However, these parameters do compare better at the other target regions. For instance, a driver requirement of 100 *J* per stroke will result in a modified engine efficiency of between 0.26 and 0.29, and at a driver requirement of 60 *J* per stroke will result in a modified engine efficiency of between 0.21 and 0.25. *Table 4.2* was generated by taking extracts from *Figure 4.11*.

Table 4.2: Extracts from the efficiency-load mapping. Note: compressed air efficiency represents the performance factor multiplied by the compressed air usage efficiency.

| **Driver requirements** | 60 J | 100 J | 160 J |
|---|---|---|---|
| Base efficiency | 0.12 | 0.17 | 0.22 |
| Required efficiency (10% improvement) | 0.22 | 0.27 | 0.32 |
| **Compressed air efficiency** | | | |
| 1.2 | 90 J | 140 J | 150 J |
| 1.1 | 98 J | 160 J | 170 J |
| 1.0 | 110 J | na | na |
| 0.9 | 127 J | na | na |
| 0.8 | 144 J | na | na |

### 4.3.6 Receiver sizing and time taken to reach final receiver pressure

The receiver will be sized as 0.06 $m^3$ (equal to the average petrol tank), and this has been done because of the space limitations of a typical motor vehicle. The amount of time required to

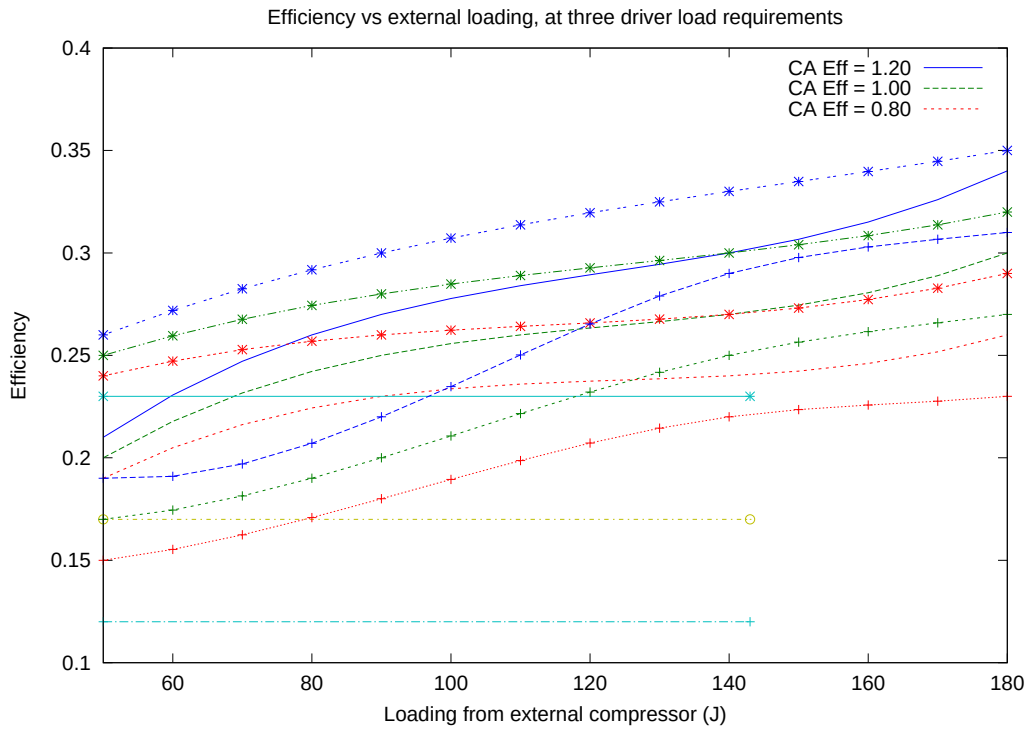



Figure 4.11: Overall system efficiency for a range of driver load requirements, for various amounts of external loading and a range of performance factors.

increase the pressure of this receiver from 6 *bar* to 12 *bar* can be calculated assuming that the engine is operating at 2000 RPM and that the gear ratio between the engine and the external compressor is 1. If 288 strokes are required to increase the pressure of the receiver from 6 *bar* to 12 *bar*, and two compression strokes occur per revolution, then $\frac{228}{2\times2000} \times 60 = 3.42\ s$ will pass before the receiver reaches 12 *bar* and compressed air can be used to propel the engine. This is clearly not a desirable time span as the system will have to rapidly move between compressed air storage and usage modes of operation. The effect of switching so rapidly between compressed air storage and compressed air usage has not been analysed, and is left for future work. Increasing the receiver volume to 0.5 $m^3$ will result in a 28.5 *s* compressed air storage time period, but this size of the receiver is not practical to be installed as a retrofit. Decreasing the swept volume of the compressor to 150 $cm^3$ does not significantly lengthen the charging time of the receiver, and reduces the loading capacity. Increasing the maximum receiver pressure also does not significantly increase the charging time, and reduces the performance factor

of the system. Receiver sizing has proved a major weakness of this retrofit.

## 4.4 Conclusion

In the above sections it has been shown that the concept of energy storage and reuse through compressed air can work, and has significant advantages when combined with heat transfer from some source of ”waste” heat energy. It is also subject to significant constraints, in that the way in which the compressed air is used can seriously degrade the feasibility of the energy storage and reuse system - as seen when using the internal combustion engine to expand the compressed air. The internal combustion engine is not designed to expand compressed air at 12 bar (for example) to atmospheric pressure - it has been designed to expand gases at much higher temperatures and pressures, and has been built accordingly.

Target efficiencies for two of the three investigated regions of operation have been reached with the proposed design. There is still room for improvement of with regard to heat transfer, as final receiver temperature is less than exhaust temperature when the receiver has reached maximum pressure.

# 5 Conclusions and recommendation

The intended mandate for this project is to improve the overall operating efficiency of a spark ignition internal combustion engine, by loading the engine with an energy storage device when it is operating at an efficiency lower than optimum. The engine tends to operate more efficiently when unthrottled, so such loading is used to allow the engine to operate with less throttling. The stored energy is later reused to propel the engine. The loading process could be external or internal to the engine, where cylinders within the engine are used to compress air into a receiver. This loading mechanism was discarded as a potential application option due to the associated impracticalities. An external loading mechanism (external compressor) was used accordingly, but was subject to the space limitations of the engine bay, and the engine could not be loaded by the full difference between driver requirements and the torque produced when operating at the point of optimum efficiency, so the full efficiency benefit of this modification was not realisable.

The engine was dynamically modelled (on a differential basis), and this engine model was used to create an efficiency mapping (presented as a table) which would indicate whether loading an engine was feasible based on the combined efficiency of the energy storage and reuse processes. This dynamic model also formed the basis for the analysis of how efficiently compressed air could be used to propel the engine, which was fairly low (approximately 53%). The operational parameters of the system were also examined and specified to achieve feasible operating pressures for the system, these being between 6 and 12 bar. An excessively low receiver pressure is undesirable because little useful torque can be produced by the engine, and an excessively high receiver pressure is undesirable because a multistage external compressor would be required. The idea of using compressed air in conjunction with the combustion process is also presented, but was not pursued further because an external compressor capable of producing very high pressures was required.

The use of heat transfer from the exhaust gases to improve process efficiency was also investigated, and is actually required to make this compressed air augmentation system feasible. The heat transfer process can still be improved, because the final temperature of the air within the receiver once the final pressure (pressure at which the compressed air storage process will cease, and the compressed air usage process will begin) is reached, is still less than the exhaust gas temperatures. The receiver size has been limited to $0.06m^3$ due to space limitations within

the vehicle, which makes for impracticably short compressed air loading and usage cycle. The compressed air augmentation system has been shown to be feasible, but the constraints imposed by applying this technology to an existing motor vehicle are numerous.

## 5.1 Future work

The idea of using compressed air to propel the engine under transient conditions could be explored, to determine whether compressed air could be used more effectively for acceleration than conventional fuel. The effect of switching frequently between loading the engine with an external compressor and using compressed air to propel the engine has not been addressed and is left for future work. The idea of disengaging the compressor from the engine at some intermediate pressure, so that heat transfer to the compressed air is allowed to continue before compressed air is used to propel the engine, could also be explored.

Yet another topic for future work includes applying the compressed air energy storage and reuse mechanism elsewhere, such as a peak load generator system at a power station or industrial plant with waste heat generation. Base load would be used to store compressed air into a receiver, and this compressed air would be later expanded when peak demand was required. Heat which would normally be expelled to the atmosphere via the cooling towers etc. could be used to improve the system performance - in the same way as the exhaust gases are used when applying the system to an internal combustion engine. The sizes of both the heat exchanger and the receiver would no longer be design constraints, and the way in which the compressed air is expanded could also be optimised for the application so that the usage efficiency is higher, because the constraint of having to use an existing internal combustion engine would be removed (one would design a compressed air expander specifically).

# References


[1] M. S. Ashhab, A. G. Stefanopoulou, J. A. Cook, and M. B. Levin. "Control oriented model for camless intake process - part I." *Mechanical engineering department, University of California in conjunction with the Ford Motor Company*.

[2] T. Miyake and H. Okada. "An Electrically Operated EGR Valve that Reduces Automotive Emissions." September 1999. `global.mitsubishielectric.com/pdf/advance/vol87/87tr6.pdf`.

[3] M. Bassett. "Investigation of Technologies to Improve Drive-cycle Fuel Economy." *Lotus Engineering*. `www.lesoft.co.uk/files/Hyb_Veh_2005.pdf`.

[4] H. stuff works. "Toyota Prius." `http://auto.howstuffworks.com/hybrid-car7.htm`. Last accessed: 14/02/09.

[5] R. Pfiffner, L. Guzzella, and C. H. Onder. "Fuel-optimal control of CVT powertrains." *Science Direct - Control Engineering Practice 11 (2003) 329336*, October 2001.

[6] C. F. Taylor. *The Internal Combustion Engine in Theory and Practice*. John Wiley and Sons, New York, London, 1960.

[7] OTA-E-504. *Improving automobile fuel economy: new standards, new approaches*. 1991. Http://books.google.com/book.

[8] M. W. Coney, C. Linnemann, and H. S. Abdallah. "A thermodynamic analysis of a novel high efficiency internal combustion engine - the isoengine." *Science Direct - Energy 29 (2004) 25852600*, 2004.

[9] Y. Takagi. "A New Era In Spark-Ignition Engines Featuring High-Pressure Direct Injection." *Twenty-Seventh Symposium (International) on Combustion/The Combustion Institute, 1998/pp. 20552068*, 1998.

[10] "The Beaumont compressed air engine." *The London Times*, Aug. 1880.

[11] J. Broderick. *Combined Internal Combustion and Compressed Air Engine*. United States Patent Office: Patent number 1,013,528, January 1912.

[12] G. Simington. *Air drive adaptor*. United States Patent Office: Patent number 3,885,387, June 1973.

[13] H. C. Stricklin. *Converting an internal combustion engine into a single acting engine driven by steam or compressed air*. United States Patent Office: Patent number 4,102,130, April 1976.

[14] K. Miller and W. Froloff. *Air-hybrid and utility engine*. United States Patent Office: Patent number 7,177,751, February 2007.

[15] "MDI - the air car." `http://www.theaircar.com/howitworks.html`. Last accessed 24/02/11.

[16] "MDI - Comparative analysis summary. Compressed air mono, compressed air dual, all electric, hybrids, and combustion engines." `www.mdi.lu`. Last accessed 24/10/11.

[17] "Cargine - Engineering AB." `http://www.cargine.com/ExhaustHeatRecycling.htm`. Last accessed 24/02/11.

[18] "Encyclopedia Britannica Student Edition." http://student.britannica.com/elementary/art-89315/An-internal-combustion-engine-goes-through-four-strokes-intake-compression. Last accessed 22/04/09.

[19] M. J. Moran and H. N. Shapiro. *Funtamentals of Engineering Thermodynamics*. John Wiley and Sons, 5th ed., 2006.

[20] G. Hoogers. *Fuel Cell Technology Handbook*. CRC Press, 2003.

[21] Kutlar, H. Arslan, and T. Calik. "Methods to improve efficiency of four stroke, spark ignition engines at part load." *Science direct - Energy Conversion and Management 46 (2005) 32023220*, March 2005.

[22] Y. Zhao, J. He, and J. Chen. "Optimization criteria for the important parameters of an irreversible Otto heat-engine." *Applied Energy 83 (2006) 228238*, 2006.

[23] C. D. Perez-Segarra, J. Rigola, M. Soria, and A. Oliva. "Detailed thermodynamic characterization of hermetic reciprocating compressors." *Science Direct - International Journal of Refrigeration 28 (2005) 579593*, January 2005.

[24] A. Bejan. *Entropy generation through heat and fluid flow*. John Wiley and Sons, 1982.

[25] C. D. Rakopoulos. "Evaluation of a Spark Ignition Engine Cycle Using First and Second Law Analysis Techniques." *Energy Convers. Mgmt Vol. 34, No. 12, pp. 1299-1314, 1993 0196-8904/93 Pergamon Press Ltd*, 1993.

[26] C. D. Rakopoulos and E. G. Giakoumis. "Second-law analyses applied to internal combustion engines operation." *Progress in Energy and Combustion Science 32 (2006) 247*, 2005.

[27] J. A. Caton. "Results from the second-law of thermodynamics for a spark-ignition engine using an engine cycle simulation." *Paper No. 99ICE239 ICEVol. 333, 1999 Fall Technical Conference ASME 1999*, 1999.

[28] B. Ribeiro, J. Martins, and A. Nunes. "Generation of Exergy in Spark Ignition Engines." *Int J. of Thermodynamics Vol. 10 (No. 2), pp. 53-60, June 2007*, 2007.

[29] J. A. McGovern and S. Harte. "An exergy method for compressor performance analysis." *Int. J. Refrig. Vol. 18, No. 6, pp. 421-433*, 1995.

[30] K. P. Dudek and M. K. Sain. "A Control-Oriented Model for Cylinder Pressure in Internal Combustion Engines." *IEEE Transactions on Automatic Control Vol 34 No 4 April 1989*, 1989.

[31] Y. Shiao and J. Moskwa. "Cylinder Pressure and Combustion Heat Release for SI Engine Diagnostics Using Nonlinear Sliding Observers." *IEEE Transactions on Control Systems Technology. Vol. 3, No. I March 1995*, 1995.

[32] P. K. Houpt and H. N. Tan. "Identification of a Thermodynamic Model for Spark Ignited Internal Combustion Engines." *Massachusetts Institute of Technology*, 1989.

[33] J. B. Heywood. *Internal combustion engine fundamentals*. McGraw-Hill, 1988.

[34] G. A. Longo and A. Gasparella. "Unsteady state analysis of the compression cycle of a hermetic reciprocating compressor." *International Journal of Refrigeration 26 681689*, 2003.

[35] B. Silowash. *Piping systems manual*. McGraw Hill, 2009.

[36] "Engineering toolbox, thermal conductivity of air." http://www.engineeringtoolbox.com/air-properties-d_156.html. Last accessed 22/04/09.

[37] "CFD online." `http://www.cfd-online.com/Wiki/Sutherland's_law`. Last accessed 22/04/09.

[38] T. H. R. Jones. *Toyota Corolla Owners Workshop Manual*. Haynes Publishing Group, 1992.

[39] R. W. Moss, A. P. Roskilly, and S. K. Nanda. "Reciprocating Joule-cycle engine for domestic CHP systems." *Applied Energy 80 (2005) 169185*, 2004.

[40] P. Kuo. "Cylinder Pressure in a Spark-Ignition Engine: A Computational Model." *J. Undergrad. Sci. 3: 141-145 (Fall)*, 1996.

[41] B. W. Williams. "Using Hybrid Automata to Model Four Stroke Engines with Variable Valve Timing in Simulink/Stateflow." *ISIS Vanderbilt University, Nashville*.

[42] S. Quinn, A. Grace, P. Barnard, L. Michaels, and B. Aldrich. "Using Simulink and Stateflow in Automotive Applications." *Simulink and stateflow technical examples*, 2005.

[43] C. Bohn, T. Bhme, A. Staate, and P. Manemann. "A Nonlinear Model for Design and Simulation of Automotive Idle Speed Control Strategies." *Proceedings of the 2006 American Control Conference Minneapolis, Minnesota, USA, June 14-16*, 2006.

[44] A. G. Stefanopoulou, J. A. Cook, J. W. Grizzle, and J. S. Freudenberg. "Control-Oriented Model of a Dual Equal Variable Cam Timing Spark Ignition Engine." *Department of electrical engineering and computer science, University of Michigan, Ann Arbor. Ford Motor Company*, 1997.

[45] C. D. Rakopoulos. "Evaluation of a spark ignition engine cycle using first and second law analysis techniques." *Energy Convers. Mgmt Vol. 34, No. 12, pp. 1299-1314, 1993*, 1993.

[46] H. R. Ricardo. *The High Speed Internal Combustion Engine*. Blackie and Son Limited, 4th ed., 1953.

[47] C. E. Goering and H. Cho. "Engine Model for Mapping BSFC Contours." *Proc 6th International Conference on Mathematical Modelling*, 1988.

[48] M. Lindgren. "A Transient Fuel Consumption Model for Non-road Mobile Machinery." *Biosystems Engineering (2005) 91 (2), 139147*, 2005.

[49] R. Kurz, B. Winkelmann, and S. Mokhatab. "Efficiency And Operating Characteristics Of Centrifugal And Reciprocating Compressors." *Pipeline and Gas Journal*, October 2010.

[50] "Toyoland - information about Toyota engines." `http://www.toyoland.com/engines/4A-F.html`. Last accessed 21/12/10.

[51] T. Denton. *Advanced Automotive Fault Diagnosis*. Elsevier Butterworth-Heinemann, 2006.

[52] S. E. Wood and R. Battino. *Thermodynamics of chemical systems*. Cambridge University Press, 1990.

[53] F. Ma and Y. Wang. "Study on the extension of lean operation limit through hydrogen enrichment in a natural gas spark-ignition engine." *International journal of hydrogen energy 33 (2008) 1416 1424*, 2008.

[54] "SAAB Combustion Control." `http://www.saabnet.com/tsn/press/001004.html`. Last accessed 1/08/10.

[55] "Autoignition Temperature Summary." `www.engineeringtoolbox.com`. Last accessed 10/08/10.

[56] "CatalyticConverter.org." http://catalyticconverter.org/. Last accessed 01/02/11.

[57] H. P. Bloch and J. J. Hoefner. *Reciprocating compressors: operation and maintenance*. Gulf Professional Publishing, 1996.

[58] R. K. Shah and D. P. Sekulic. *Fundamentals of heat exchanger design*. John Whiley and Sons, 2003.

[59] A. S. Foust, L. A. Wenzel, C. W. Clump, L. Maus, and L. B. Andersen. *Principles of unit operations*. John Whiley and Sons, 1964.

[60] F. Incropera and D. DeWitt. *Introduction to Heat Transfer*. John Wiley and Sons, 1990.

[61] "School of mechanical industrial and aeronautical engineering, Fluid and Thermodynamics Course Notes - MECN3016." 2007.

[62] R. E. Simons. "Estimating Natural Convection Heat Transfer for Arrays of Vertical Parallel Flat Plates." *Electronics Cooling*, February 2002.

[63] A. D. Kraus, A. Aziz, and J. R. Welty. *Extended surface heat transfer*. John Whiley and Sons, 2001.

[64] G. Nellis and S. Klein. *Heat transfer*. Cambridge University Press, 2009.

[65] H. Shokouhmand and A. Ahmadpour. "Heat Transfer from a Micro Fin Array Heat Sink by Natural Convection and Radiation under Slip Flow Regime." *Proceedings of the World Congress on Engineering 2010 Vol II WCE 2010*, June 2010.

[66] J. Burrows, R. Hemp, W. Holding, and R. Stroh. *Environmental Engineering in South African Mines*. Mine Ventilation Society of South Africa, 1989.

[67] F. Angulo-Brown, J. A. Rocha-Martinez, and T. D. Navarrete-Gonzalez. "A non-endoreversible Otto cycle model: improving power output and efficiency." *Journal of applied Physics D. 29 (1996) 8083*, 1995.

[68] Y. Ge, L. Chen, and F. Sun. "Finite-time thermodynamic modelling and analysis of an irreversible Otto-cycle." *Applied Energy 85 (2008) 618624*, 2007.

[69] S. Bhattacharyya and D. A. Blank. "Power optimized work limit for internally irreversible reciprocating engines." *International Journal of Mechanical Sciences 42 (2000) 1357-1368*, 1999.

[70] K. H. Hoffmann, J. M. Burzler, and S. Schubert. "Endoreversible Thermodynamics." *Journal for non-equilibrium thermodynamics. Volume 22. Number 4*, 1997.

[71] J. M. Burzler. "Performance Optima for Endoreversible Systems." *Doctor rerum naturalium - Technische Universitat Chemnitz*, 2002.

[72] A. Durmayaza, O. S. Sogutb, B. Sahinc, and H. Yavuzd. "Optimization of thermal systems based on finite-time thermodynamics and thermoeconomics." *Progress in Energy and Combustion Science 30 (2004) 175217*, 2003.

[73] P. Roberts. "Personal communication." May 2008.

[74] X. Qin, L. Chen, F. Sun, and C. Wu. "The universal power and efficiency characteristics for irreversible reciprocating heat engine cycles." *European Journal of Physics 24 (2003) 359366*, 2003.

[75] X. Qin, L. Chen, F. Sun, and C. Wu. "The universal power and efficiency characteristics for irreversible reciprocating heat engine cycles." *European Journal of Physics 24 (2003) 359366*, 2003.

[76] L. A. Arias-Hernandez, G. A. de Parga, and F. Angulo-Brown. "On Some Nonendoreversible Engine Models with Nonlinear Heat Transfer Laws." *Open System and Information Dynamics 10: 351-375, 2003*, 2003.

[77] A. Bejan. *Advanced Engineering Thermodynamics*. John Wiley and Sons, 1988.

# A Finite-time thermodynamics

## A.1 Overview

The differential equation model based on the Otto cycle now gives an analyst an idea of the effect of irreversibility on process efficiency, but is still not very useful as an analytical tool, as a time consuming numerical simulation must be performed before any results are obtained. One of the required outputs of this project is to evaluate process efficiency for a particular set of system conditions; and a possible avenue of investigation may be found in the field of finite-time thermodynamics. This tool allows a process to be abstracted into two distinct parts: an internally reversible part, and an irreversible part that includes interactions with the surroundings (i.e. heat transfer between the surroundings and the working fluid) [67]. This methodology has been successfully applied to the Otto cycle [68], reciprocating engines [69], the CurzonAhlborn heat engine, which is based on the Carnot cycle [70], the Diesel engine [71], and numerous other thermodynamic power cycles including the Stirling cycle, Joule-Brayton, Atkinson, Ericsson and Lorentz cycles [72]. From the previously mentioned applications of finite-time thermodynamics, it is apparent that this tool has only been applied to cycles, while the internal loading process may not necessarily operate in a cycle; but no evidence was found in the literature indicating why this thermodynamic tool can not be applied to a process not operating in a cycle, and an example of finite-time thermodynamics applied to such a process is known to Dr Paul Roberts [73] - a visiting lecturer at the University of the Witwatersrand. Finite time thermodynamics is particularly useful in characterising the upper operating limit of real cycles where the rate at which work is done becomes an important factor, [69]. Carnot analysis is based on a reversible process, and so all states visited during a process are equilibrium states, and so does not provide an accurate description of real power cycles. A quasistatic process is carried out at an infinitesimally slow rate and as stated by Qin et al: ”a finite amount of work produced by the engine over an infinite amount of time delivers no power” [74]. The concept of endoreversibility has been used to derive abstracted models of heat engines for the purpose of optimisation.

## A.2 Internal Combustion Engine Model

The combustion process can be modelled according to differential equation models which prove particularly useful to the analysis of engine control projects. One of the objectives of modelling the internal combustion process is to obtain an efficiency mapping which would vary with engine speed and load, and finite-time thermodynamics is used to obtain such a mapping as significantly less computational resources are required to solve a finite-time model than a differential model.

As mentioned above, finite time thermodynamics is used in the optimisation of power cycles; and in a sense, the compressed air system is similar to the Joule cycle - as air will be compressed, and heated (to improve overall processes efficiency) and finally expanded. It may prove beneficial to analyse this cycle using finite time thermodynamics, and as a precursor to this analysis, finite time thermodynamics is used to characterise the efficiency of a spark ignition internal combustion engine (of which numerous examples exist). Finite time thermodynamics has been successfully applied to Otto and Diesel cycle models [68, 71] and will be used to obtain a qualitative description of the efficiency mapping of an internal combustion engine.

Much work has been done by Qin *et al* on the modelling of reciprocating heat engines as endoreversible cycles [75]; and by Blank *et al* [69] and Angulo-Brown *et al* [67, 76] in which engines are modelled as non-endoreversible cycles. The concept of endoreversibility is used extensively in finite time thermodynamics; an endoreversible process is internally reversible but externally irreversible - i.e. irreversibility is due to heat transfer to the working fluid, no entropy is generated by the working fluid when producing work [77], which has applicability limits as all realistic power cycles produce entropy. This leads to the concept of non-endoreversible cycles, where entropy is produced when work is done by the working fluid. For an endoreversible cycle:

$$\frac{Q_1}{T_{1w}} = \frac{Q_2}{T_{2w}} \tag{A.1}$$

For a non-endoreversible cycle [76]:

$$\begin{aligned} \sigma_i &= \frac{Q_1}{T_{1w}} - \frac{Q_2}{T_{2w}} \\ &= (1-R)\frac{Q_2}{T_{w2}} \end{aligned}$$

Combining the above:

$$\frac{Q_1}{T_{1w}} = R\frac{Q_2}{T_{2w}} \tag{A.2}$$

Where $R$ is a measure of the departure from an endoreversible process. Expressions for power and efficiency were obtained from [67, 75] :

$$P(R,K_1,K_2) = \frac{C_{V2}(R - r_v^{1-\gamma}}{K_1 + K_2 r_v^{1-\gamma}} - \mu v^2 \tag{A.3}$$

$$\eta(R,K_1,K_2) = 1 - \frac{1}{R}\left(r^{1-\gamma} + \frac{\mu v^2}{C_{v2}}(K_1 + K_2 r^{1-\gamma})\right) \tag{A.4}$$

Where:

- $K_1$ = Inverse of the rate of heat transfer ($k_1$) where $k_1 = \frac{dT}{dt}$ for a constant volume heating process
- $K_2$ = Inverse of the rate of heat transfer ($k_2$) where $k_2 = \frac{dT}{dt}$ for a constant volume cooling process
- $r_v$ = Maximum volume over the minimum volume
- $C_{v1}$ = Heat capacity at constant volume, during the combustion process
- $C_{v2}$ = Heat capacity at constant volume, during the exhaust process
- $\mu v$ = Power lost due to friction, where $\mu$ is the coefficient of friction and $v$ is the average piston speed.

$K_1$ and $K_2$ are related to the time taken for heat transfer to occur to and from the working fluid respectively, which implies that these variables are a function of the engine speed. Power lost due to friction is also a function of the engine speed, so equations A.3 and A.4 provide a power and efficiency relationship as a function of engine speed and the irreversibility factor $R$. The effect of loading on the Otto cycle is taken into account by including the term: $(P_{atm} - P_{in})\Delta V$, where $\Delta V$ is the displaced volume and $P_{in}$ is the inlet pressure which is less than atmospheric pressure due to throttling; as the degree to which an engine is loaded is determined by the extent to which it is throttled. Equations A.3 and A.4 were modified to include the effects of throttling in the model. The work done per cycle is given by the net heat transfer to the system, as per the first law of thermodynamics.

$$W_c = C_v(T_3 - T_2) - C_v(T_4 - T_1) - (P_{atm} - P_{in})\Delta V$$

The power per cycle is given as follows, where $\mu v^2$ is the power lost to friction.

$$P = \frac{W_c}{\tau_c} - \mu v^2 \tag{A.5}$$

Where $\tau_c$ is the cycle time of the process. The compression and expansion processes are modelled as instantaneous adiabats [67] and have no contribution to the cycle time of the process, which is determined by the engine speed. For instance, an engine speed of $3600RPM$ will have a cycle time of $33.33ms$, and it is assumed that the time spent on each of the heat transfer processes is half of the cycle time [68]. The cycle time is then represented as follows:

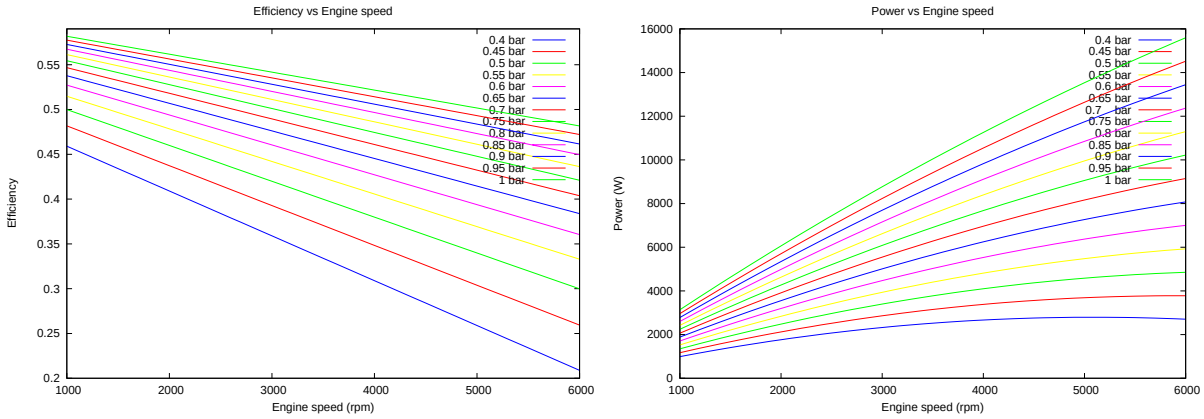
$$\tau_c = K_1(T_3 - T_2) + K_2(T_4 - T_1)$$

Where $K_1 = t_{12}\backslash(T_3 - T_2)$ and $K_2 = t_{41}\backslash(T_4 - T_1)$ obtained assuming that heat transfer to and from the working fluid occurs at the rate given by $\frac{dT}{dt} = \frac{1}{K_1}$ and $\frac{dT}{dt} = \frac{1}{K_2}$ respectively, and assuming that $t_{12} = t_{41} = \tau_c\backslash 2$. The efficiency of the cycle is given by:

$$\eta = \frac{P}{Q_{in}\backslash\tau_c} \tag{A.6}$$

Where $Q_{in} = C_v(T_3 - T_2)$.

Efficiency and power curves plotted for a range of engine speeds and throttle settings are shown in *Figure A.1*. The results are qualitatively correct in that efficiency decreases as power increases. Although similar, this behavior is not strictly the same as the behavior typically demonsatrated by finite time thermodynamic models of power cycles; which is calculated for a fixed engine speed to yield an expression for power per cycle against efficiency. It is well known that cycle efficiency is maximum when the power produced per cycle is zero, and that cycle efficiency is less than maximum efficiency at maximum power [72]. Although qualitatively correct, this finite-time model of the Otto cycle can be greatly improved; for instance some researchers have taken into account the variation of specific heat with temperature [68], and Burzler incorporated the irreversibility due to combustion in a diesel cycle [71]. *Table A.1* shows sample data for a throttle setting corresponding to an inlet pressure of 0.8 *bar*, and an engine speed of 3600 *RPM*.




(a) Otto cycle efficiency for a number of different throttling conditions

(b) Power generated for an Otto cycle for a number of throttling conditions

Figure A.1: Finite-time thermodynamic model - Power and efficiency curves

Table A.1: Sample data for the FTT model, for a throttle setting corresponding to an inlet pressure of 0.8 *bar*, and an engine speed of 3600 *RPM*

| | | | | | |
|---|---|---|---|---|---|
| $T_1$ | = | 300 $K$ | $K_1$ | = | $8.5 \times 10^{-6}$ |
| $T_2$ | = | 756 $K$ | $K_2$ | = | $21.6 \times 10^{-6}$ |
| $T_3$ | = | 2699 $K$ | $\mu$ | = | 12 $kg.s^{-1}$ |
| $T_4$ | = | 1071 $K$ | $r_v$ | = | 10 |
| $P$ | = | 7713 $W$ | $\eta$ | = | 0.49 |

This method shows promise but is not used to characterise process efficiency due to the large discrepancy between actual and predicted engine efficiency.

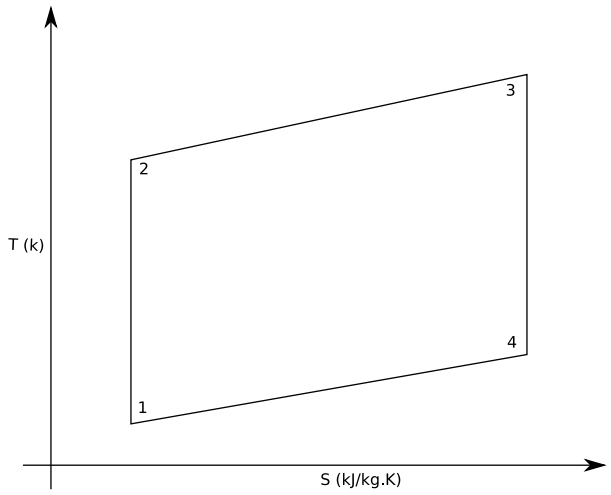



Figure A.2: TS diagram representation of an Otto cycle

# B Sample calculation for the differential equation model

The following sample calculation is used to demonstrate how the differential equation models have been handled. The equations are solved with the LSODE solver, which is a function native to the OCTAVE mathematical simulation package. The sample calculation is for the cylinder drawing air in from a manifold at a pressure of 0.5 bar. The temperature of the air (in the manifold and the cylinder) is 300 K. As the piston moves downwards, the pressure and temperature of the air within the cylinder decrease (as seen by the negative partial differential for each).

$$\dot{m} = \begin{cases} \frac{\eta_v A_{th} P_{tank}}{\sqrt{RT_{tank}}} \gamma^{\frac{1}{2}} \left(\frac{2\gamma}{\gamma+1}\right)^{\frac{\gamma+1}{2(\gamma-1)}} & \text{if } \frac{P_{cyl}}{P_{tank}} > \frac{2}{\gamma+1}^{\frac{\gamma+1}{2(\gamma-1)}} \\ \frac{\eta_v A_{th} P_{tank}}{\sqrt{RT_{tank}}} \left(\frac{P_{cyl}}{P_{tank}}\right)^{\frac{1}{\gamma}} \left[\frac{2\gamma}{\gamma-1}\left(1 - \frac{P_{cyl}}{P_{tank}}^{\frac{\gamma-1}{\gamma}}\right)\right]^{\frac{1}{2}} & \text{if } \frac{P_{cyl}}{P_{tank}} \leq \frac{2}{\gamma+1}^{\frac{\gamma+1}{2(\gamma-1)}} \end{cases} \tag{B.1}$$

$$\begin{aligned} \frac{2}{\gamma+1}^{\frac{\gamma+1}{2(\gamma-1)}} &= \frac{2}{2.4}^{\frac{2.4}{2(0.4)}} \\ &= 0.578 \\ \frac{p_{cyl}}{p_{tank}} &= \frac{5.499 \times 10^4}{5.5 \times 10^4} \\ &= 0.99 \\ \therefore \dot{m} &= \frac{\eta_v \times \pi\left(\frac{0.02}{2}\right)^2 \times 5.5 \times 10^4}{\sqrt{28.97 \times 300}} 1.4^{\frac{1}{2}} \left(\frac{2 \times 1.4}{1.4+1}\right)^{\frac{1.4+1}{2(1.4-1)}} \\ &= 2.497 \times 10^{-4}\ kg/s \end{aligned}$$

$$\begin{aligned} \eta_v &= 0.597071 + N \times 5.51605 \times 10^{-5} + p_{cyl} \times 9.30417 \times 10^{-7} \\ &= 0.597071 + \frac{104.7 \times 60}{2\pi} \times 5.51605 \times 10^{-5} + (5.5 \times 10^4) \times 9.30417 \times 10^{-7} \\ &= 0.7 \end{aligned}$$

$$
\begin{aligned}
V_{cyl} &= V_c \times \left[1+0.5\left(\frac{Vd+Vc}{Vc}-1\right)\left(\frac{l}{a}+1-\cos\theta-\left(\frac{l}{a}^2-(\sin\theta)^2\right)^{0.5}\right)\right] \\
&= 4.407\times10^{-5}\left[1+0.5\left(\frac{3.967\times10^{-4}+4.407\times10^{-5}}{4.407\times10^{-5}}-1\right)\ldots\right. \\
&\quad \left.\left(\frac{0.1}{0.0385}+1-\cos(0.0146)-\left(\frac{0.1}{0.0385}^2-(\sin(0.0146))^2\right)^{0.5}\right)\right] \\
&= 4.4099\times10^{-5}\ m^3
\end{aligned}
$$

$$
\begin{aligned}
\dot{V_{cyl}} &= \frac{V_c}{2}\times\left(\frac{V_d+V_c}{V_c}-1\right)\times\left[\omega\sin(\pi-\theta)+\left(0.5\times\ldots\right.\right. \\
&\quad \left.\left.\left(\frac{l}{a}^2-(\sin(\pi-\theta))^2\right)^{-0.5}\right)\times(-2\sin(\pi-\theta)\cos(\pi-\theta))\times\omega\right] \\
&= \frac{3.967\times10^{-4}}{2}\times\left(\frac{3.967\times10^{-4}+4.407\times10^{-5}}{4.407\times10^{-5}}-1\right)\times\ldots \\
&\quad \left[104.7\sin(\pi-0.0146)+\left(0.5\times\left(\frac{0.1}{0.0385}^2-(\sin(\pi-0.0146))^2\right)^{-0.5}\right)\times\ldots\right. \\
&\quad \left.(-2\sin(\pi-0.0146)\cos(\pi-0.0146))\times104.7\right] \\
&= 4.199\times10^{-4}\ m^3/s
\end{aligned}
$$

$$
\begin{aligned}
A_{cyl} &= A_{ch}+A_p+\pi B(l+a-a\cos(\theta)+\sqrt{l^2-(a\sin(\theta))^2}) \\
A_p &= \pi(B/2)^2 \\
&= \pi(0.08/2)^2 \\
&= 5.02\times10^{-3}\ m^2 \\
A_{ch} &= A_p \\
A_{cyl} &= 2\times5.02\times10^{-3}+\pi\times0.08\times(0.1+0.0385-0.0385\times\cos(0.006)+\sqrt{0.1^2-(0.0385\sin(0.006))^2}) \\
&= 0.001
\end{aligned}
$$

$$
\begin{aligned}
R &= \frac{8314}{28.97} \\
&= 286.99
\end{aligned}
$$

$$
\begin{aligned}
m &= \frac{p \times V_{cyl}}{R \times T} \\
&= \frac{5.499 \times 10^4 \times 4.4075 \times 10^{-5}}{286.99 \times 300} \\
&= 2.815 \times 10^{-5}\ kg
\end{aligned}
$$

$$
\begin{aligned}
\rho &= \frac{5.499 \times 10^4}{278.9 \times 300} \\
&= 0.638\ kg/m^3
\end{aligned}
$$

$$
\begin{aligned}
N_{Re} &= \frac{\rho \times \frac{\omega}{2 \times \pi} \times D}{\mu} \\
&= \frac{0.638 \times \frac{104.7}{2\pi} \times 0.08}{1.84 \times 10^{-5}} \\
&= 3544.4
\end{aligned}
$$

$$
\begin{aligned}
\dot{Q}_{ht} &= A_{cyl}\left[0.3\lambda \frac{{N_{Re}}^{0.7}}{D}(T_{cyl} - T_w) + 1 \times 10^{-8}({T_{cyl}}^4 - T_w^4)\right] \\
&= 0.001\left[0.3 \times 0.026\left(\frac{3544}{0.08}\right)^{0.7}(300 - 300) + 1 \times 10^{-8}(300^4 - 300^4)\right] \\
&= 0kW
\end{aligned}
$$

$$
\begin{aligned}
\dot{T} &= \frac{1}{mCv}\left[\dot{Q} - p\dot{V} + h_i\dot{m} - h_e\dot{m} - u\dot{m}\right] \\
&= \frac{1}{(2.815\times10^{-5})(718)}\Big[0 - (5.499\times10^{4})(4.199\times10^{-4}) + \ldots \\
&\quad (300.19\times10^{3})(2.497\times10^{-4}) - 0 - (214.07\times10^{3})(2.497\times10^{-4})\Big] \\
&= -75.99\ K/rad \\
\dot{p} &= \frac{R(\dot{m}T + \dot{T}m) - \dot{V}p}{V} \\
\frac{dp}{d\theta} &= \frac{dp}{dt}\times\frac{dt}{d\theta} \\
&= \frac{R(\dot{m}T + \dot{T}m) - \dot{V}p}{V}/\omega \\
&= \frac{286.98(2.497\times10^{-4}\times300 - 75.99\times2.815\times10^{-5} - 4.199\times10^{-4}\times0.5\times10^{5})}{4.4099\times10^{-5}\times104.7} \\
&= -4531.4\ pa/rad
\end{aligned}
$$

# C Heat transfer sample calculations

## C.1 Heat transfer coefficient from exhaust gas to heat exchanger

The following calculation serves to demonstrate how the heat transfer coefficient from the exhaust gases would be calculated, assuming the following parameters:

| | | | | |
|---|---|---|---|---|
| $T_{exh} = 900\ K$ | $T_{rec} = 300\ K$ | $p_{exh} = 1.5\ bar$ | $c_p = 1120.8\ J/kg.K$ | $d = 0.04\ m$ |
| $\lambda = 0.06\ W/K.m$ | $\mu = 3.89 \times 10^{-5}\ kg/m.s$ | $L = 1\ m$ | $\dot{m} = 0.02$ | |

Note: $p$ is the pressure in the exhaust pipe, $d$ and $L$ are the diameter and length of the segment of the heat exchanger through which the exhaust gas passes, $\dot{m}$ is the mass flow rate through the exhaust pipe, and the remainder of the properties are considered at a temperature of $T = 900\ K$

$$
\begin{aligned}
\rho &= \frac{P}{RT} \\
&= \frac{1.5 \times 10^5}{\frac{8314}{28.97} 900} \\
&= 0.58\ kg/m^3 \\
A_{pipe} &= \pi \times 0.02^2 \\
&= 1.25 \times 10^{-3}\ m^2 \\
\bar{\dot{m}} &= \frac{\rho(V_i - V_f)}{30/N} \\
&= \frac{0.58(4.407 \times 10^{-4} - 4.407 \times 10^{-5})}{30/2600} \quad \textit{Assuming an engine speed of } 2600\ \textit{RPM} \\
&= 0.02\ kg/s
\end{aligned}
$$

Note: the exhaust gas air will actually be pulsed rather than steady - hence the averaged value above is used. The outside diameter of the exhaust pipe is $0.04\ m$.

$$
\begin{aligned}
u_m &= \frac{\dot{m}}{\rho A_{pipe}} \\
&= \frac{0.02}{(0.58)(1.25\times10^{-3})} \\
&= 27.4\ m/s \\
N_{Re} &= \frac{d\rho u_m}{\mu} \\
&= \frac{(0.04)(0.58)(27.4)}{(3.89\times10^{-5})} \\
&= 16345 \\
\bar{h} &= 0.023\frac{\lambda}{d}\left(\frac{u_m d\rho}{\mu}\right)^{0.8}\left(\frac{c_p\mu}{\lambda}\right)^{0.3} \\
&= 0.023\frac{0.081}{0.04}\left(\frac{27.4\times0.04\times0.58}{3.89\times10^{-5}}\right)^{0.8}\left(\frac{1120\times3.89\times10^{-5}}{0.06}\right)^{0.3} \\
&= 75.9\ W/K.m^2
\end{aligned}
$$

$$
\begin{aligned}
\bar{h}\times A &= (75.9)(\pi\times0.04\times1) \\
&= 9.53\ W/K
\end{aligned}
$$

## C.2 Heat transfer coefficient from heat exchanger surface to receiver gases

| | | | |
|---|---|---|---|
| $T_w = 900\ K$ | $T_{rec} = 300\ K$ | $p = 1.5\ bar$ | $c_p = 1005\ J/kg.K$ |
| $\lambda = 0.026\ W/K.m$ | $\mu = 1.84\times10^{-5}\ kg/m.s$ | $L = 1\ m$ | $N_{cpr} = 1000\ rpm$ |

$$
\begin{aligned}
\rho &= \frac{1.5\times10^5}{\frac{8314}{28.97}300} \\
&= 1.74\ kg/m^3 \\
\dot{m} &= \frac{\Delta m}{1/N} \\
&= \frac{2\times\rho(V_i - V_f)}{1/N_{cpr}} \quad (\textit{two cylinders discharge air per revolution}) \\
&= \frac{2\times1.74(2.2\times10^{-4} - 2.2\times10^{-5})}{30/1000} \\
&= 22.96\times10^{-3}\ kg/s
\end{aligned}
$$

$$
\begin{aligned}
u_m &= \frac{\dot{m}}{A} \\
&= \frac{22.96 \times 10^{-3}}{8 \times 0.01 \times 0.08} \\
&= 3.58\ m/s \\
N_{Re} &= \frac{L \rho u_m}{\mu} \\
&= \frac{(1)(1.74)(3.58)}{1.84 \times 10^{-5}} \\
&= 97170 \\
N_{Pr} &= \frac{c_p \mu}{\lambda} \\
&= \frac{(1005)(1.84 \times 10^{-5})}{0.026} \\
&= 0.707 \\
\overline{h} &= \frac{\lambda (N_{Re}{}^{\frac{1}{2}})(N_{Pr}{}^{\frac{1}{3}})}{L} \\
&= \frac{0.026(97170^{\frac{1}{2}})(0.707^{\frac{1}{3}})}{1} \\
&= 6.81\ W/K.m^2
\end{aligned}
$$

$$
\begin{aligned}
\overline{h} \times A &= (5.15)(8)(2 \times (1 \times 0.08) + (0.01 \times 1) \\
&= (6.81)(8)(0.17) \\
&= 9.26\ W/K
\end{aligned}
$$

## C.3 Heat transfer via natural convection

| | | | | |
|---|---|---|---|---|
| $T_w = 900\ K$ | $T_{rec} = 300\ K$ | $p = 1.5\ bar$ | $c_p = 1005\ J/kg.K$ | $b = 0.01\ m$ |
| $\lambda = 0.026\ W/K.m$ | $\mu = 1.846 \times 10^{-5}\ kg/m.s$ | $L = 0.08\ m$ | | |

$$\begin{aligned}\rho &= \frac{1.5\times10^5}{\frac{8314}{28.97}300}\\ &= 1.74 kg/m^3\end{aligned}$$

$$\begin{aligned}Ra &= \frac{\rho g\beta c_p b^3\Delta T}{\mu\lambda}\\ &= \frac{(1.74)(9.8)(1/300)(1005)(0.01^3)(900-300)}{(1.846\times10^{-5})(0.026)}\\ &= 7.21\times10^4\end{aligned}$$

$$\begin{aligned}h &= \frac{\lambda Ra}{24b}\left(1-e^{-\frac{35}{bRa}}\right)^{0.75}\\ &= \frac{(0.026)(0.01)(7.21\times10^4)}{(24)(0.01)}\left(1-e^{-\frac{35}{(0.01)(7.21\times10^4)}}\right)^{0.75}\\ &= 1.6\, W/m^2.K\end{aligned}$$

$$\begin{aligned}\bar{h}\times A &= (1.6)(16\times0.03\times1)\\ &= 0.512\, W/K\end{aligned}$$

# D Sample calculation for the compressed air storage model

$$\begin{aligned} V_b &= V_a / \left(\frac{p_{rec}}{p_{in}}\right)^{1/\gamma} \\ &= 2.2 \times 10^{-4} / \left(\frac{6 \times 10^5}{1.01 \times 10^5}\right)^{1/1.4} \\ &= 6.16 \times 10^{-5}\ m^3 \end{aligned}$$

$$\begin{aligned} work &= p_{rec}(V_f - V_x) + \frac{p_{rec}V_x - p_{in}V_i}{1-\gamma} \\ &= 6 \times 10^5 (2.2 \times 10^{-5} - 6.16 \times 10^{-5}) + \frac{(6 \times 10^5)(6.16 \times 10^{-5}) - (1.01 \times 10^5)(1.1 \times 10^{-4})}{1 - 1.4} \\ &= -60.64\ J \end{aligned} \tag{D.1}$$

$$\begin{aligned} torque &= \frac{2 \times 60.64}{2 \times \pi} \\ &= 19.3\ N.m \end{aligned} \tag{D.2}$$

The workings of the model can be demonstrated by considering a single compression stroke of the external compressor. Consider the receiver initially at a pressure of 6 *bar*, 300 *K*. One

compression stroke of the external compressor will add $1.65 \times 10^{-4}\ kg$ of air into the receiver:

$$\begin{aligned}
T_b &= T_a\left(\frac{p_b}{p_a}\right)^{\frac{\gamma-1}{\gamma}} \\
&= 300\left(\frac{6\times10^5}{1.01\times10^5}\right)^{\frac{1.4-1}{1.4}} \\
&= 499\ K \\
V_b &= \frac{V_a}{\left(\frac{p_b}{p_a}\right)^{\frac{1}{\gamma}}} \\
&= \frac{2.2\times10^{-4}}{\left(\frac{6\times10^5}{1.01\times10^5}\right)^{\frac{1}{1.4}}} \\
&= 6.15\times10^{-5}\ m^3 \\
\rho_b &= \frac{p_b}{RT_b} \\
&= \frac{6\times10^5}{\frac{8314}{28.97}499} \\
&= 4.19\ kg/m^3 \\
\Delta m &= \rho_b(6.15\times10^{-5} - 2.2\times10^{-5}) \\
&= 4.19(V_b - V_c) \\
&= 1.65\times10^{-4}\ kg
\end{aligned}$$

The state of the receiver will change as this air is added, and heat will be transferred into the incoming air as it blows across the heat exchanger:

$$\begin{aligned}
u_i &= 214.07\times10^3\ J/kg \\
m_i &= \frac{(6\times10^5)(0.5)}{\frac{8314}{28.97}300} \\
&= 3.4\ kg \\
\Delta Q &= \dot{Q}\times\Delta t \\
\Delta t &= \frac{30GR}{N} \\
&= \frac{30\frac{1}{2.5}}{2000} \\
&= 6\times10^{-3}\ s
\end{aligned}$$

The rate of heat transfer to the air is determined according to the method described in *Section 4.2.6*, and for this case was determined to be 2622 $W$. The heat transferred into the air is determined by multiplying the rate of heat transfer by the time over which the stroke occurs:

$$
\begin{aligned}
\Delta Q &= \dot{Q} \times \Delta t \\
&= 2622 \times 6 \times 10^{-3} \\
&= 15.7\ J \\
u_f &= \frac{h_{in} \times \Delta m + \Delta Q + u_i \times mrec_i}{\Delta m + mrec_i} \\
&= \frac{(501.99 \times 10^3)(1.65 \times 10^{-4}) + 15.7 + (214.07 \times 10^3)(3.4)}{1.65 \times 10^{-4} + 3.4} \\
&= 214.25\ kJ/kg \\
T_{rec} &= 300.25\ K \\
p_{rec} &= 6.01\ bar \\
work &= p_b(V_b - V_c) + \frac{p_a V_a - p_b V_b}{1-\gamma} \\
&= 6 \times 10^5 (6.15 \times 10^{-5} - 2.2 \times 10^{-5}) + \frac{(1.01 \times 10^5)(2.2 \times 10^{-4} - (6 \times 10^5)(6.15 \times 10^{-5})}{1 - 1.4} \\
&= 60.6\ J
\end{aligned}
$$